Annual Report FY 2003

平成 15 年度活動報告

Institute for Geothermal Sciences

Graduate School of Science

Kyoto University

京都大学

大学院理学研究科

附属地球熱学研究施設

Institute for Geothermal Science
Graduate School of Science, Kyoto University

京都大学大学院理学研究科
附属地球熱学研究施設

Beppu Geothermal Research Laboratory
Noguchibaru, Beppu, Oita 874-0903,
Japan
Telephone: +81-977-22-0713
Racsimile: +81-977-22-0965

別府
〒874-0903 大分県別府市野口原
電話: 0977-22-0713
ファックス: 0977-22-0965
Homepage: http://www.vgs.kyoto-u.ac.jp

Aso Volcanological Laboratory
Choyo, Aso, Kumamoto
869-1404, Japan
Telephone: +81-967-67-0022
Facsimile: +81-967-67-2153

阿蘇(火山研究センター)
〒869-1404 熊本県阿蘇郡長陽村河陽
電話: 0967-67-0022
ファックス: 0967-67-2153
Homepage: http://w3.vgs.kyoto-u.ac.jp

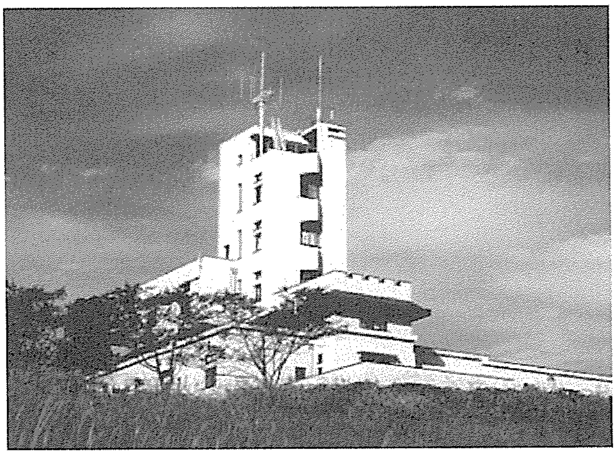

Front Cover Image : A strombolian explosion in the 1st crater of Mt.Nakadake, Aso volcano in October 1979.(Photo by M.Sako)
表紙の写真：1979年10月の阿蘇中岳第一火口のストロンボリ噴火の様子（迫幹夫撮影）

Editional complilation by M.Utsugi
Printed in Japan by Touka Shobo (TEL 092-565-7678)

目次　Contents

序

法人化に関連して大学運営の効率化を志向する傾向が強い。見かけの研究成果を急ぐあまり、解決しやすい研究のみを取り上げる危険にさらされている。観測的研究においてはデータの収集に多大の労力を費やすことが多く、他分野に較べて論文の少ない傾向は否めず、評価面で苦戦を強いられる事になる。元来、京都大学は１０年に一人の優秀な研究者が育てば良いとのスタンスで研究を進めてきたと理解している。評価を気にするあまり、資産の食い潰しに走ることなく、本質をついた研究には時間を要しても、じっくりと取り組みたいものである。

人事においては、由佐教授が退官され、名誉教授となられました。長年にわたり、研究はもとより、施設運営に尽力されましたことに感謝いたします。阿蘇における補任人事と合わせて補任の選考が開始されました。施設の将来計画を決定することになる重要事項であるため時間がかかるかもしれませんが悔いのない人事を行いたいと考えています。
昨年度末の鈴木助手の離職に伴い、山本順司博士が助手に任用され１２月に着任されました。また、適任者が見出せず空席になっていた技官に、井上寛之氏が内定されました。活躍を期待しています。外国人客員であった、陳中華博士が９月末で離職し、Jianguo Du 博士が１０月に着任されました。これを契機に、中国との共同研究の進展を期待しています。

学生においては、長谷英彰、吉川美由紀氏が博士学位を取得されました。しかし、適切な就職口が見出せず、研修生となることを余儀なくされる状況にあります。機関研究職員では、宮田佳樹・宮崎隆氏の後任として後藤秀作・中川毅氏が着任しました。中川氏は１０月末にニューキャスル大学の専任講師として転出され、網田和宏氏が補任されました。また、追加要求枠で森健彦氏が桜島から移籍されました。

一方、２１世紀ＣＯＥが本格的に開始され、地球熱学研究施設では竹村教授を中心としてプレート収斂域における水･熱フローをキーワードとして研究が進展しています。また、地球熱学研究施設において多目的観測研究の拠点を形成するべく教室との密な連携が進展しつつあります。学部等教育に関しては地球熱学を開講しました。これに伴い、京都における教官や学生の居室が不可欠であり、理学部１号館に２スパンの使用が認められました。しかし、教官の京都常駐勤務は認められていません。地球熱学に関する教育の充実に支障を来たすと考えられるので対策が必要です。火山噴火予知に関しては、第７次火山噴火予知計画事業が建議されたにもかかわらず、新規の設備要求は認められませんでした。観測設備の老朽化が危惧されます。

この活動報告が施設全員の相互理解と研鑽の拠り所として活用されることを願い、施設外の方々には、私たちの活動をご理解戴き、ご指導とご助言を賜る機会となれば幸いです。諸般の事情により出版が遅れたことをお詫び申し上げます。

地球熱学研究施設長
田中　良和

Preface

Recently, it was demanded to make out many research papers effectively with low cost in related with reformation of juridical personalization of national universities. This requirement includes a risk to select easier subjects to get more results in shorter time.In geophysical observational studies, data collection in long time is very important. As a result, output is not so many compared with the other fields, and we are in trouble. Instead of such situations we want to spend enough time to resolve essential problems as a peculiarity of Kyoto University.

In personnel affairs, Professor Yuki Yusa retired and took up a title of honorable professor. We praise his geophysical studies and thank for his contributions in the administration of our institute. As a post Yusa, supplemental personnel affairs are in progress. We want to search for a best scientist to fit our future study plan. In December, Dr. Junji Yamamoto arrived as associate post at Beppu, and Mr. Hiroyuki Inoue was appointed as a technical professional at Aso. As a visiting faculty, Dr. Chang-Hwa Chen left at the end of September, and Dr. Jianguo Du arrived. We hope to get more deeply involved in cooperative studies with Taiwan and Republic of China through these personnel exchanges. As a postdoctoral associate, Dr. Takehiko Mori arrived at Aso from Sakurajima volcanological Laboratory.

In our graduate school, Mr. Hideaki Hase and Miss Miyuki Yoshikawa obtained Doctor of Science, and they stay as unemployed researchers. It is serious problems for us. While, 21 COE program of earth science started, study of water and heat flows in the convergent regions of plates is main subject of our institute lead by Professor Takemura. Also the project to build a base for multiple observational studies in Aso and Beppu is in progress along with closer connection to the Kyoto campus. For undergraduate students, we opened advanced courses for geothermal sciences and volcanology. In order to achieve further educational tasks, we kept two rooms for our students in Kyoto campus. Stay of our staff member at the Kyoto campus was not approved positively yet. We must search the best way to do. The 7th project for prediction of volcanic eruption started, but none of budget for new devises was obtained. We are apprehensive about our aged observational devices.

I wish this annual report be put to practical use for improving the mutual understanding among the staffs and providing study materials for our daily activities. I would like to beg all people to read this to understand our activities and we look for guidance on further development of the Institute.

Yoshikazu Tanaka, Professor/ Director

構成員　Members

教授	*Professors*
竹村恵二	Keiji Takemura
田中良和	Yoshikazu Tanaka
(施設長 Director)	
由佐悠紀	Yuki Yusa
(2004 年 3 月退官)	

助教授	*Associate Professors*
古川善紹	Yoshitsugu Furukawa
大沢信二	Shinji Ohsawa
大倉敬宏	Takahiro Ohkura
須藤靖明	Yasuaki Sudo

助手	*Assistant Professors*
山本順司	Junji Yamamoto
(2003 年 12 月着任)	
川本竜彦	Tatsuhiko Kawamoto
柴田知之	Tomoyuki Shibata
宇津木充	Mitsuru Utsugi

技官	*Technical Professionals*
馬渡秀夫	Hideo Mawatari
吉川　慎	Shin Yoshikawa

外国人客員	*Visiting Faculty*
陳　中華	2003 年 9 月退職
杜　建国	2003 年 10 月着任

非常勤研究員	*Resarch Assosiates*
網田和宏	Kazuhiro Amita
後藤秀作	Shusaku Goto
井上（北田）直人	Naoto Kitada
中川　毅	Nakagawa Tuyoshi
西村光史	Koshi Nishimura
森　健彦	Takehiko Mori

教務補佐員	*Research Assistant*
芳川雅子	Masako Yoshikawa

研究支援推進員	
迫　幹雄	Mikio Sako

大学院生	*Graduate students*
中坊　真	Makoto Nakaboh
長谷英彰	Hideaki Hase
山田　誠	Makoto Yamada
吉川美由紀	Miyuki Yoshikawa

事務補佐員	*Secretaries*
今村町子	Machiko Imamura
後藤君子	Kimiko Goto
土屋寿子	Toshiko Tutiya

臨時用務員	
山崎咲代	Sakiyo Yamazaki

研究活動 Research Activities

施設内共同研究 (In-house collaboration)

Crystallization processes of Unzen 1991–1995 dacite inferred from melt inclusion analyses

K. Nishimura, T. Kawamoto** and **K. Takemura

Collaboration with T. Kobayashi (Kagoshima Univ.), T. Sugimoto (Kyushu Univ.) and S. Yamashita (Okayama Univ.)

Previous petrological studies of the 1991–1995 dacite of the Unzen volcano have suggested mixing of high- and low-temperature (T) end member magmas. Before the mixing, the high- and low-T magmas were aphyric and crystal-rich, respectively (Nakamura 1995). In order to further understand the evolution of the Unzen dacite, we investigated pressure and temperature records of the low-T magma by the use of phenocrysts and melt inclusion chemistry. Melt inclusions are small volumes of silicate melt that are entrapped during crystallization of phenocrysts and variably cooled depending on quench rate. Such inclusions can retain concentrations of volatile elements at the time of entrapment because they are contained within relatively incompressible phenocryst hosts. Analysis of these inclusions, therefore, provides direct information on pre-eruptive conditions in the magma reservoir.

The water contents of melt inclusions of plagioclase and quartz phenocrysts were determined by using Fourier Transform Infrared (FT-IR) spectroscopy. A typical IR absorption spectrum is shown in Figure 1. The variation in water content of the melt inclusions (5.1–7.2 wt. % H_2O) reflected the degassing history of the low-T magma ascending from deeper levels (~250 MPa) to a shallow magma chamber at ~140 MPa (Figure 2). The ascent rate of the low-T magma decreased markedly towards the emplacement level as increasing crystal content. In such conditions, cooling of magma as well as degassing-induced undercooling drived crystallization. With the decreasing ascent rate, degassing-induced undercooling decreased in importance, and cooling became more dominant in crystallization, causing local and rapid crystallization along the margin of the magma body. Some crystals contain scores of melt inclusions, whereas there are some crystals without any inclusions. This heterogeneous distribution suggests the variation in the crystallization rate within the magma body; it also suggests that cooling was dominant cause for melt entrapment. Numerical calculations of the cooling magma body suggest that cooling caused rapid crystal growth and enhanced melt entrapment once the magma became a crystal-rich mush at low temperature (Figure 3). The crystal fraction and temperature conditions during the melt inclusion formation in Unzen dacite (Figure 2) are consistent with this model. Based on the estimated P-T conditions and the crystallization mechanisms of the low-T magma using the melt inclusion analyses, we draw a picture showing a plausible magma plumbing system under the Unzen volcano in Figure 4.

(submitted to Bulletin of Volcanology)

References

Huppert HE, Sparks RSJ (1988a) The generation of granitic magmas by intrusion of basalt into continental crust. J Petrol 29:599–642

Huppert HE, Sparks RSJ (1988b) Melting the roof of a chamber containing a hot, turbulently convecting fluid. J Fluid Mech 188:107–131

Koyaguchi T, Kaneko K (1999) A two-stage thermal evolution model of magmas in continental crust. J Petrol 40:241–254

Koyaguchi T, Kaneko K (2000) Thermal evolution of silicic magma chambers after basalt replenishments. Trans Royal Soc Edinburgh: Earth Sci 91:47–60

Kusakabe M, Sato H, Nakada S, Kitamura T (1999) Water contents and hydrogen isotopic ratios of rocks and minerals from the 1991 eruption of Unzen volcano, Japan. J Volcanol Geotherm Res 89:231–242

Nakamura M (1995) Continuous mixing of crystal mush and replenished magma in the ongoing Unzen eruption. Geology 23:807–810

Piwinskii AJ, Wyllie PJ (1968) Experimental studies of igneous rock series: a zoned pluton in the Wallowa batholith, Oregon. J Geol 76:205–234

Sato H, Nakada S, Fujii T, Nakamura M, Suzuki–Kamata K (1999) Groundmass pargasite in the 1991–1995 dacite of Unzen volcano: phase stability experiments and volcanological implications. J Volcanol Geotherm Res 89:197–212

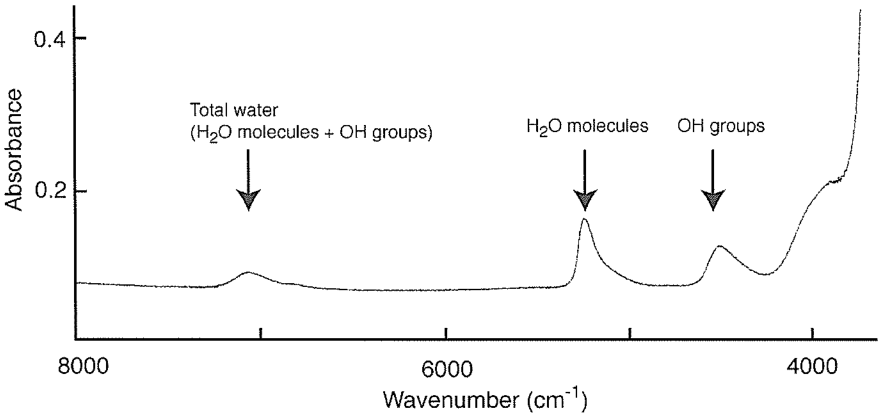

Figure 1 Typical IR spectrum of the melt inclusion analyzed in this study (Bomb 02: rhyolitic melt inclusions trapped within quartz phenocryst). The combination bands at 4500 cm^{-1} and at 5200 cm^{-1} were used for total water determination.

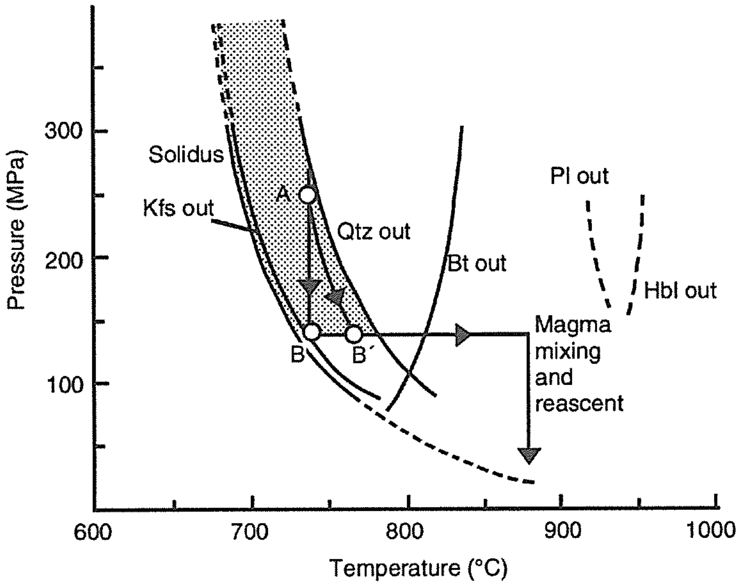

Figure 2 Schematic P-T section for dacite with 67.4 wt. % SiO_2 (based on Piwinskii and Wyllie 1968; sample 779). Shaded area represents possible P-T conditions for melt inclusion formation. Line A-B and line A-B′ represent a possible magma ascent path of extremely cooled magma and that of insulated magma, respectively. In the case of adiabatic magma ascent, latent heat of degassing crystallization increases magma temperature.

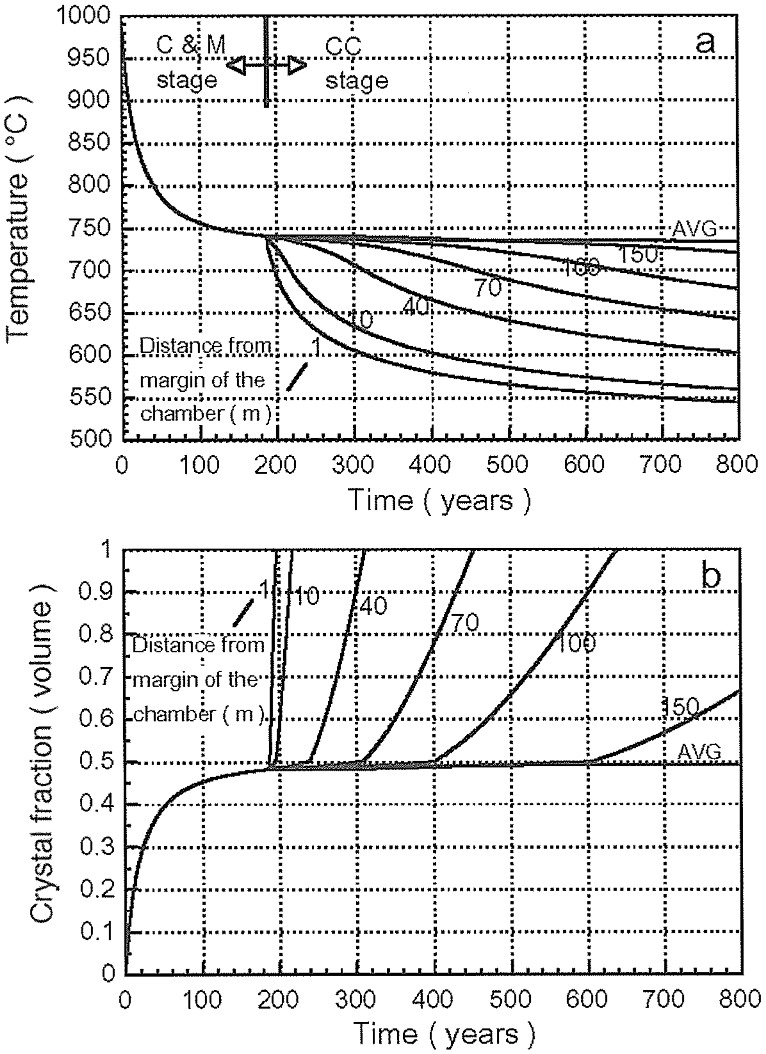

Figure 3 Variations in magma temperature (a) and crystal fraction (b) with time after contact of hot magma with a cold solid on the basis of a heat and mass transfer model which is developed out of the ideas of fluid mechanics in Huppert and Sparks (1988a; 1988b) and Koyaguchi and Kaneko (1999; 2000) In the Convection and Melting (C&M) stage, the magma has uniform temperature throughout the chamber due to vigorous convection. In the Conductive Cooling (CC) stage, on the other hand, the magma temperature decreases towards the margin of the chamber (a). After the C&M stage, the crystal fraction increases rapidly near the margin of the magma chamber (b).

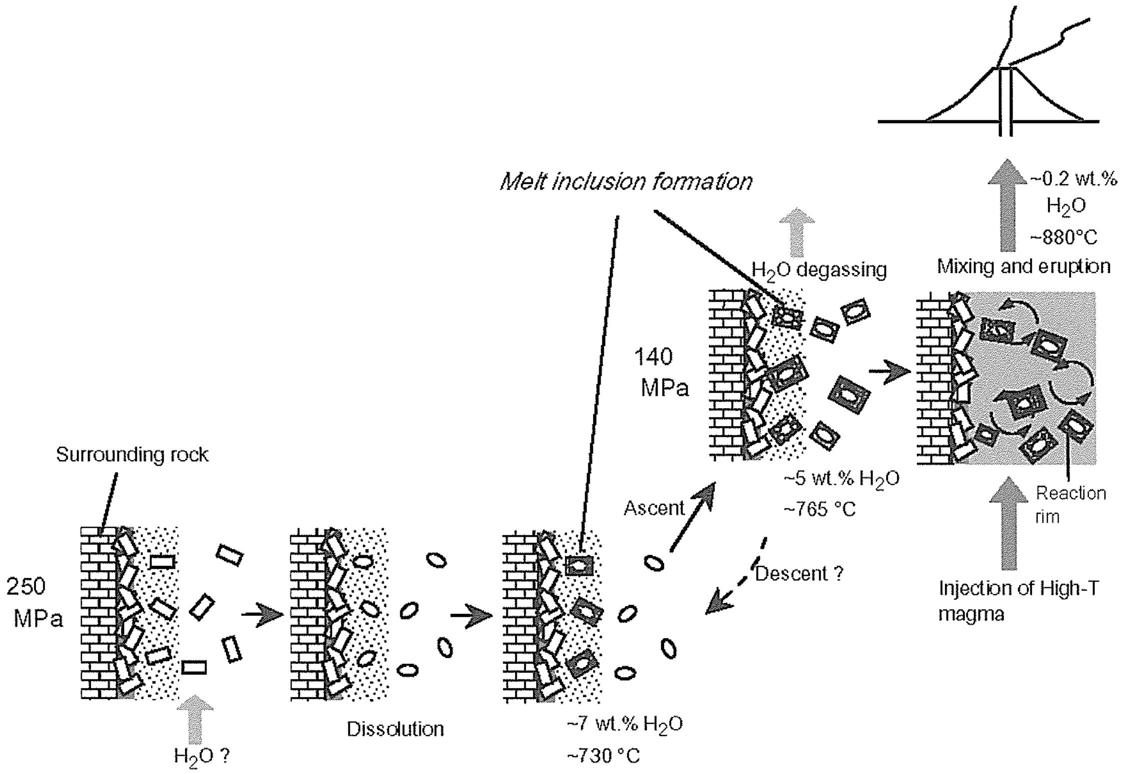

Figure 4 Schematic illustration of the evolution of the Unzen dacite showing formation processes of melt inclusions in phenocrysts. The depths below the summit are shown in km. The resorbed crystal surfaces caused by input of H_2O-rich fluid become favorable substrates for inclusion entrapment during subsequent growth events. Rapid crystal growth induced by cooling causes entrapment of melt inclusions along the margin of the low-T magma body (dotted area). During the magma ascent, the cooling-driven crystallization and degassing-induced crystallization occur simultaneously (see text for details). The injection of the high-T magma results in the An-rich reaction rim. The groundmass water content (<0.5 wt. %; Kusakabe et al. 1999) and crystallization temperature of the groundmass (~880 °C; Sato et al. 1999) are also shown.

Geochemical and Colorimetric Study on Yudamari Crater Lake, Aso Volcano, Japan

S. Ohsawa, Y. Sudo, H. Mawatari, *G. Shimoda,* ***M. Utugi, K. Amita, S. Yoshikawa, M. Yamada,*** *K. Iwakura, Y. Onda, N. Takamatsu*

(I) Some geochemical features of Yudamari crater lake

On August 4 in 2000 and on April 22 in 2003, water samples for chemical and isotopic analyses were collected from Yudamari crater lake formed in the 1st crater of Mt. Nakadake, Aso Volcano, central Kyushu, Japan (Fig.1; Fig.2). The lake water, which shows very high temperatures (above 50℃), has extremely high acidity (below pH 1) and contains chloride and bisulfate ions in large quantities (Table 1). These features indicate that high temperature volcanic gas discharged from volcanic gas conduit under the lake floor directly and/or indirectly inputs heat and HCl and SO_2 to the crater lake water. Aqueous SiO_2 concentration of the lake water is extremely higher than saturation value with respect to every SiO_2 mineral at the lake water temperature (Fig.3). Dissolved sulfate enriched in ^{34}S is probably formed by SO_2 disproportionation and/or hydrolysis of elemental sulfur at an elevated temperature (Table 1). These would be signs that sublimnic hydrothermal environment has been established under the lake floor and the hydrothermal water may circulate between the sublimnic hydrothermal system and the cater lake.

(II) Change in water color of Yudamari crater lake prior to the mud eruption at the lake bottom on July 10, 2003

Water of Yudamari is colored by Rayleigh scattering of sunlight from aqueous colloidal sulfur particles and also by reason of absorption of sunlight by dissolved iron ion [1]. The lake water previously colored in greenish blue made the color more greenish from the middle of 2002 and then was suddenly colored in yellowish green in early 2003 (Fig. 4). From a colorimetric measurement of the lake water color by the use of a remote colorimeter in this period, it is objectively demonstrated that the color change sensed by naked eye surely occurred (Fig. 5). Moreover, it is shown that the color change from greenish blue to yellowish green began at least 4 months before the mud eruption at the lake bottom on July 10, 2003 (Fig. 6) and was ahead of the start of gradual increase of surface temperature of the crater lake water about 1 month (Fig. 7). It is known that geochemical behavior of dissolved components in crater lakes formed in summit craters of active volcanoes [2], such as Yudamari, is affected by volcanic gas discharged from subaqueous fumaroles [3]. Therefore, we are now considering the causal relation between the color change of the Yudamri crater lake water and volcanic activity of Aso Volcano.

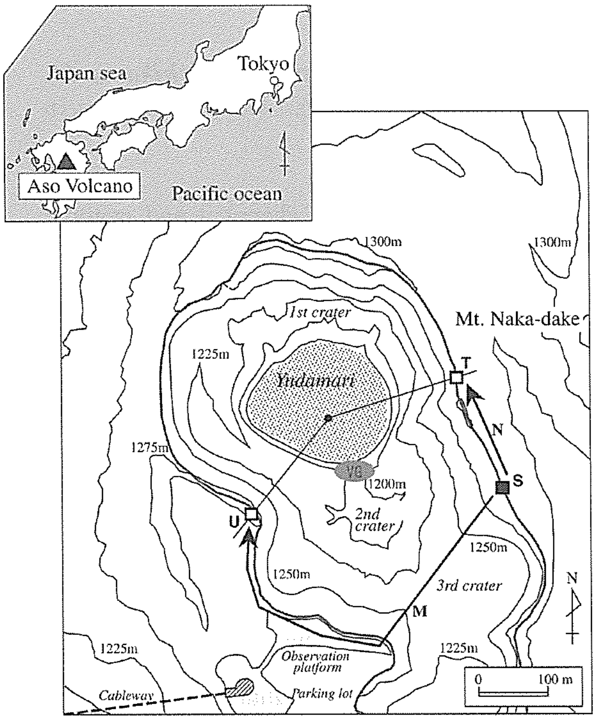

← Fig.1 Location map of Aso Volcano and map showing main topographic features of Yudamari crater lake.

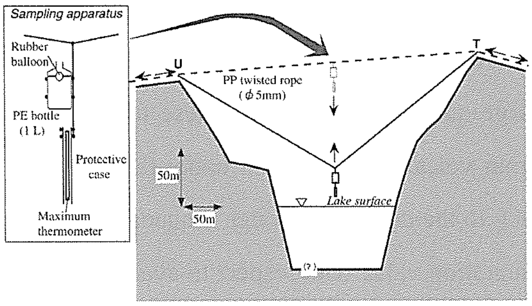

Fig.2 Simplified explanation showing water sampling and sampling apparatus for lake water.

Table 1 Results of chemical and isotopic analyses of water samples from Yudamari crater lake.

Sampling Date	Apr. 22, 2003	Aug. 4, 2000	Oct. 19, 1993
Water temp. (℃)	71.2	55.3	66.2
pH	−0.72	0.81	0.38
Na (mg/L)	5810	1740	785
K (mg/L)	2460	700	385
Ca (mg/L)	1360	2190	1090
Mg (mg/L)	7720	1760	880
ΣFe(mg/L)	16000	4050	1800
Al (mg/L)	19300	5510	2590
Cl (mg/L)	112000	28600	15700
SO_4(mg/L)	103000	43700	14100
F (mg/L)	12000	2350	
SiO_2(mg/L)		430	
δD (‰)		+8.0	
$\delta^{18}O$ (‰)		+11.9	
$\delta^{34}S$ (‰)		+15.6	

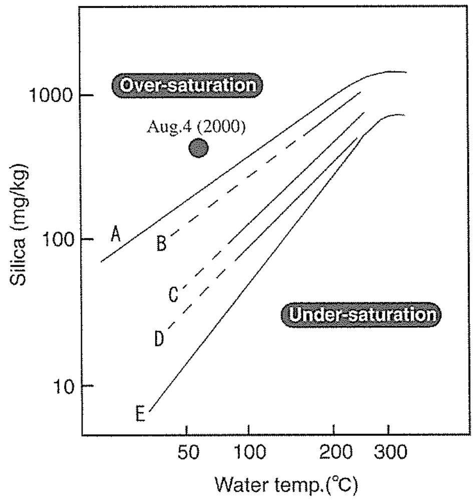

Fig.3 Relation between SiO_2 content and temperature of Yudamari crater lake water, and temperature dependence of solubility of various silica minerals (A: amorphous silica, B: opal-CT, C: α-cristobalite, D:chalcedony, E:quartz; Fournier, 1985).

Fig.4 Change in water color of Yudamari crater lake before the mud eruption at the lake bottom on July 10, 2003.

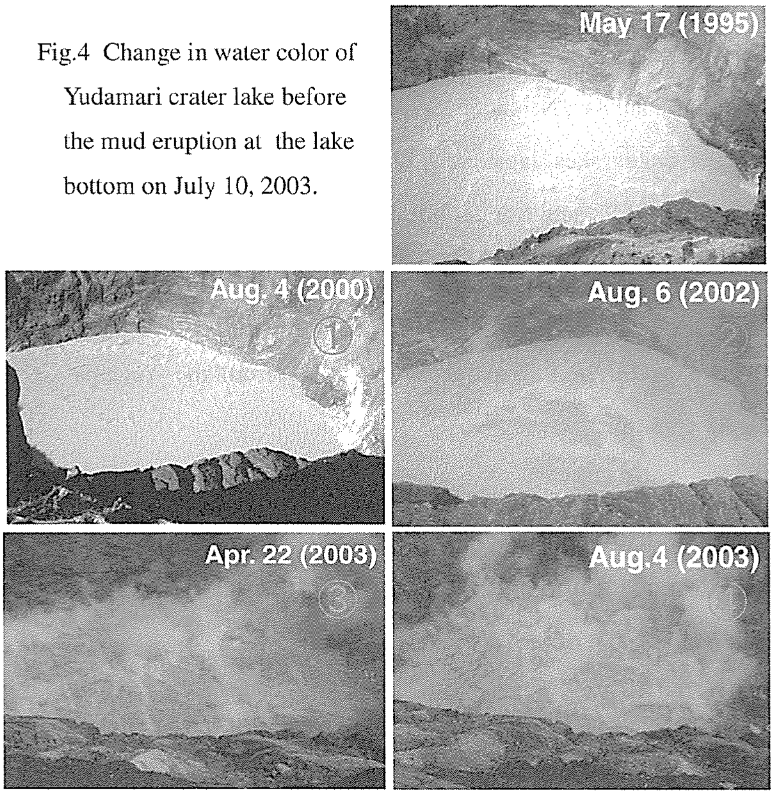

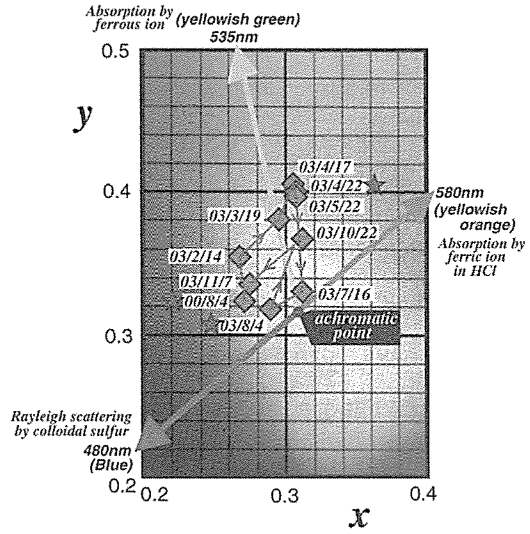

← Fig. 5 Plot on the CIE1931 chromaticity diagram of colorimetric measurement data of Yudamari crater lake water from 2000 to 2003. Directions of three vectors from the achromatic point indicate hues of colloidal sulfur solution, ferrous ion solution and ferric ion in hydrochloric solution. Number with red asterisk corresponds to photograph number in Fig. 4.

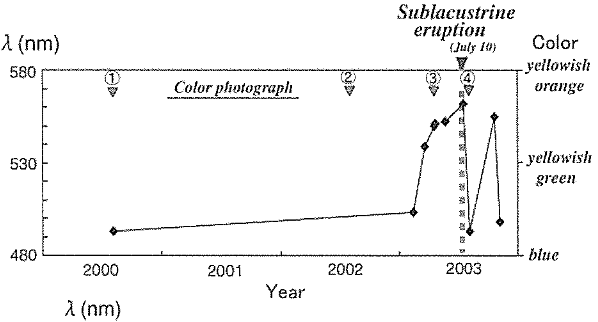

Fig. 6 Temporal variation in water color (λ : dominant wavelength) of Yudamari crater lake from 2000 to 2003. Number with inverted delta corresponds to photograph number in Fig. 4.

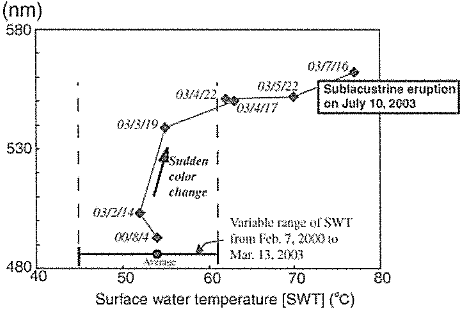

Fig. 7 Relation between surface water temperature and water color (λ : dominant wavelength) of Yudamari crater lake before the lacustrine phreatic eruption on July 10, 2003. Variable range of SWT means range of seasonal variation in surface water temperature observed before the 2003 lacustrine phreatic eruption.

References

[1] Onda, Y., Ohsawa, S., Takamatsu, N. (2003) A colorimetric and geochemical study of the coloration factor of hyper-acid active crater lakes. Japanese J. Limnol., 64 : 1 - 10.

[2] It is said that there are about 28 active crater lakes in the world. ; Takano, B. (2001) Geoscience of Active Crater Lakes. J. Balneol. Soc. Japan, 50 : 161 - 182.

[3] e.g., Ohsawa, S., Takano, B., Kusakabe, M., Watanuki, K. (1993) Variation in Volcanic Activity of Kusatsu-Shirane Volcano as Inferred from $\delta^{34}S$ in Sulfate from the Yugama Crater Lake. Bull. Volcanol. Soc. Japan, 38 : 95-99.

Along-arc variations of trace element compositions from Quaternary volcanic rocks in Kyushu-arc, Japan

Tomoyuki SHIBATA, Masako Yoshikawa** and **Keiji Takemura

Quaternary volcanoes are linearly arranged in Kyushu, Japan, forming a clear volcanic front (Fig.1). In this region, Philippines sea plate is subducting to same direction from 2Ma to present (Kamata, 2002). The northeastern and southern extensions of the volcanic chain are Southwestern Japan and Ryukyu arc, respectively. Adakites, which are thought to be generated from a partial melts of subducting slab, are widely distributed in Southwestern Japan arc (e.g. Morris, 1995). On the other hand, it is observed that chemical characteristics of Quaternary volcanics are gradually changed from southern Kyushu to Ryukyu Islands Shinjo et al., 2000). Accordingly, we can point out a possibility that the along arc variations of chemical characteristics are observed from arc volcanics distributed in Kyushu Island. The along arc variations must be caused by differences of mechanism of material transfer form subducting slab, chemical characteristics of the mantle wedge and constituents of crustal materials. Therefore, we compiled trace element compositions of Quaternary volcanics from Kyushu.

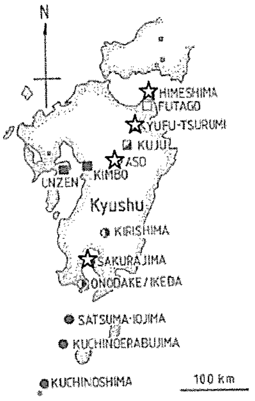

Fig. 1 Distribution of Quaternary volcanoes modified from Nakata (1986). Star shows volcanoes, of which trace element compositions were compiled in this report.

The results of compilations are shown in Fig 2. Most of the Sr/Y ratios and Y contents of Hime-Shima show high and low values, respectively. The Sr/Y ratios and Y contents increase toward the south. This might be suggested that mechanism of material transfer (dehydration or partial melting) from subducting Philippines Sea plate to mantle wedge changes at northern and southern part of Kyushu. The relationship between Nb and Zr concentrations are shown in Fig.1b. The Zr/Nb ratios are increasing from north to south, except for those of Hime-Shima. Ratio of Zr/Nb is nearly constant during magmatic processes so that the observed change of the Zr/Nb ratio may indicates that the chemical characteristics of mantle wedge below Kyushu changes with along arc direction.

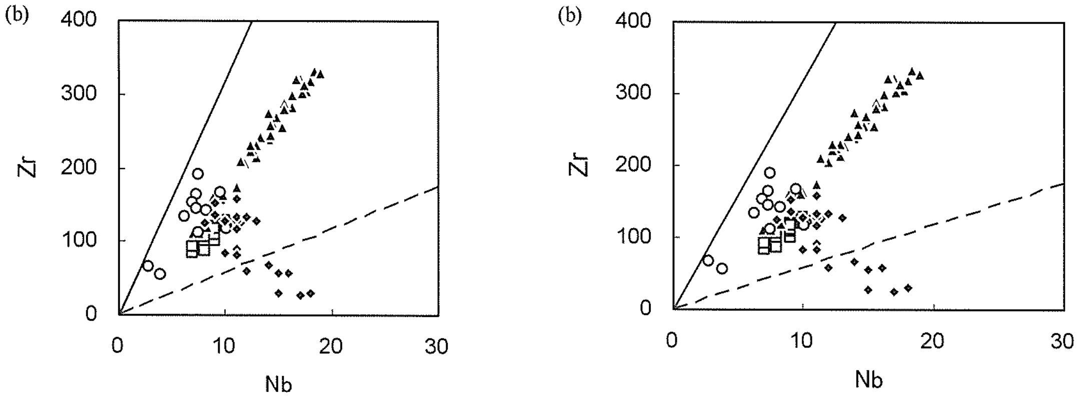

Fig. 1. The compiled data of trace element compositions of Quaterny volcanics from Kyushu along the volcanic front. (a) corrlation between Y concentrations and Sr/Y ratios. (b) corrlation between Nb and Zr concentrations. Legends are as follows, solid diamond: Hime-Shima; open square: Tsurumi-dake and Yufu-dake; solid triangle: Aso; open circle: Aira. The solid and dashed lines in (a) indicate a fields of adakite and general arc magma, respectively. Those lines in (b) represent averaged trend of MORB and OIB, respectively. Data are from Ito et al. (1997), Hunter (1998), Ohta et al. (1990), and Arakawa et al. (1998)..

Characteristics of tephra erupted from large calderas in Kyushu recorded in Lake Biwa sequence

Keiji Takemura, *Chan-Hwa Chen*[1], *Tom, Kwe-Gi Fung*[2] , ***Tomoyuki Shibata***, ***Takeshi Nakagawa*** *and Tohru Danhara*[3]

1. Institute of Earth Sciences, Academia Sinica, Taipei, Taiwan
2. Institute of Geosciences, National Taiwan University
3. Kyoto Fission-Track Co., Ltd, Japan

There are large calderas located in Kyushu, from which tephras were erupted and transported by mainly westerly wind system and preserved in Japanese island and ocean areas. Lake Biwa located in central Japan is one of the good and important reservoirs for the recorder of those tephra. The Lake Biwa has at least 910m thick sediments, which were deposited in lacustrine or fluvial environments in the Quaternary. The upper most unit is a continuous and massive sequence of lacustrine clay with thickness of 250 m and the age of at least 430 thousand years (Meyers et al., 1993; Takemura, 1990), and the most important reservoir of wide-spread tephras. We have rechecked tephras in the Lake Biwa on the physical appearance, mineralogy, refractive index and chemical composition of glass and correlate the tephras with those in the large calderas in Kyushu (Aso, Kakuto, Aira, Ata and Kikai Caldera) based on the preliminary data.

1. Physical appearance, mineralogy and refractive index of tephras

58 samples were collected for the tephra analysis. Some characteristic tephras related to wide-spread tephra are listed below.

No. B3-3 (ca. 10.3m depth) is intercalated as a lens in slime, and is composed of mainly bubble wall type of glasses with brown glasses. The glass has refractive index ranging from 1.508 to 1.514 (mode: 1.511). This tephra is correlated to wide spread one (K-Ah tephra) from Kikai Caldera. No. B15-2 (ca 27.2m depth) found in slime clay is composed of mainly bubble wall type of glasses with refractive index of 1.498 – 1.501 (mode: 1.500) and correlated to AT tephra came from Aira Caldera of south Kyushu. No. B43-1 (66.83 – 66.88 m depth) has bubble wall and pumice types of glasses with crystals of two kinds of pyroxenes and green hornblende. Refractive index of glass ranges from 1.506 to 1.514 (mode: 1.508 and 1.512). This is correlated to Aso-4 tephra erupted from Aso caldera. No. B45-3 at about 70.5 m depth was found as a lens in slime mud, containing quartz grains as light minerals. Glasses are composed of bubble-wall and pumice types. The mode value of refractive index for three-fourth of the glasses is 1.508. The sample must be included grains from K-Tz tephra at Kikai Caldera. No. B53-3 (74.56 – 74.58 m depth) is glassy ash containing heavy minerals composed mainly of Opx. Glasses are composed of bubble-wall and pumice types. Refractive index of glasses ranges from 1.510 to 1.512 (mode: 1.511). This ash is correlated with Ata tephra from Ata caldera. No. B186CC (ca.170.74m depth) has thin bubble-wall type of glasses with brown glasses. Refractive index of glasses ranges from 1.519 to 1.521 (mode: 1.520 – 1.521). This tephra is correlated to Aso-1 tephra from Aso caldera. No.236CC (207.74 m depth) is vitric ash, and is composed mainly of bubble wall-type of glasses with refractive index ranging from 1.500 to 1.503 (mode: 1.502). This tephra is correlated to Kkt tephra from Kakuto Caldera.

2. Chemical composition of glasses and correlation to wide spread tephra from Kyushu

The total 18-tephra layers were sampled from the upper 640 m part of the Lake Biwa 1400 m core drilled in 1982 for chemical analysis. The chemical analyses of pure glass shards picked up under microscope have been done by the electron microprobe in the IES, AS. Correlation between tephras in the core and those in the calderas can be depicted by the plots of K_2O vs. SiO_2 concentrations (Fig.1 and 2). The tephra derived from Ulreung-Oki with higher K_2O and lower SiO_2 can be clearly identified in Tephra Layer 2 at the 13.5 m depth. The Tephra Layer 4 at the 66.85 m depth and Tephra Layer 10 and 11 at around 169.2 – 170.9 m depth with relatively higher K_2O and lower SiO_2 are consistent with those of Aso-4 and Aso-1, respectively. Moreover, it is notable that the K_2O contents of tephra glasses from the Hohi and Kakuto areas are higher than 4 wt %, which do not vary with time. This phenomenon will offer an important criterion to distinguish the tephra sources from central Kyushu. Therefore, the results highly indicate that the source of Layer 19 (635.1 m depth) was suggested from the Hohi area. In the Fig. 2, other tephra layers belonged to calc-alkaline series, scatter in the areas of eruptions from southwestern Kyushu and Daisen area. The advanced isotopic studies shall significantly help distinguishing sources of these tephra layers. However, the studies of mineral assemblages and particle sizes of tephra layers are also needed for understanding the tephra sources and paleo-wind systems.

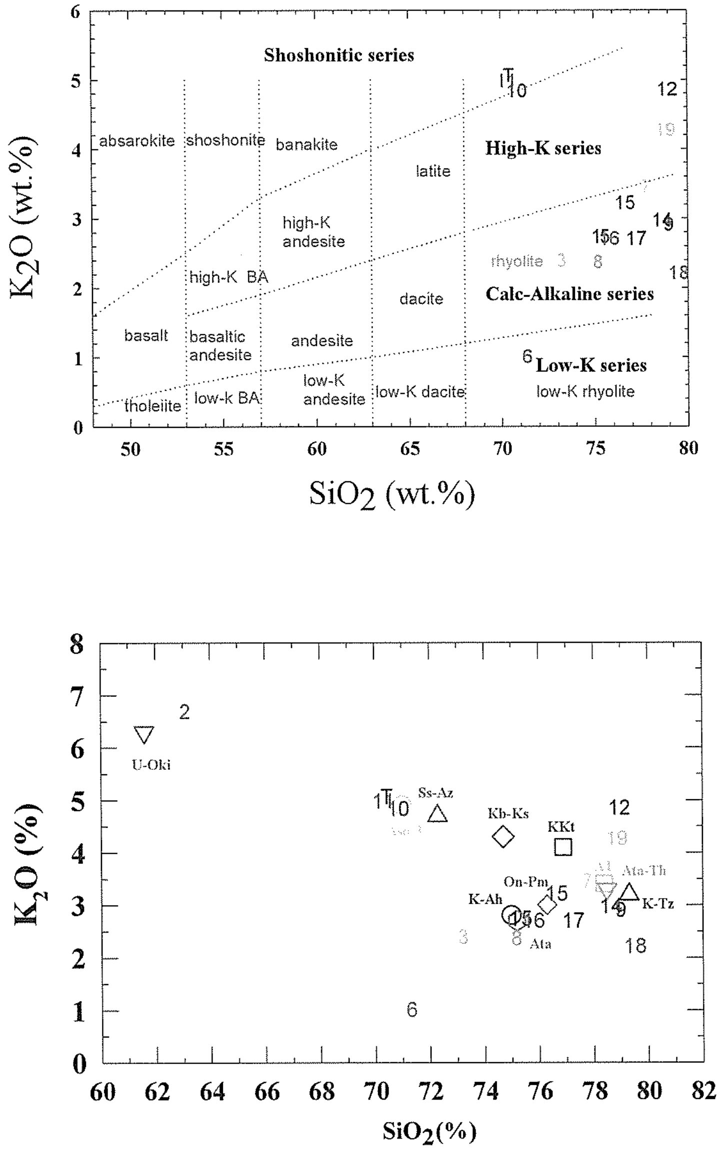

Fig.1 (upper) and Fig. 2 (lower), The K_2O vs. SiO_2 contents of glass shards in tephra layers collected from Lake Biwa 1400 m core.

The numerical sequence represents tephra layers in the core from top to bottom. The open symbols with names indicated the data of the selected Japanese tephra deposits (data from Machida, 1999).

Detection of seawater intrusion into thermal groundwater using strontium isotopes: A case study in Beppu hydrothermal system, Japan

Yuki Yusa, Tomoyuki Shibata and Masako Yoshikawa

At the southeastern coastal area of Beppu hydrothermal field, Japan, Kikkawa and Kitaoka (1977) defined the zone of seawater intrusion into thermal groundwater, in which the chloride concentration is over 500ppm, and showed a spreading tendency of the zone by compiling chloride concentration data obtained by repeated surveys from 1926 to 1976. However their definition is convenient only in this area. The effectiveness of stable isotopes of Sr (^{87}Sr/^{86}Sr ratios) has been proved in the study of surface- and ground-water systems (Satou and Nakano, 1994; Yusuhara et al., 1999). As the Sr isotopes hardly fractionate in nature unlike the stable isotopes of O and H, it is expected that ^{87}Sr/^{86}Sr will be a surpassing tracer in the identification of saline sources and waters (Barbieri and Morotti, 2003). This abstract treats validity of ^{87}Sr/^{86}Sr as an index for seawater intrusion into thermal groundwater and the subsequent change in the zone of seawater intrusion at the southeastern coastal area of Beppu.

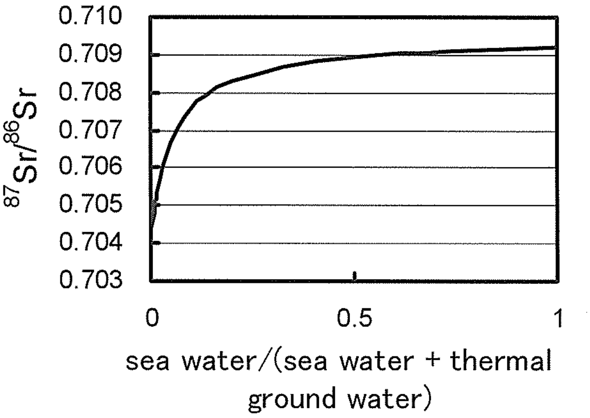

Fig. 1. 87Sr/86Sr of thermal groundwater for various mixing rates of seawater and original thermal groundwater in Beppu.

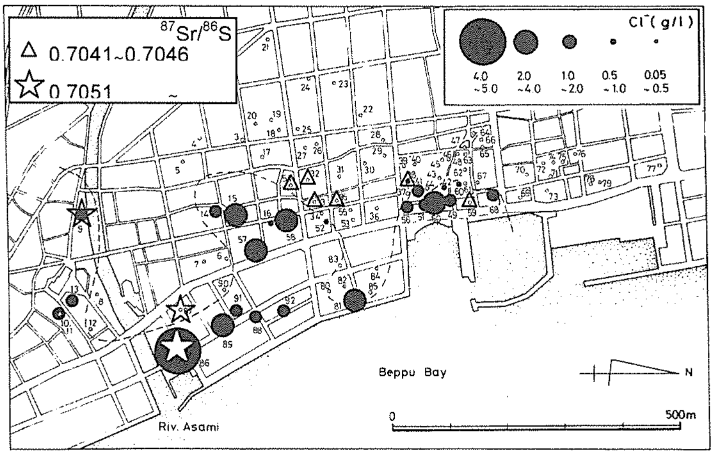

Fig. 2. Distribution of ^{87}Sr/^{86}Sr compared with the zone of seawater intrusion in 1976 shown by Kikkawa and Kitaoka (1977)

The values of ^{87}Sr/^{86}Sr in 10 water samples from the present area ranges from 0.7041 to

0.7054. The lowest value is almost the same as that of the formation (Notsu et al., 1990) through which thermal groundwater flows. Assuming the lowest value is that of the original thermal groundwater, thermal waters having ^{87}Sr/^{86}Sr over 0.7050 can be produced by 1.3% or more mixing of seawater (Fig. 1). This sensitiveness shows that ^{87}Sr/^{86}Sr is a powerful index for the seawater intrusion into groundwater. The distribution of ^{87}Sr/^{86}Sr in present water samples matches the zone of seawater intrusion in 1976, which indicates that the zone of seawater intrusion did not spread in the last 30 years (Fig. 2).

研究報告 Scientific Reports

Climatic and environmental changes at southeastern coast of Lake Biwa over past 3000 years, inferred from borehole temperature data

Shusaku Goto, *Hideki Hamamoto**, Makoto Yamano*
*Earthquake Research Institute, University of Tokyo

An effect of temperature change at the earth's surface propagates into the underground and disturbs the underground temperature structure that is determined by the thermal conductivity distribution and heat flow from the deep. Analyzing disturbances in the underground temperature structure carefully, the past ground surface temperature change closely related to the past climate change can be reconstructed. Reconstruction of the ground surface temperature history from borehole temperature data has been performed over the world and provided information on regional and global past climatic changes (e.g. Wang, 1992; Huang et al., 2000; Harris and Chapman, 2001).

In order to infer past climatic change in central Japan, we repeatedly measured temperatures in a borehole at the Karasuma site on the southeastern coast of Lake Biwa and reconstructed the sediment surface temperature history during the last 3000 years from the temperature profiles. The reconstructed temperature history shows Medieval Warm Period (Broecker, 2001), Little Ice Age (Overpeck et al., 1997; Mann et al., 1999), and contemporary temperature warming (Fugure 1). The pattern of the change in the past sediment surface temperature at the Karasuma site is consistent with that of the proxy temperatures estimated from δ^{13}C variation of Japanese cedars during the last 2000 years in Yakushima Island, southern Japan (Kitagawa and Matsumoto, 1995). However, the amplitude of the past sediment surface temperature change at the Karasuma site is significantly larger than that of proxy temperature change in Yakushima Island. Based on temporal change in the height of the archaeological sites, Hama (1994) suggested that the water level of Lake Biwa rose in the late 12th century A.D., corresponding to the beginning of the decrease in the sediment surface temperature in the late 12th century. Furthermore, timings of two destructive earthquakes (1185 A.D. and 1662 A.D., Usami (1966)) that caused water level changes of Lake Biwa correspond to the beginnings of changes in the sediment surface temperature, suggesting that the reconstructed sediment surface temperature history reflects environmental changes due to tectonically induced water level changes of the lake. Comparison of contemporary temperatures of the air and ground surface measured by Lake Biwa Museum, Shiga Prefecture, and lake bottom in shallow depth measured by Center for Ecological Research, Kyoto University indicates that the mean temperature of lake bottom in shallow depth is 1 K higher than that of air temperature and 1 K lower than that of ground surface temperature. Applying these relations to the suggested environmental changes, the pattern and amplitude of past air temperature change at the Karasuma site agree with those of the change in proxy temperature in Yakushima Island. Thus, we suggest that the sediment surface temperature history reconstructed from the Karasuma borehole temperature data reflects the past climate change but is biased by environmental changes due to tectonically induced past water level changes of Lake Biwa.

References

Broecker, W.S., 2001. Was the Medieval Warm Period global?, Science 291, 1497-1499.

Hama, O., 1994. Off shore sites of Lake Biwa and the distribution of ancient villages. Research Report of the Lake Biwa Museum Project Office 2, 97-110 (in Japanese.)

Harris, R.N., Chapman, D.S., 2001. Mid-latitude (30°-60°N) climatic warming inferred by combining borehole temperatures with surface air temperatures. Geophys. Res. Lett. 28, 747-750.

Huang, S., Pollack, H.N., Shen, P.-Y., 2000. Temperature trends over the past five centuries reconstructed from borehole temperatures. Nature 403, 756-758.

Kitagawa, H., and Matsumoto, E., 1995. Climatic implications of δ^{13}C variations in a Japanese cedar (*Cryptomeria japonica*) during the last two millenia. Geophys, Res. Lett. 22, 2155-2158.

Mann, E.M., Bradley, R.S., Hughes, M.K., 1999. Northern hemisphere temperatures during the past Millennium: inferences, uncertainties, and limitations. Geophys. Res. Lett. 26, 759-762.

Overpeck, J., Hughen, K., Hardy, D., Bradley, R., Case, R., Douglas, M., Finney, B., Gajewski, K., Jacoby, G., Jennings, A., Lamoureux, S., Lasca, A., MacDonald, G., Moore, J., Retelle, M., Smith, S., Wolfe, A., Zielinski, G., 1997. Arctic Environmental change of the last four centuries. Science 278, 1251-1256.

Usami, T., 1966. Descriptive table of major earthquakes in and near Japan which were accompanied by Damages. Bull. Earthq. Res. Inst. 44, 1571-1622 (in Japanese, with English Abstr.)

Wang, K., 1992. Estimation of ground surface temperatures from borehole temperature data. J. Geophys. Res. 97, 2095-2106.

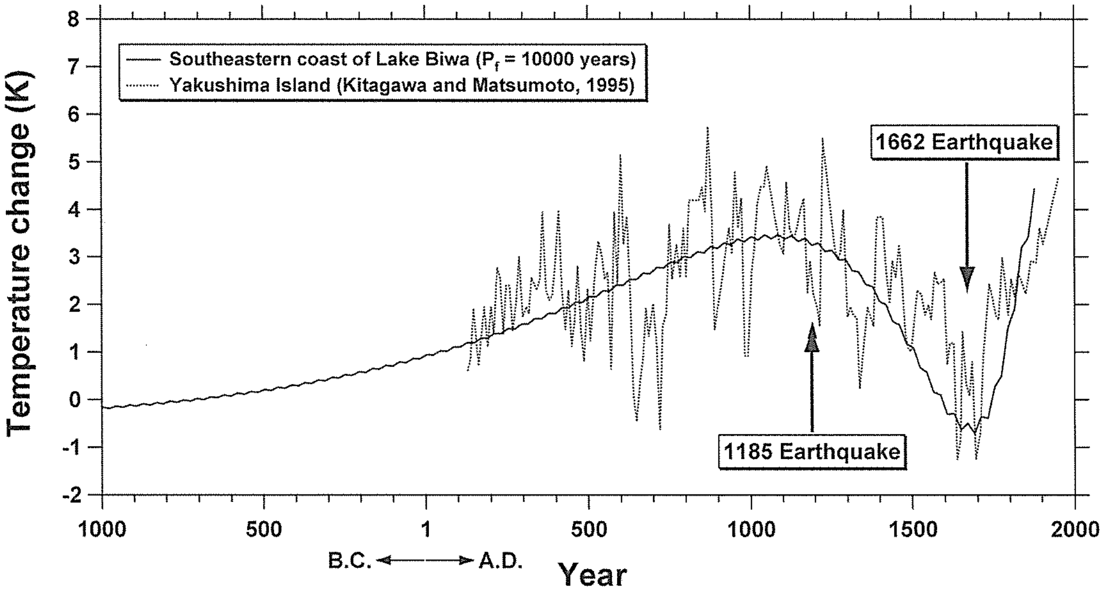

Figure 1 Sediment surface temperature history at southeastern coast of Lake Biwa over past 3000 years. For comparison, proxy temperature change estimated from $\delta^{13}C$ variation of Japanese cedars in Yakushima Island, southern Japan (Kitagawa and Matsumoto, 1995) is also plotted. Timings of the 1185 and 1662 earthquakes are indicated.

A model of subsurface water flow estimated from a self-potential profile on Mt. Kishimadake, Aso volcano

H. Hase

Mt. Kishimadake is one of the youngest cones among Aso caldera that is mainly composed of scoria and lava of 2,000 to 3,000 yeas old. The volcano has a summit crater with about 200 m in diameter. The height difference between the summit rim and the crater bottom is 50 m. The volcano also has a large flanking crater with a diameter of about 400 m on the east of the summit.

Figure 1(a) shows the measurement points of self-potential survey on Kishimadake. The SP is plotted against topographic elevation in Fig. 1(b). The SP-elevation diagram shows a negative correlation between them. However, there seems to be two separate trends which correspond to the areas within the summit crater and outer flanking areas. A negative correlation between SP and elevation is normally attributed to the streaming potential due to ground water flow from the summit to flanking areas. If the flow is continuous through the volcanic edifice, the SP-elevation trend should be aligned on a single line. I consider that the two separate trends are produced by the discontinuity of flow system due to an impermeable layer (strongly welded deposits) which probably lies beneath the summit crater. This impermeable layer is detected as a high electrical resistivity layer by the DC electric sounding (details are presented in another article of this issue).

To verify the above idea I performed numerical model calculations assuming that the areas where ground water permeates into the ground and flows out of the ground correspond to electric current sink and source, respectively. The calculation was performed by using the relaxation method with grid size of 61x61x40. I assumed concentric symmetries for the topography, resistivity structure and equivalent current sources with a rotation axis at the summit crater (See Fig. 2). Since I here assumed that water flow causing the streaming potential is separated by the impermeable layer, I again symmetrically emplaced two pairs of equivalent current sources and sinks in and out of the summit crater. Electrically neutral condition should be imposed for these pairs. Then I searched the positions and intensities of the equivalent sources and sinks which minimize the misfit between the potentials of the model and observations. The best fit model gives the currents of 50 mA and 250 mA for inner and outer current pairs, respectively.

Figure 3(a) compares the observed and modeled SP profile plotted against the distance from the center of the summit crater. The SP-elevation diagram is also presented in Fig. 3(b). These two plots well explain the real SP profile and support the validity of the hypothesis above.

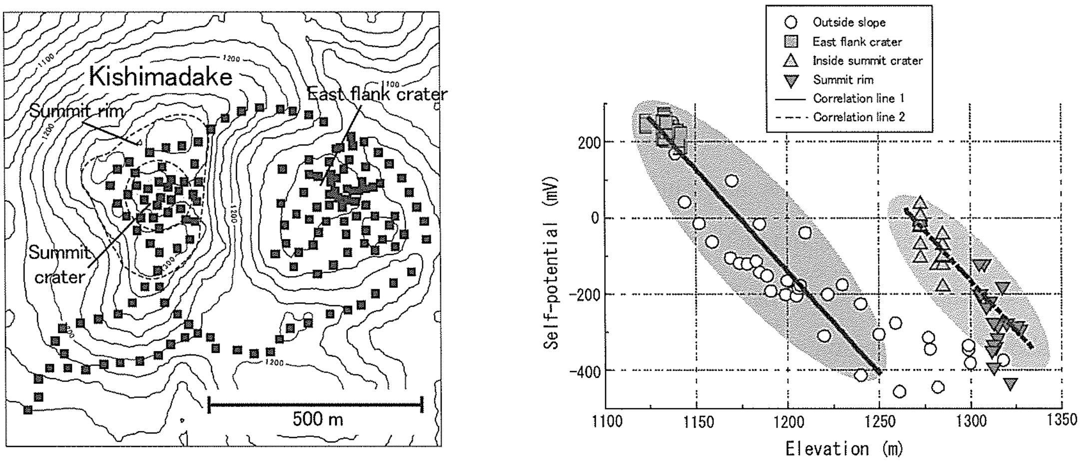

(a) (b)

Figure 1. (a) Measurement points of SP on Mt. Kishimadake. (b) SP plotted against topographic elevation.

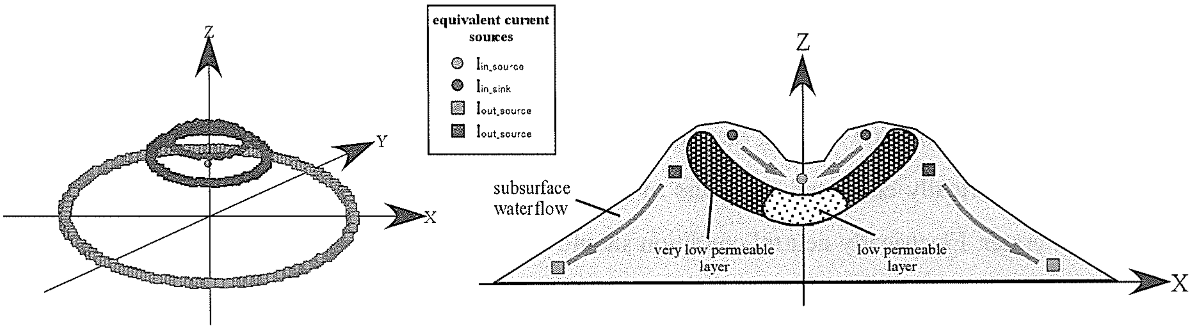

(a) **(b)**

Figure 2. Schematic images of (a) equivalent current sources and sinks in the numerical calculations and (b) hypothetic ground water flow causing the equivalent currents.

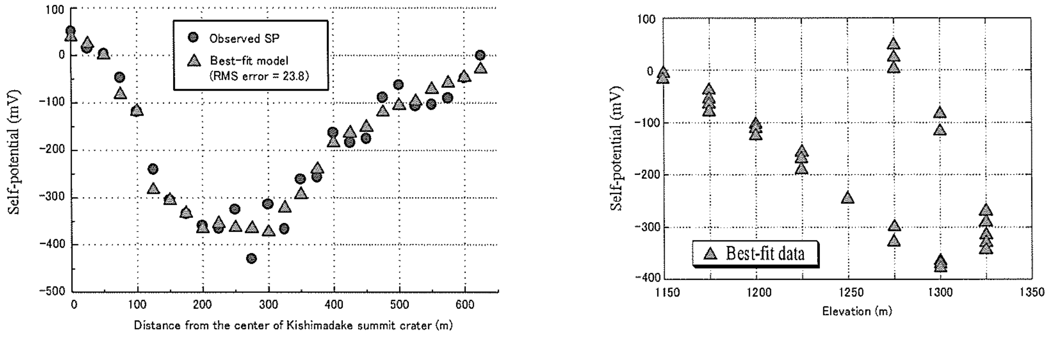

(a) (b)

Figure 3. (a) Comparison between observed and modeled SP profile plotted against the distance from the center of the summit crater. (b) Modeled SP plotted against the topographic elevation.

DC electric exploration on Mt. Kishimadake, Aso volcano

H. Hase, M. Utsugi, *T. Hashimoto*,* ***S. Yoshikawa*** *and* ***M. Nakaboh***

*Institute for Seismology and Volcanology, Graduate School of Science, Hokkaido Univ.

The occurrence of streaming potential is controlled by the ground water its flow volume and pattern, which is strongly influenced by subsurface structural variation around there. Therefore, it is important to know the subsurface structure for interpreting self-potential data.

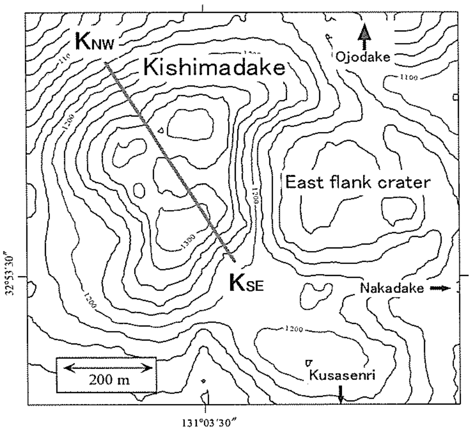

Figure 1. Location map of electric exploration line in the summit area of Mt. Kishimadake.

One of the authors (H. Hase) conducted a self-potential survey on Mt. Kishimadake and found two separate trends of topographic effect which correspond to the area within the summit crater and outer flank areas (details are presented in another article of this issue). We inferred that the characteristic self-potential profile is formed by structural variation on the summit area of the volcano.

We conducted DC electric exploration (Wenner and Eltran methods) over the summit crater of Kishimadake, one of the central cones of Aso volcano (Fig. 1). The length of the survey line is 600 m and electrodes interval is 10 m. 2-D resistivity structure around the summit of Kishimadake was inverted from measured apparent resistivity using ABIC-minimizing deconvolution method (Fig. 2). The resistivity structure shows a roughly symmetric pattern in vertical cross-section from the center of the crater. A low-resistive layer, less than 1k □m, is located under the summit crater to the depth of 50 m (A). On the contrary, high-resistive layer is located just below the crater rim (B). The maximum resistivity of this layer exceeds over 10km.

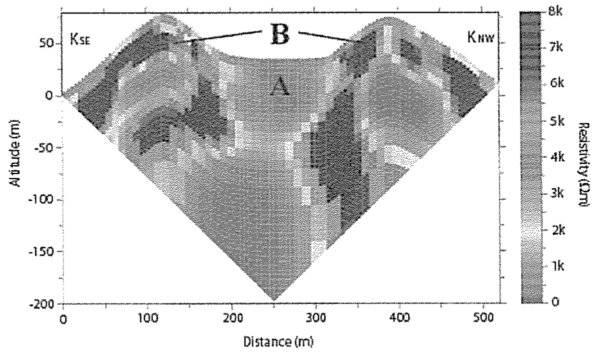

Figure 2. Two-dimensional inversion resistivity model in the summit area of Mt. Kishimadake

Basement configuration of Yamashina Basin inferred from gravity survey

INOUE (KITADA), N.**, Doshida, S. (DPRI) and **TAKEMURA, K.

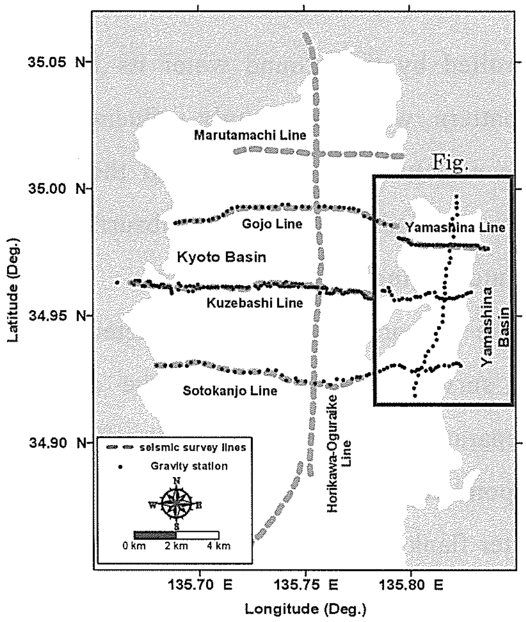

Fig. 1. Location map of gravity stations and seismic survey lines. Broken lines and solid circles in figure indicate the seismic survey lines and gravity stations, respectively.

From 1998 to 2003, the Kyoto City has been conducted various subsurface surveys for the estimation of seismic hazards. The seismic refraction and reflection surveys reveal the framework of subsurface structure of the Kyoto and Yamashina Basins (Fig. 1). The geophysical data coverage is sparse in the Yamashina Basin. We carried out gravity analysis for the purpose of estimating the basement configuration of the Yamashina Basin. We conducted gravity survey with station interval of 100 – 300 m along the Gojo, Yamashina, and Sotokanjo seismic lines. The gravity data of Inoue et al. (2004) were adopted for Kuzebashi line. We extended the gravity measurement lines of the Kuzebashi and Sotokanjo lines to the Yamashina Basin. The N-S gravity measurement was carried out with station interval of 500m. The 195 gravity data were obtained from Nov. 2003 to Jan. 2004. The reduction density 2.65 g/cm^3 was applied by reference to the analysis of the Kyoto City. The basement configuration was derived by two-layer analysis constrained with the results of the seismic surveys. The N-S basement configuration was obtained based on the E-W results. Density contrast 0.5 g/cm^3 between the basement and overlaying deposits was decided by calculating in several density contrasts. Fig. 2 indicates the basement configuration of the Yamashina Basin. The basement configuration relief gently tilts towards to the south. Depth to the in the central part of the Yamashina Basin, where the basin is narrow, is shallow.

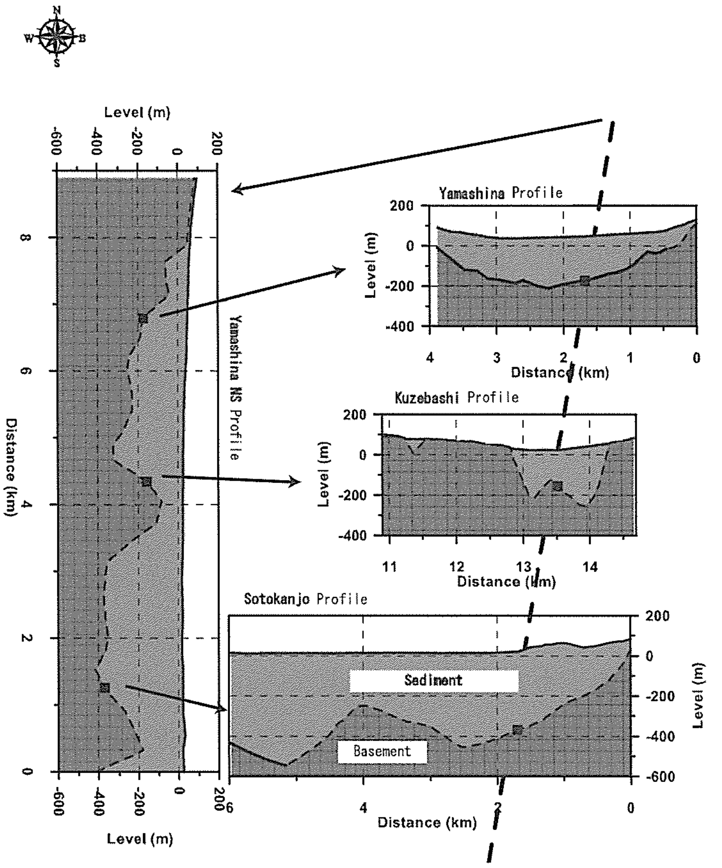

Fig. 2. Basement configuration of the Yamashina Basin. Density contrast is 0.5 g/cm^3. Solid line is the top of the basement obtained from the Yamashina seismic survey line. Broken line indicates the top surface of the basement inferred from the gravity analysis. Solid squares in figure indicate the control point of the basement.

References

Inoue, N., Tanaka, Y. Itoh, H., Iwano, S., Kitada, N. Fukuda, Y. and Takemura, K., 2004, Density of Sediment in Kyoto Basin Inferred from 2D Gravity Analysis

along Horikawa-Oguraike and Kuzebashi Seismic Survey Lines, Zishin 2, 57, in press.

Underground structure of Yufu Basin inferred from 2D gravity analysis

INOUE (KITADA), N., TAKEMURA, K. and YUSA, Y.

The Yufu Basin is located in the southwestern Yufu – Tsurumi graben. The seismic reflection survey was carried out in order to reveal the underground structure in the Yufu Basin (Yusa et al., 1995). The gravity measurement (Fig. 1) also was conducted along the seismic survey line (Fukuda et al., 1995, Kusumoto et al, 1996). We analyzed the gravity data reported by Fukuda et al. (1995). The reduction density 2.30 g/cm^3 was decided by the correlation method in which an optimum density is adopted when Bouguer anomaly least correlates with topography.

Fig. 1. Gravity station map. Solid circles in figure indicate the gravity measurement stations.

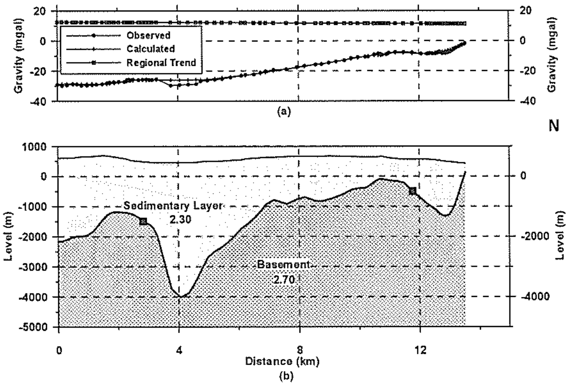

Fig. 2. Two-layered model of Yufu basin. (a) Gravity anomaly. (b) Density structure. Numerical values in figure indicate the density in g/cm^3. Solid squares in figure indicate the control point of the basement.

We constructed the two-layer model of the Yufu Basin. The control point of the basement and density contrast were refereed from the report of NEDO (1989) and Kusumoto et al. (1996). The difference between observed and calculated gravity anomalies exceeds few mgals around the Yufu Basin in the two-layer model (Fig. 2). This difference corresponds to subsurface low density materials in the Yufu Basin. The result of seismic reflection survey indicates the low velocity surface layer. We attempted to construct the multi-layer model considering subsurface low density layer. The boundaries of multi-layer were iteratively revised to improve the difference between observed and calculated gravity anomalies. The initial levels of boundaries (low density and basement) were 400 and -1000m, respectively. Fig.3 indicates the result of multi-layer analysis. The low density layer corresponds to the low velocity layer of the seismic profiles and the Yufu Basin. The basement relief, between the Yufuin and Beppu-kita faults, tilts to the south.

References

Kusumoto, S., Fukuda, Y., Takemoto, S. and Yusa, Y., 1996, Three-dimensional subsurface structure in the eastern part of the Beppu-Shimabara Graben, Kyushu, Japan, as revealed by Gravimetric Data, J. Geod. Soc. Jpn., 42, 167-181.

NEDO, 1989, Regional exploration of geothermal fluid circulation system, Report of Gravity Survey, Tsurumi area. National Geothermal Resources Exploration Project, New Energy Development Organization, Tokyo. pp98.

Yusa, Y., Fukuda, Y., Kitaoka, K., Ohsawa, S., Ikawa, T. and Abe, S., 1995, Seismic reflection survey in Yufu Basin, 1995 Japan Earth and Planetary Science Joint Meeting, Abstract, 61.

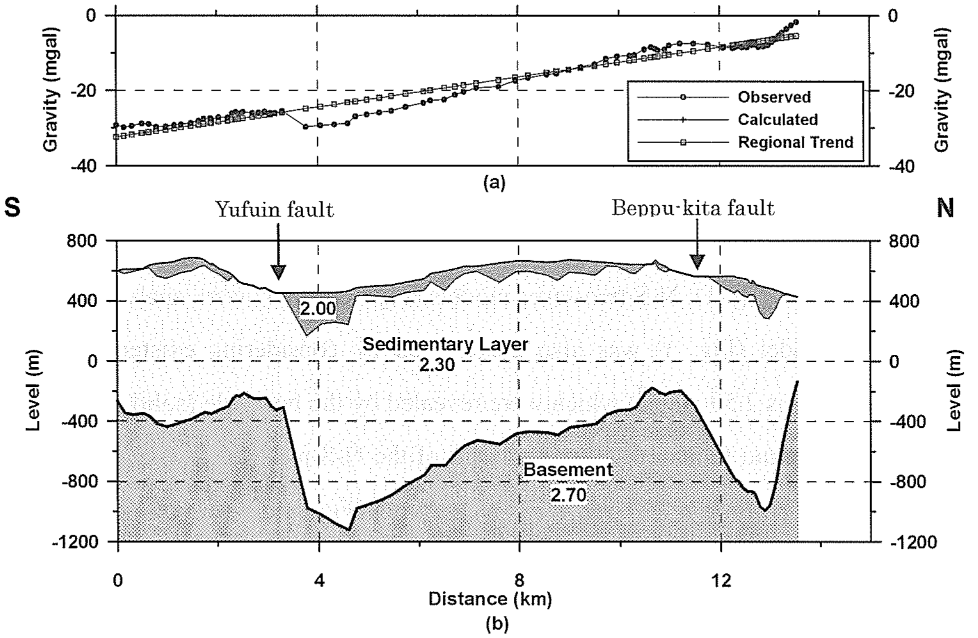

Fig. 3. Multi-layered model of Yufu basin. (a) Gravity anomaly. (b) Density structure. Numerical values in figure indicate the density in g/cm^3.

Underground structure of Shimabara Peninsula inferred from 2D gravity analysis

INOUE (KITADA), N. and TAKEMURA, K.

The Unzen Scientific Drilling Project (USDP) investigates the subsurface structure, geological history and physical property around the Unzen volcano in the eastern part of the Shimabara Peninsula. The acquired various and significant information provides the detailed geological longitudinal section around the Unzen (Hoshizumi et al., 2002). On the contrary, the New Energy Development Organization (NEDO) have been conducted various survey for the geothermal filed research project in the western part of the Shimabara Peninsula and suggested the underground structure model (NEDO, 1984). Based on the subsurface model of the western part of the Shimabara Peninsula, we inferred the N-S subsurface structure around Unzen volcano to compare with the result of USDP. The gravity data around Unzen volcano were adopted from the gravity CD-ROM published by the Geological Survey of Japan (GSJ, 2000).

We constructed two-layer model (basement and overlaying layer) in consideration of the previous geological and geophysical works (NDEO, 1984). The basement corresponds to the Paleogene deposits. The outcrop or borehole information about distribution of the Paleogene deposits is sparse in the study area (open triangle in Fig. 1). The overlaying layer of the model consisted of the Unsen volcano products and the Neogene - Quaternary deposits. Based on the previous study, the density of the basement and overlaying layer were decided 2.50 and 2.30 g/cm^3, respectively. The top surface of the basement was iteratively adjusted to improve the difference between the observed and calculated gravity anomalies. The E-W two-layer models were obtained constrained with the basement constrain (open triangles in Fig. 1). Based on the result of E-W models (solid squares in Fig. 1), N-S two-layer models (Figs. 2 and 4) were analyzed. The western N-S multi-layered model (Fig. 3) was also constructed by considering existence high density volcanic rocks (density is 2.50 g/cm^3) which were revealed by the borehole (solid circles in Fig. 1). The basement relief around faults in the western part of the N-S profiles (Figs. 2 and 3) is steeper than that of the eastern part (Fig. 4). The eastern N-S profile (Fig. 4) suggests high density material under the Mt. Fugen.

References

Geological Society of Japan, 2000, Gravity CD-ROM of Japan, Digital Geoscience Map Series, P-1.

Hosizumi, H., Uto, K., Matsumoto, A., Xu, S. and Oguri, K., 2002 Geology of Unzen volcano and core stratigraphy of the flank drillings, Unzen Workshop 2002, 4-8.

NEDO, 1984, Regional exploration of geothermal fluid circulation system, Western Unzen area. National Geothermal Resources Exploration Project, New Energy Development Organization, Tokyo. pp1060.

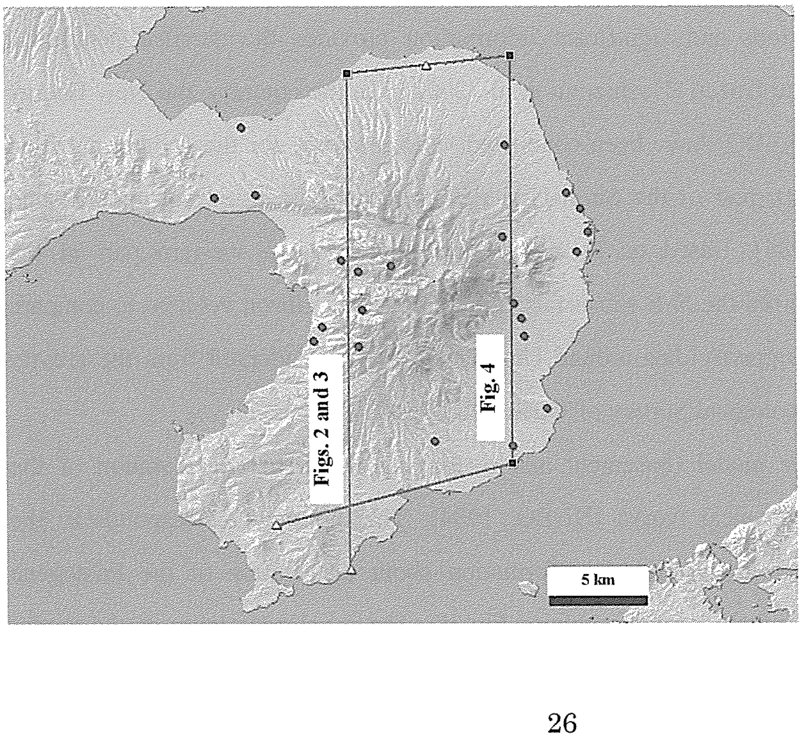

Fig. 1. Index map of the Shimabara Peninsula. Open triangles, solid squares and solid circles in figure indicate the outcrop or obtained the depth of the Paleogene deposit, basement constrains derived from gravity analysis and boreholes, respectively.

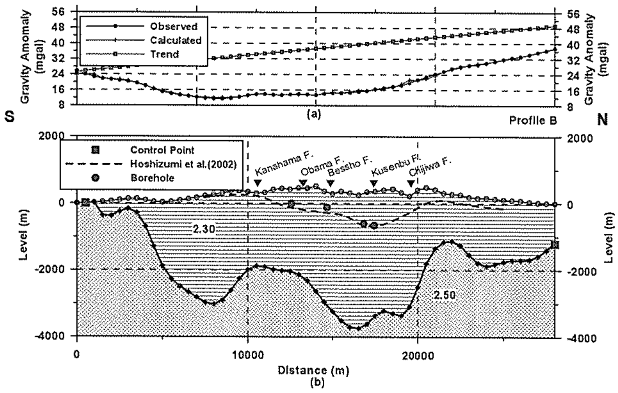

Fig. 2. Two-layer western N-S profile. (a) Gravity anomaly. (b) Density structure. Broken line in figure and solid circle indicate the basement of Unzen volcano deposit (Hoshizumi et al., 2002) and location of borehole, respectively. Numerical values in figure indicate the density in g/cm³.

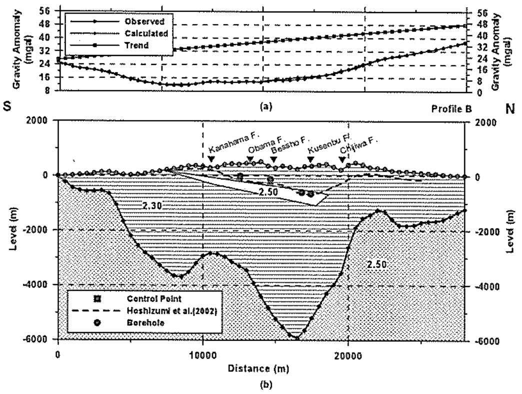

Fig. 3. Multi-layer western N-S profile. (a) Gravity anomaly. (b) Density structure. Broken line in figure and solid circle indicate the basement of Unzen volcano deposit (Hoshizumi et al., 2002) and location of borehole, respectively. Numerical values in figure indicate the density in g/cm³.

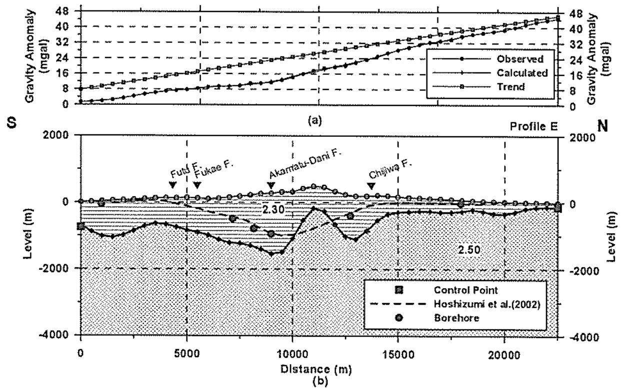

Fig. 4. Two-layer eastern N-S profile. (a) Gravity anomaly. (b) Density structure. Broken line in figure and solid circle indicate the basement of Unzen volcano deposit (Hoshizumi et al., 2002) and location of borehole, respectively. Numerical values in figure indicate the density in g/cm³.

Hydrous phase stability and partial melt chemistry of H_2O-saturated KLB-1 peridotite up to the uppermost lower mantle conditions

Kawamoto, T.

Stability of hydrous phases and partial melt chemistry in 13.6 wt. percent H_2O bearing mantle peridotite are reported in a pressure range up to 24 GPa and a temperature range from 900 to 1400 °C. Various hydrous phases like phase E, phase D, superhydrous B, hydrous wadsleyite and ringwoodite are observed between 14 and 24 GPa. The phase boundary between wadsleyite and ringwoodite under hydrous conditions is found to be at higher pressure than under the dry conditions. The H_2O-undersaturated solidus temperature of a model mantle is estimated up to 11 GPa based on (1) the reported solubility of H in nominally anhydrous minerals and (2) linearity of H_2O-undersaturated solidus between the dry and wet solidus (Kawamoto and Holloway, 1997) with respect to H_2O abundance at a constant pressure.

Under H_2O-saturated conditions at pressures greater than 10 GPa, the (Mg+Fe)/Si atomic ratios of partial melts decrease with increasing temperature: from 2.5 at 1100 °C to 1.6 at 1300 °C at 14 GPa, from 3.3 at 1100 °C to 1.8 at 1300 °C at 17 GPa, and from 2.8 at 1200 °C to 1.7 at 1400 °C at 20 GPa. This is in contrast to the reported constant value of dry partial melts. A partial melt coexisting with Mg-perovskite at 24 GPa and 1400 °C has (Mg+Fe)/Si and Ca/Al atomic ratios of 2.2 and 11, respectively. Ultramafic hydrous melts similar to those observed experimentally under uppermost lower mantle conditions may have contributed to chemical differentiation between the upper and lower mantle. (Physics of Earth and Planetary Interior, 143-144, 387-395, 2004)

Critical phenomena between magmas and aqueous fluids

Kawamoto, T.

A series of direct observation of complete miscibility between aqueous fluids and the Fuji 1707 calc-alkaline andesite - rhyolite magmas has been conducted using Bassett's type externally heated diamond anvil cell (Figure). Supercritical behaviors are observed between aqueous fluids and andesitic (62 weight % SiO_2) or rhyolitic (69 % SiO_2) melts. The critical temperatures for the andesite and water (900 - 1000 °C at 1.2 - 0.5 GPa) are found to be higher than those for the

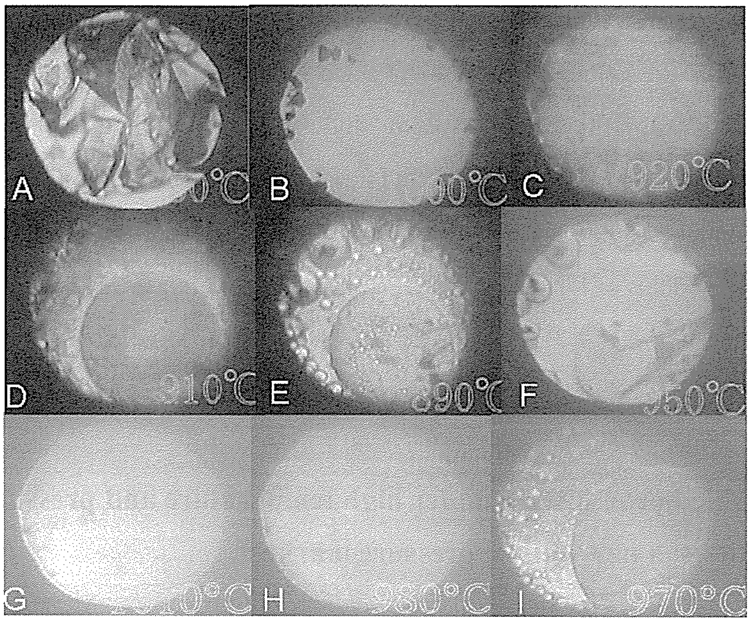

rhyolite and water (780 - 800 °C at 0.7 - 0.5 GPa). This suggests that more mafic magmas and the aqueous fluid have higher critical temperatures. Chemical fractionation between the andesitic melt and the aqueous fluid were observed: (1) Na_2O and K_2O preferentially enter into the aqueous fluid, (2) CaO, MgO and Al_2O_3 into silicate-rich melt, and (3) TiO_2, FeO, and SiO_2 are almost equally partitioned into them. Even if a second critical point between the aqueous fluids and silicate melts exists in the earth's mantle, such a supercritical fluid can be separated into a melt and a fluid eventually along its migration to the surface. Under such circumstances elemental fractionation between the aqueous fluid and the melt should control the chemical characteristics of volcanic rocks. (Review of High Pressure Science and Technology, in Japanese, August 2004, Rejected by Geochim. Cosmochim. Acta).

The compressibility of a natural apatite

Matsukage, K.N. (Ibaraki University), Ono, S. (JAMSTEC), ***Kawamoto, T.****, Kikegawa, T. (High Energy Accelerator Research Organization)*

Apatite is one of the accessory minerals but is commonly found in various kinds of crustal rocks, such as sedimentary, igneous and metamorphic rocks. It is an important reservoir of rare earth elements (REE) and large ion lithophile elements (LILE). Apatite also contains volatile elements (F, Cl, and OH) as major components. We determined the isothermal bulk modulus and its pressure derivative using diamond anvil cell under hydrostatic conditions and to understand the compressional properties of apatite.

In-situ synchrotron X-ray diffraction (XRD) experiments of a natural apatite with the formula of $Ca_5(PO_4)_3F_{0.94}Cl_{0.06}$ were carried out using a diamond anvil cell and angle-dispersive technique at Photon Factory (PF), Japan. Pressure-volume data were collected up to 7.12 GPa at 300K. The pressures were determined from the ruby fluorescence spectra shift. The unit-cell parameters and volume decreased systematically with increasing pressure, and a reliable isothermal bulk modulus and its pressure deviative were obtained in this study. The third order Birch-Murnaghan equation of state yielded the isothermal bulk modulus of $K_T = 91.5(38)$ GPa, its pressure derivative $K_T' = 4.0$ (11), and the zero-pressure volume $V_0 = 524.2(3)$ A^3. (Physics and Chemistry of Minerals. In press)

Raman spectroscopy of cubic boron nitride under high temperature and pressure conditions: a new optical pressure marker

Kawamoto T., *Matsukage, N. K. (Ibaraki University), Nagai, T. (Hokkaido University), Nishimura, K., Mataki, T., Ochiai, S. (ST Japan), Taniguchi, T. (Advanced Materials Laboratory, National Institute for Materials Science)*

Pressure dependence of Raman peaks of cubic boron nitride (cBN) is determined at 100, 200 and 300 °C using pressure scales of ruby and gold. In pressures lower than 6 GPa, the pressure dependences of cBN Raman determined with ruby pressure scale for transverse-optical (TO) and longitudinal-optical (LO) modes are 3.45 ± 0.02 and 3.36 ± 0.02 cm $^{-1}$/GPa at 100 °C and 3.43 ± 0.02 and 3.44 ± 0.07 cm $^{-1}$/GPa at 300 °C, respectively. These values are consistent with the

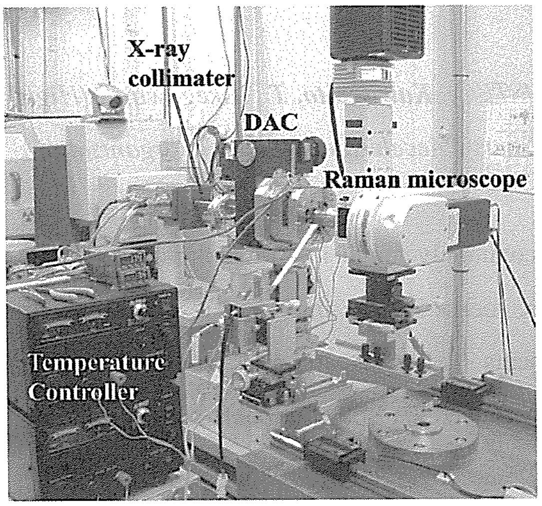

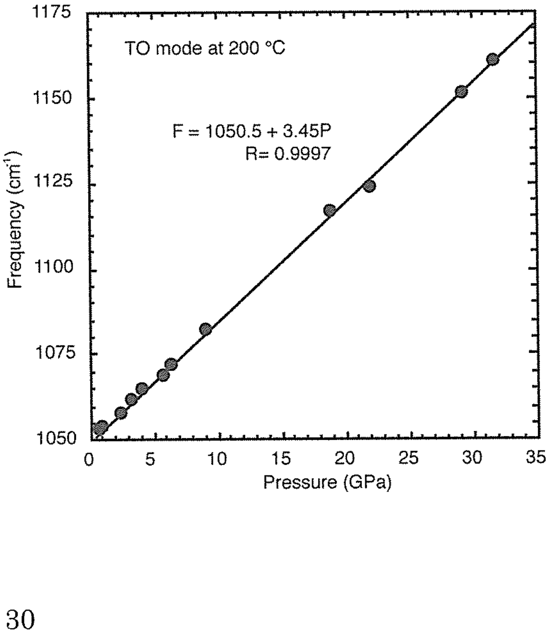

previous study conducted at room temperature using ruby pressure scale. Synchrotron X-ray diffraction experiments using gold pressure marker at SPring-8 (Photo) also yields 3.45 ± 0.03 cm $^{-1}$/ GPa for TO mode at 200 °C in a pressure range up to 32 GPa (Figure). Under the present pressure and temperature conditions, the pressure dependence of Raman peaks of cBN seems to be independent from temperature conditions. CBN can be used as an optical pressure marker under high temperature conditions. (Review of Scientific Instruments, 75, 2451-2454, 2004)

Changes in the structure of water deduced from the pressure dependence of the Raman OH frequency

Kawamoto, T.*, Ochiai, S. (ST Japan), Kagi, H. (University of Tokyo)*

We report on the Raman spectra of water under high temperature and pressure conditions and show a discontinuity in the pressure dependence of the OH stretching frequency. As pressure increases, the strength of hydrogen bonding increases rapidly in the pressure ranges up to 0.4 ± 0.1 GPa at 25 °C, 1.0 ± 0.1 GPa at 100 °C and 1.3 ± 0.1 GPa at 300 °C, and slowly above these pressures (Figure 1). This finding clearly demonstrates the existence of discontinuities in the pressure-response of the hydrogen bonds of water, which suggests a possible structural change under these conditions (Figure 2).

The present experimental data are limited to 300 °C. However, structural change of hot water, may occur at higher temperature conditions. In this case, the structural change should affect the chemical and physical properties of the aqueous fluid in the earth's subduction zones. The Mg/Si

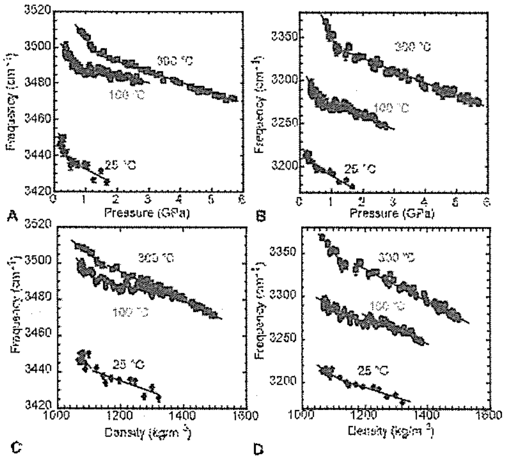

Figure 1

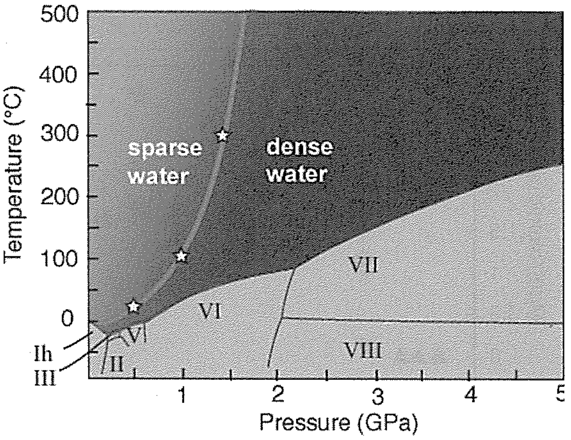

Figure 2

ratios of silicate component dissolved into aqueous fluid are found to change drastically from SiO_2-rich to MgO-rich at about 2 - 3 GPa and 1000 °C. Such changes may be explained by a structural change of water. (Journal of Chemical Physics (Communications section). 120, 5867-5870, 2004)

Mg/Si ratios of aqueous fluids coexisting with forsterite and enstatite based on the phase relations in the Mg_2SiO_4-SiO_2-H_2O system

Kawamoto, T., *Matsukage, K. N. (Ibaraki University), Mibe, K. (geophysical Laboratory), Nishimura, K., Isshiki, M. (JASRI, SPring-8), Ishimatsu, N. (Hiroshima University) and Ono, S. (JAMSTEC)*

Direct observation of aqueous fluids coexisting with $MgSiO_3$ enstatite and/or Mg_2SiO_4 forsterite is performed at 0.5 – 5.8 GPa and 800 -1000 °C with an externally heated diamond anvil cell and synchrotron X-rays. In the $MgSiO_3$ – H_2O system, at 1000 °C forsterite crystallizes below 3 GPa and not above that pressure. In the Mg_2SiO_4 – H_2O system, forsterite congruently dissolves into the aqueous fluids up to 5 GPa at 1000 °C. These observations suggest that the aqueous fluids coexisting with enstatite and forsterite have $Mg/Si < 1$ below 3 GPa and $1 < Mg/Si < 2$ above that pressure.

Comparison with the previous studies reporting Mg/Si ratios of the aqueous fluid coexisting with enstatite and forsterite indicates that the Mg/Si ratios change rapidly from SiO_2-rich to MgO-rich features at around 3 GPa and 1000 °C (Figure). This can be related to possible structural changes of liquid water under these conditions. The aqueous fluids coexisting with enstatite and forsterite do have similar Mg/Si ratios to those found in the partial melts of H_2O-saturated peridotite. Somewhere within the upper mantle these two fluids unite to form a single

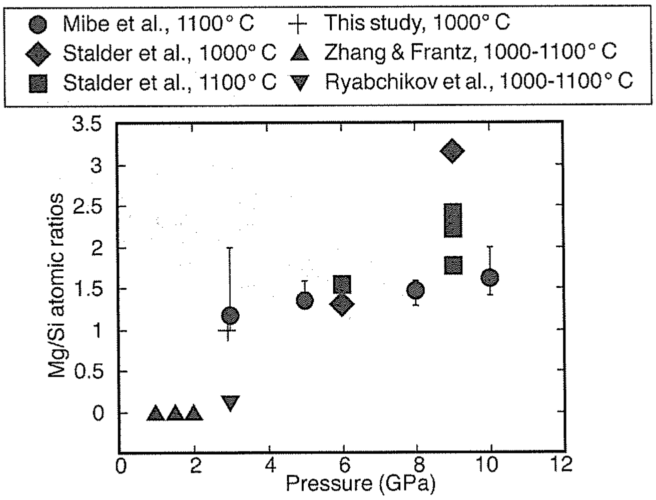

regime and cannot be distinguished from each other. (American Mineralogist. in press, October 2004).

Determination Investigation of Critical Behavior in Basalt-H_2O System Using High-pressure and High-temperature X-ray Radiography

Mibe, K. (Geophysical Laboratory), Kanzaki, M. (Okayama University at Misasa), ***Kawamoto,*** *T., Matsukage, K. N. (Ibaraki University), Fei, Y. (Geophysical Laboratory), and Ono, S. (JAMSTEC)*

To investigate the critical phenomena between aqueous fluid and hydrous silicate magma in the Earth's interior, a new method for making direct observations of immiscible fluids was developed using X-ray radiography technique together with the Kawai-type double stage multianvil system driven by a DIA-type cubic press (SPEED-1500) installed at BL04B1, SPring-8, Japan. Basalt-H_2O and Sr-plagioclase-H_2O systems were investigated. A new sample container comprising of a metal (Pt or AuPd) tube with a pair of lids made of single crystal diamonds was used under pressures between 2 and 5 GPa and temperatures up to 1500 °C. The sample inside the container can be directly observed through the diamond lids.

At around 800-900 °C and pressures up to about 3 GPa in both basalt- H_2O and Sr-plagioclase-H_2O systems, we observed light-gray spherical bubbles moving upward in the darkgray matrix. The light-gray spheres that absorb less X-rays represent an aqueous fluid, whereas the dark-gray matrix represents a silicate melt. At least up to 1200 °C, immiscible two phases (i.e., both aqueous fluid and silicate melt) were observed up to about 3 GPa in the basalt- H_2O system. At pressures above about 4 GPa, no bubbles appeared when heating to about 1200 °C, suggesting the possibility that the second critical end-point in basalt- H_2O system could be around 3 to 4 GPa. Our new technique can be applied to the direct observations of various coexisting 2-fluids under deep mantle conditions that could not be achieved by previous experimental methods. (J. Geography 112, 970-978, 2003, in Japanese).

Genesis and evolution of the enriched subcontinental lithospheric mantle beneath South India

T. Miyazaki, ***T. Shibata*** *and* ***M. Yoshikawa***

The Dharwar craton of South India was a main part of the earth's oldest continental assembly named Ur (-3000Ma) and also existed in later supercontinents emerged during earth history (Rogers and Santosh, 2003). Revealing the histories of the Dharwar craton and added periphery crust are profitable for tracing the history of supercontinents (their amalgamation, evolution and dispersion). Similar to the geological and geochlonological evidences of crastal rocks, the geochemical information from lithospheric mantle keel beneath the craton is also an important constraint for unraveling the long history of the Dharwar craton. The existence of long lived enriched lithospheric mantle is known beneath the Dharwar and periphery area. It is anticipated that the genesis and evolution of this enriched mantle reflect the major geological event in the history of the Dharwar craton.

The existence of alkali metal- and LREE-enriched lithospheric mantle beneath southeastern periphery of the Dharwar craton has been inferred based on Sr-Nd-Pb isotopic data on carbonatites and alkaline silicate rocks (Kumar et al., 1998; Schleicher et al., 1998; Miyazaki et al., 2000; Pandit et al., 2002; etc.). The Sr and Nd isotopic data also suggest that the sub-continental enriched lithospheric mantle remained a closed system from 2.6-2.5 Ga to 800-750 Ma and survived from convective disruption (Kumar et al., 1998; Miyazaki et al., 2003). The tholeiite dyke swarms of 1.6 and 1.8 Ga in this region also have evidence deriving from this enriched mantle source (Radhakrishna and Joseph, 1998). On the basis of difference in the isotopic signatures between coexisting carbonatites and syenites, Miyazaki et al (2003) have envisaged isotopically different enriched mantle sources and indicated mantle heterogeneity.

The event of mantle enrichment occurred at the late Archaean is now controversial, but it is significant topic to reveal the early history of the Dharwar craton. Although Jayananda et al. (2000) proposed the existence of an enriched mega-mantle-plume during the Late Archaean, there are many evidences approving the mantle enrichment by earlier subduction event. Miyazaki et al. (2003) indicated that the Neoproterozoic syenites and other mantle-derived intrusives have diagnostic trace-element signatures, typical to the magmas erupted in convergent margin. They inferred that slab-derived component played a major role for the genesis of long-lived enriched lithospheric mantle. The C isotope of the carbonatites also shows subduction related signature. Pandit et al. (2002) indicated that the relative enrichment of ^{13}C in the Neoproterozoic carbonaties as compared to the Paleoproterozoic carbonatites is a result of the equilibration of CO_2 derived from the ocean crust with existing carbon reservoir. Geological evidence of late Archaean subduction was summarized by Chadwick et al. (2000) who interpreted the whole craton in terms of accreted island arc. Moreover, in southeastern periphery of the Dharwar craton, several types of basement gneiss with age about 2.5 Ga have geochemical composition similar to the sanukitoids or average TTG(tonalite-trondhjemite granitic rock), favoring the active subduction event of late Archaean

(Moyen et al., 2001). According to the view points mentioned above, it is understood that the late Archaean subduction was major event in the history of the Dharwar craton and generated the long lived enriched lithospheric mantle.

The spatial extent of the enriched lithospheric mantle may reflect the scale of the late Archaean subduction. Nd isotope investigations of the charnockites and basic granulite from the Eastern Ghats Belt and eastern Antarctica revealed prolonged development of enriched lithospheric mantle (Arima et al., 2001). Although detailed investigations are required, the late Archaean subduction might occur in large area of old continental assembly.

References

Arima, M., Takano, N., Saradhi, P. and Kagami, H. (2001) Crustal and mantle evolution of the Proterozoic Eastern Ghats Belt, India. Gondwana Res. 4, 564-565.

Chadwick, B., Vasudev, V.N. and Hegde, G.V. (2000) The Dharwar craton, southern India, interpreted as the result of Late Archaean oblique convergence. Precamb. Res. 99, 91-111.

Jayananda, M., Moyen, J.–F., Martin, H., Peucat, J.–J., Auvray, B. and Mahabaleswar, B. (2000) Late Archaean (2550-2520 Ma) juvenile magmatism in the Eastern Dharwar craton, southern India: constraints from geochronology, Nd-Sr isotopes and whole rock geochemistry. Precamb. Res. 99, 225-254.

Kumar, A., Charan, S.N., Gopalan, K. and Macdougall, J.D. (1998) A long-lived enriched mantle source for two Proterozoic carbonatite complexes from Tamil Nadu, southern India. Geochim. Cosmochim. Acta 62, 515-523.

Miyazaki, T., Kagami, H., Ram Mohan, V., Shuto, K. and Morikiyo, T. (2003) Enriched subcontinental lithospheric mantle in the northern part of the South Indian Granulite Terrain: Evidence from Yelagiri and Sevattur syenite plutons, Tamil Nadu, South India. Gondwana Res, 6, 585-594.

Miyazaki, T., Kagami, H., Shuto, K., Morikiyo, T., Ram Mohan, V. and Rajasekaran, K. C. (2000) Rb-Sr geochronology, Nd-Sr isotopes and whole rock geochemistry of Yelagiri and Sevattur syenites, Tamil Nadu, South India. Gondwana Res. 3, 39-53.

Moyen, J-.F., Martin, H. and Jayananda, M. (2001) Multi-element geochemical modeling of crust-mantle interactions during late-Archaean crustal growth: the Clospet granite (South India). Precamb. Res. 112, 87-105.

Pandit, M.K., Sial, A.N., Sukumaran, G.B., Pimentel, M.M., Ramasamy, A.K. and Ferreira, V.P. (2002) Depleted and enriched mantle sources for Paleo- and Neoproterozoic carbonatites of southern India: Sr, Nd, C-O isotopic and geochemical constraints. Chem. Geol. 189, 69-89.

Radhakrishna, T. and Joseph, M. (1998) Geochemistry and petrogenesis of the Proterozoic dykes in Tamil nadu, southern India: another example of the Archaean lithospheric mantle source. Geol. Rundsch. 87, 268-282.

Rogers, J.J.W. and Santosh, M. (2003) Supercontinents in earth history. Gondwana Res. 6, 357-368.

Schleicher, H., Kramm, U., Pernicka, E., Schidlowski, M., Schmidt, F., Subramanian, V., Todt, W. and Viladkar, S.G. (1998) Enriched subcontinental upper mantle beneath southern India:

evidence from Pb, Nd, Sr and C-O isotopic studies on Tamil Nadu carbonatites. J. Petrol. 39, 1765-1785.

Genesis of tholeiitic and calcalcaline series of Zao volcano, NE Japan arc, employing trace element and isotopic compositions

T. Shibata, *C. Qing, A. Sakayori, Y. Tatsumi*

Genesis of co-existing tholeiitic series (TH) and calcalkaline series (CA) in island arc and their relationship has been a focus of attention because it is critical to understanding magma genesis in island arc and continental crust formation. The Zao is Quaternary volcano situated on the Tohoku Backbone Ranges, Northeastern Japan arc, and both of TH and CA co-exist in continuous volcanic activity. In addition, geology and petrology of the Zao volcano is well understood by Sakayori (1991) so that Zao volcano is one of the suitable volcanos to elucidate the genetical relationship of TH and CA magma series. We already reported the preliminary results of Sr, Nd and Pb isotope and trace element compositions of Zao volcano, and shown that at least four components are necessary to explain the chemical characteristics of TH and CA of Zao volcano (Shibata et al, 2003). However, the sources and relationships of those components were still ambiguous. Therefore, we developed the discussions of the genesis of TH and CA from Zao volcano employing the Sr, Nd, Pb isotope and trace element compositions.

The volcanic activity of Zao volcano started about 1 Ma and continues to the present, and is divided into Stage 1 to Stage 4 (Sakayori, 1991). According to Sakayori (1991), the rocks of Stage 1 belong to TH (low-K), and all the other to CA (midium-K). And on the Harker Diagrams, volcanic rocks of Stage 1 and Stage 3 show obvious different trend and those of the other stage plotted in between those two trends. Thus, we selected the 5 samples from Stage 1 and 5 from Stage 3 as a representative of TH and CA, respectively. The trace element compositions of the studied samples show the typical characteristics of island arc magma in the diagram of MORB normalized pattern, such as enrichment of LILEs and negative Nb spike. Positive Pb and Sr spikes are also apparent. The LILEs enrichment and negative spikes of Nb are relatively larger in CA than TH. Although abundance ratios of Cs/Nb of TH are restricted to 0.09 - 0.20, those of CA can be divided into two ranges, such as 0.20 – 0.25 and 0.42 – 0.57.

The isotopic compositions of TH are more enriched compared to CA. In all the diagrams presenting the relationship of the isotope compositions, TH and CA make different liner trends, which indicate the mixing relation. Furthermore, Pb isotopic compositions suggest that two depleted endmember is necessary to explain the trend of TH and CA. The depleted endmenber of TH is relatively enriched than that of CA. On the other hand, tow enriched endmembers are required from the relationships between parent/daughter and the isotope ratios, because TH and CA show different linier trends in those relation and the liner trends are diverse in the direction of isotopically enriched side. The both of the enriched direction of TH and CA is differ from the mixing trend of mantle wedge and recycled materials form subducting slab observed from Northeastern Japan (Shibata and Nakamura, 1997). Therefore, slab component can not be a candidate of enriched endmember of TH and CA. Alternatively, it has to take account for the involvement of different crustal material. When we look at more in detail, isotopic trend of CA can be divided in to two trends on the bases of the low and high Cs/Nb ratios. The isotopic trends of CA with low Cs/Nb can have same isotopicaly enriched component. On the other hand, the isotopic trends of CA with high Cs/Nb differ from the direction of enriched extension of TH, and show a linier trends with pyroclastics occurred around the Zao volcano, which is considered as crust origin. From the observations in the above, it can be concluded that four components are necessary to explain the chemical characteristics of TH and CA from Zao volcano and the different two enriched components are derived from different crustal materials, although the sources of those are not obvious yet.

Funai Fault beneath downtown Oita, east central Kyushu, southwest Japan

Chida, N., ***Takemura, K.*** *et al.*

Drilling surveys, the seismic reflection survey and the Geo-slicer investigation reveal the location and active mode of a fault (Funai Fault) lying concealed under the town area of Oita City. The Funai Fault is the southeast continuation of the Horita-Asamigawa fault (Beppu) and total length is about 20km.

Wide-spread tephra K-Ah volcanic ash layer found in drill cores is the effective key marker for calculating the activity of fault. The average rate of vertical displacement of Funai Fault after the K-Ah volcanic ash (6,300 yBP) is 2.2-2.5 m/1000 years, and the fault is estimated as one of the A class active faults in Japan. The latest activity is inferred before 1,540 yBP and after 2,350 yBP according to the displacement of sedimentary layer and age determination by carbon-14 dating. It is necessary to elucidate accurate distribution and the activity of the concealed faults lying under the Oita Plain.

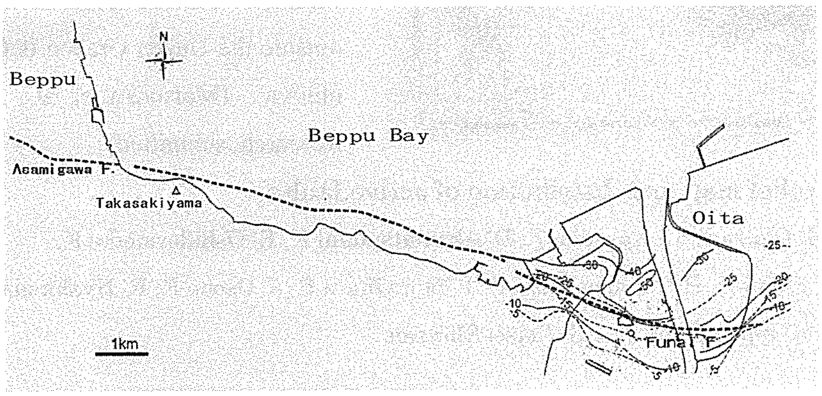

Fig. Location of Funai Fault lying under the Oita Plain (Chida et al, 2003)
Contour line is the bottom depth of K-Ah volcanic ash layer, and contour interval is 5m.(Chida et al., Active Fault Research, 23, 93-108, 2003)

Late Quaternary Activity of active faults in the Unzen Graben, western Kyushu, based on tectonic geomorphology

Matsuoka, A., Tsutsumi, H. and ***Takemura, K.***

The Unzen Graben, which is bounded by normal faults to the north and south, is located on the western end of the Beppu-Shimabara Graben. The faults in the Unzen Graben have developed with the growth of the Unzen volcanoes and dislocated volcanic materials such as lavas and pyroclastic deposits. The detailed location and vertical offsets of the active faults have been reported by previous studies, but the timing of faulting was poorly constrained.

We estimated the vertical offsets based on topographic profiling, and calculated vertical slip rate based on recently obtained ages of volcanic rocks and sediments. In addition, we excavated two trenches at Chijiwa Town (western part of Unzen Graben) in order to reveal the timing of recent faulting events, and also found several outcrops across the active faults.

Based on these surveys, the active faults in the Unzen Graben can be divided into four groups. Two groups of faults, which are located on the northern and southeastern margins of the Unzen Graben, have vertical slip rates as high as 0.13 to 1.0 mm/yr. A group of faults inside the Unzen Graben has slip rate 0.085 to 0.46 mm/yr except for the Akamatsudani fault which has slip rate 0.91 to 1.7 mm/yr. Three groups of faults mentioned above show cumulative vertical offsets and their rates of activity tends to be higher around the edifice of the Fugen volcano. On the other hand, the group outside the Unzen Graben is 0.026 to 0.068 mm/yr. (Matsuoka et al., Active Faults Research, submitted)

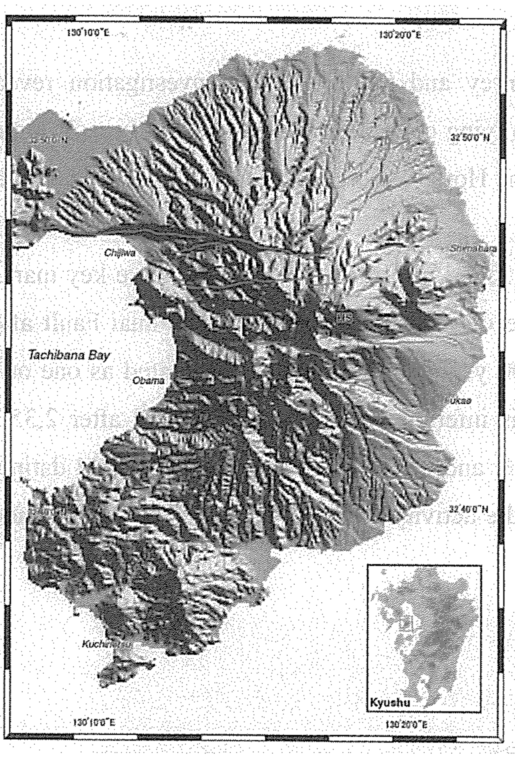

Fig. Shaded relief map and distribution of active faults

A: Chijiwa F., B: Ogura F., C: Kusenbu F., D: Akamatsudani F., E: Oshidorinoike F., F: Fukae F., G: Futsu F., H: Takaiwayama F., I: Yanagihara F., J: Osono F., K: Hyakkadai F., L: Haraiyama F., M: Ipponmatsu F., HS: Heisei Shinzan

High Density Helicopter-Borne Aeromagnetic Survey in Aso Volcano

M. Utsugi, Y. Tanaka** and **N. Kitada

Recently, geomagnetic field observation is successfully applied to many active volcanos to detect the volcano-magnetic changes, i.e., geomagnetic field changes associated with the volcanic activities. These observations are usually based on the continuous or repeated observation stations setting on the ground near the active area. From these observations, we can obtain high accurate information about the temporal geomagnetic field changes. But we can obtain only limited information about the special distribution of geomagnetic changes because of it is quite difficult to maintain many observation stations under the extremely bad environment around the active area of volcano. To interpret the geomagnetic field changes to underground heat transfer, we have to know the special distribution of the geomagnetic changes.

To obtain the detailed information about the spatial distribution, we tried to use the aeromagnetic survey. Based on the aeromagnetic survey, we can get many data of spatial distribution of the field easily. Our goal is to detect the volcano-magnetic changes from the repeated aeromagnetic survey. The main problem of aeromagnetic repeated observation is the difficulty of the observation point control. In the two flights, it will be impossible to flight exactly same position. So that, it is very difficult to separate observed field changes to temporal variation due to the volcanic activities and the spatial variation due to the difference of the observation points. If the detailed distribution of geomagnetic field is obtained on quiet period of the volcano, and the field intensity on the arbitrary point around the active area is estimated interpolating the observed data, we can correct the spatial variation of the repeated aeromagnetic survey data caused by the difference of flight position, and it may be possible to detect the field changes associated with the volcanic activities.

For this purpose, we made very high density and low altitude helicopter-borne aeromagnetic survey on Aso Volcano, central Kyushu Island of Japan, in July 2002. The survey area was NS1200 x EW1200 x 300m region above the Nakadake crater which is the most active area on Aso volcano (Fig.1). In this survey, we used a high-resolution portable cesium magnetometer. The sampling time of measurements was 0.1 second. The flight was

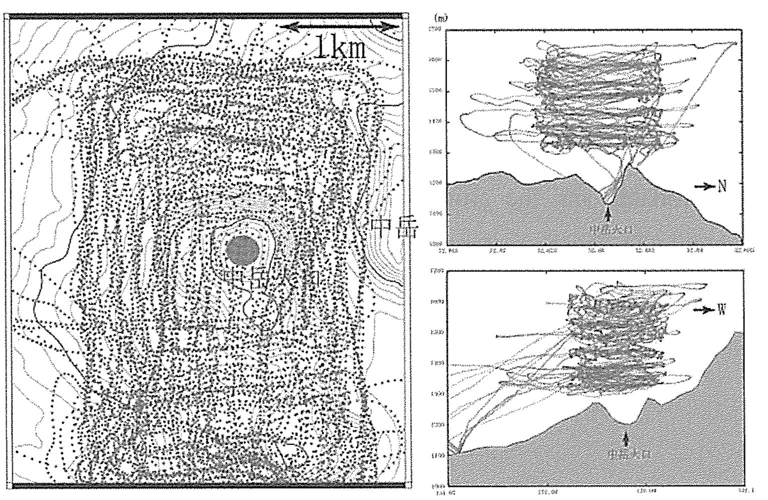

Fig. 1 The distribution of the observation points of the high-density aeromagnetic survey.

made in 8 heights (1370, 1400, 1450, 1500, 1540, 1570, 1600 and 1640 m from the sea level). The total numbers of measurements were about 8200. Using these data, we tried to estimate the special distributions of the geomagnetic field around the Nakadake crater. Observed data likely contain some noise or miss-observed data. To extract these inadequate data, we applied the technique of equivalent anomaly method. This method is usually used to calculate the upward continued aeromagnetic data. Based on this method, inharmonic component of observed data is carried away and the harmonic field distribution can be estimated in the upper region of the flight surface. In this study, we used this method to extract harmonic component from the observed data. The accuracy of the obtained distribution over the Nakadake crater is about 10nT, and if comparatively larger scale eruption is occurred, we can detect the volcano-magnetic changes using our estimated distribution of the geomagnetic field.

Origin and behavior of dissolved inorganic carbon of shallow groundwater in Kuju and Aso volcanic area

M.Yamada, S.Ohsawa, K.Kazahaya, M.Yasuhara, K.Amita,
H.Mawatari, S.Yoshikawa and Y.Yusa

Origin and behavior of dissolved inorganic carbon of shallow groundwater in Kuju and Aso volcanic area was discussed by means of isotope hydrology and geochemistry. Hydrogen and oxygen isotopic compositions of water and carbon isotopic ratio of dissolved inorganic carbon (DIC) were analyzed for 78 and 60 cold spring waters in Kuju and Aso volcanic area, respectively.

The hydrogen and oxygen isotopic ratios demonstrate definitely approved that the major source of spring waters in Kuju and Aso volcanic area are mainly derived from the meteoric water. The groundwater altitude effects on δD value in Kuju volcanic area and on δ^{18}O value in Aso volcanic area were speculated to be −1.37‰/100m and −0.2‰/100m, respectively. On the basis of the above result, the recharge area and migration direction of groundwater were determined.

DIC in shallow groundwater have generally its origin in soil CO_2 in Kuju volcanic area, however, the data of δ^{13}C and concentration of DIC approved that the magmatic gas mixed into some spring waters around Mt.Taisen and Mt.Kurodake, and the groundwater dissolved magmatic CO_2 was added in the groundwater dissolved soil CO_2 during water migration. Flux of magmatic CO_2, which is discharged from whole springs in this area, is estimated to be 12.9 ton/day in all. On the other hand, in Aso volcanic area, δ^{13}C and concentration of DIC showed that no spring water contains DIC of magmatic origin.

Noble gases in mantle-derived xenocrysts in an alkali basalt from Japan Trench oceanward slope: implications for wide distribution of MORB source over the upper-mantle

Yamamoto J., *Hirano N. (TITech) and Kagi H. (LEC)*

The source of MORB (mid-ocean ridge basalt) has generally been regarded to be derived from the suboceanic mantle, and to be located in the upper-mantle. The 3He/4He ratio in MORB shows quite uniform values of (8 +/- 1) R_A (R_A is the atmospheric $^3He/^4He$ ratio of 1.4×10^{-6}). MORB-like $^3He/^4He$ ratios have often been observed in mantle-derived rocks from island arcs and subcontinental mantle. There is a widespread consensus that the source of MORB is a ubiquitous component of the upper-mantle. Recently, however, occurrences of $^3He/^4He$ ratios lower than that of MORB have been reported for some subcontinental and island arc ultramafic xenoliths. Several possibilities are proposed to explain these low ratios including mixing with an atmospheric component; the influence of radiogenic ^4He ingrowth attributed to metasomatic enrichment of incompatible elements such as U and Th, or reduction of He/U ratio caused by preferential depletion of helium [1]. These discussions depend greatly on the implicit assumption that the source of MORB is a unique and uniform component in the upper-mantle.

To clarify the noble gas isotopic compositions of suboceanic mantle, we measured noble gas isotopic ratios of olivine xenocrysts in an alkali-basalt sampled from a northwest Pacific seamount. The xenocrysts are reported to be derived from upper-mantle from major element compositions [2,3]. The density of CO_2 fluid inclusions in the xenocryst records the pressure before entrainment into the host magma. Micro-Raman spectroscopic analysis allows us to estimate the internal pressure of the small fluid inclusions [4,5]. We applied this method to CO_2-dominated fluid inclusions in the xenocryst. The internal pressure of CO_2-dominated inclusions were up to 0.4 GPa (Fig. 1: [6]), which corresponds to a depth of up to 14 km of lithospheric mantle under the seafloor. By applying both vacuum crushing and stepwise heating extraction of the noble gases, uncontaminated $^3He/^4He$ ratios range between 7.2 and 7.7 R_A and $^{40}Ar/^{36}Ar$ ratios are up to 5000 in the xenocrysts (Table 1: [6]). These observations demonstrate that the upper mantle beneath the oceanward slope of the Japan Trench has a similar isotopic composition to the MORB source, suggesting a uniform MORB source is largely distributed in the upper mantle.

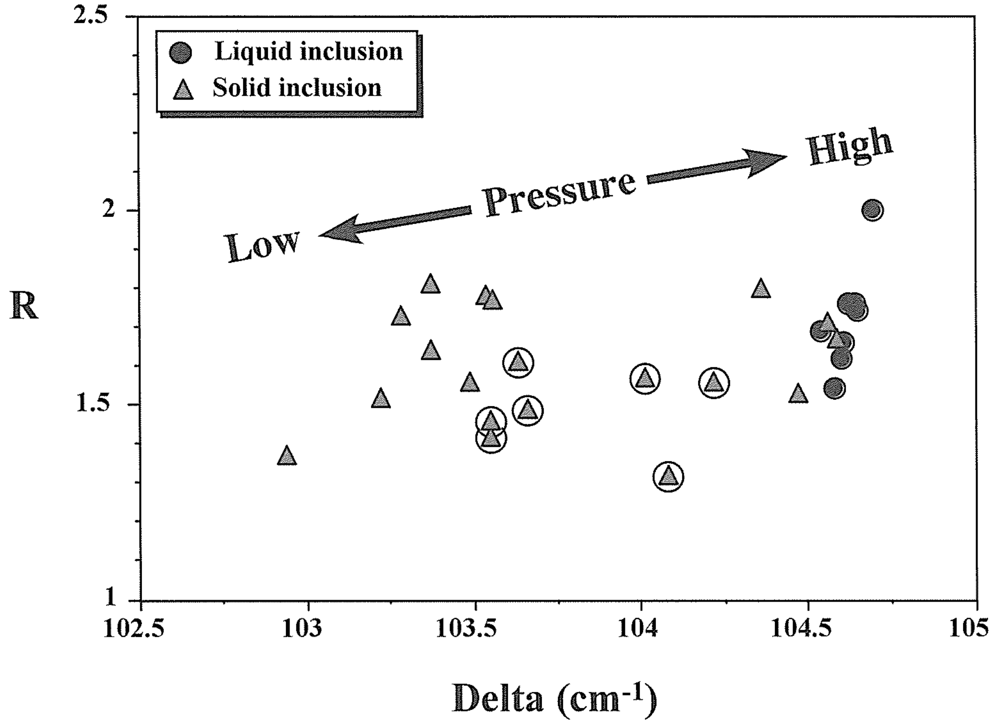

Table 1. Noble gas isotopic compositions in large olivine phenocrysts from Japan Trench oceanward slope

		weight g	^{3}He ccSTP/g	error ccSTP/g	^{4}He ccSTP/g	error ccSTP/g	^{20}Ne ccSTP/g	error ccSTP/g	^{36}Ar ccSTP/g	error ccSTP/g	^{40}Ar ccSTP/g	error ccSTP/g	^{84}Kr ccSTP/g	error ccSTP/g	^{132}Xe ccSTP/g	error ccSTP/g
Crushing		0.245	6.5E-12	8.8E-13	7.6E-07	9.9E-08	1.2E-10	1.5E-11	1.4E-10	8.6E-12	2.4E-07	1.4E-08	5.4E-12	3.8E-13	4.0E-13	2.7E-14
Heating	**700IC**	1.384	1.9E-13	4.4E-14	5.0E-08	6.5E-09	8.0E-11	1.0E-11	1.5E-10	9.0E-12	4.8E-08	2.9E-09	4.8E-12	2.9E-13	2.7E-13	1.8E-14
	1200IC		4.2E-12	5.7E-13	4.7E-07	6.1E-08	2.3E-11	4.1E-12	3.1E-11	1.9E-12	1.5E-07	9.1E-09	1.4E-12	9.5E-14	1.8E-13	1.3E-14
	1900IC		7.7E-12	1.0E-12	8.9E-07	1.2E-07	2.3E-10	2.9E-11	3.8E-10	2.3E-11	5.1E-07	3.0E-08	1.8E-11	1.1E-12	1.6E-12	1.1E-13
	total		1.2E-11	1.2E-12	1.4E-06	1.3E-07	3.4E-10	3.1E-11	5.7E-10	2.5E-11	7.1E-07	3.2E-08	2.4E-11	1.1E-12	2.0E-12	1.1E-13

		weight g	^{3}He/^{4}He R/Ra	error R/Ra	^{20}Ne/^{22}Ne	error	^{21}Ne/^{22}Ne	error	^{40}Ar/^{36}Ar	error	^{38}Ar/^{36}Ar	error	^{4}He/^{40}Ar*	error
Crushing		0.245	7.20	0.31	9.70	0.30	0.0306	0.0040	1647	30	0.1891	0.0027	3.9	0.6
Heating	**700IC**	1.384	3.02	0.57	9.66	0.27	0.0272	0.0028	320	4	0.1885	0.0008	13.7	3.2
	1200IC		7.70	0.27	9.82	1.36	0.0271	0.0107	4945	71	0.1892	0.0015	3.2	0.5
	1900IC		7.36	0.13	9.75	0.11	0.0304	0.0008	1331	19	0.1895	0.0011	2.3	0.3
	total		7.30	0.12	9.73	0.23	0.0294	0.0020	732	10	0.1887	0.0007	5.7	0.6
	1200IC+1900IC								1963	27	0.1895	0.0010		

Figure 1. R-Delta plot for CO_2 Fermi diad of CO_2 inclusions in some xenocrysts. R means intensity ratio of the CO_2 Fermi diad. Delta means separation of wavenumber of the CO_2 Fermi diad. Circle: liquid inclusion; triangle: solid inclusion; triangle + circle: solid inclusion with vapor bubble. The reproducibility of the Delta and R for data with moderate intensity (counts) is typically ~0.15 cm^{-1} and ~0.2 cm^{-1}, respectively. Because the inclusions with low Delta-value have lower density than that of high Delta-value, the data tend to show wide variation particularly in the R-value.

Reference

[1]. Yamamoto J., Kaneoka I., Nakai S., Kagi H., Prikhod'ko V.S. & Arai S. (2004) Evidence for subduction-related components in the subcontinental mantle from low 3He/4He and 40Ar/36Ar ratio in mantle xenoliths from Far Eastern Russia. Chemical Geology 207, 237-259.

[2]. Hirano N., Kawamura K., Hattori M., Saito K. and Ogawa Y. (2001) A new type of intra-plate volcanism; young alkali-basalts discovered from the subducting Pacific Plate, northern Japan Trench. Geophys. Res. Lett. 28, 2719-2722.

[3]. Hirano N., Yamamoto J., Kagi H. and Ishii T. (2004) Young olivine xenocryst-bearing alkali-basalt

from the oceanward slope of the Japan Trench. Contributions to Mineralogy and Petrology in press.

[4]. Yamamoto J., Kagi H., Kaneoka I., Lai Y., Prikhod'ko V. S. and Arai S. (2002) Fossil pressures of fluid inclusions in mantle xenoliths exhibiting rheology of mantle minerals: Implications for the geobarometry of mantle minerals using micro Raman spectroscopy. Earth and Planetary Science Letters 198, 511-519.

[5]. Kawakami Y., Yamamoto J. and Kagi H. (2003) Micro-Raman densimeter for CO2 inclusions of mantle-derived minerals. Applied Spectroscopy 57, 1333-1339.

[6]. Yamamoto J., Hirano N., Hanyu T., Kagi H. and Kaneoka I. (2003) Noble gases in mantle-derived xenocrysts in an alkali basalt from Japan Trench oceanward slope. In Plume and problems of deep sources of alkaline magmatism (edited by N.V. Vladykin), pp.39-50. Irkutsk State Technical University, Irkutsk

Melt generation process in the mantle wedge under island arc recorded in the Hayachine-Miyamori ophiolitic complex

Masako Yoshikawa *and Kazuhito Ozawa*

Peridotites provide direct information of chemical fractionation processes such as melt separation and migration in the upper mantle. Recently, precise trace element analyses of peridotites have proposed a general occurrence of an open-system melting induced by melt influx in the upper mantle (e.g. Kelemen et al., 1992; Johnson and Dick, 1992; Ozawa and Shimizu, 1995). Isotopic compositions of Sr and Nd for peridotites have been believed to provide important clue to confirm origins of mantle and influxed melt. However, the precise isotopic data are not enough accumulation because of analytical difficulty.

The Hayachine - Miyamori ophiolitic complex is located in the Hayachine Tectonic belt which forms the northeast boundary of the South Kitakami Belt of the northeast Japan, that is one of the oldest geological units of Japan (Ehiro, 2000). The open system melting of hydrous mantle under island arc has been proposed in this complex by a series of Ozawa's studies (e.g. Ozawa, 1988). According to Ozawa (1984, 1988), the peridotites and pyroxenites are divided into two types on the bases of a clear gap in spinel Cr# (Cr/(Cr+Al)): i.e. an aluminous spinel (Cr# <0.4) bearing ultramafic suite (ASUS) and a chromite (Cr#>0.4) -bearing ultramafic suite (CSUS). The ASUS occurs as kilometric sized patches in the CSUS in the Miyamori complex (Ozawa, 1984).

Bulk rock compositions and forsterite value of olivine display the systematic change in this complex which can be explained by deference of degree of melting as pointed out by Ozawa (e.g. 1988). Chondrite-normalized trace element patterns tend to show more enrichment in incompatible elements as peridotites become refractory. On the basis of such reverse correlation between incompatible and major elements and occurrence of ASUS in the Miyamori complex, it is inferred that CSUS was formed by open system melting with significant melt influx and refractory ASUS was less involvement of the same influxed melt in melting during entrainment to CSUS diapir. (e.g. Ozawa and Shimizu, 1995). However, calculated trace element concentrations by applying the open system melting model (Ozawa and Shimizu, 1995) to our new data with previously reported data indicate that 1) the trace element patterns of this complex can not be explained by partial melting with a single melt influx, 2) modeled influxed melt to ASUS shows moderate enrichment in incompatible elements and slight Sr negative anomaly, and estimated influxing melt of CSUS was extensive enrichment of incompatible elements with Sr positive anomaly, and 3) two stage open system melting needs to explain a trace element pattern of a refractory ASUS.

The variation of Nd isotopic compositions of the peridotites is larger (ε_{Nd} = +4 to +20) than those of intrusive rocks (ε_{Nd} = +5 - +8) (Shibata and Ozawa, 1992; Ozawa, Shibata and Asahara, unpublished data). The more refractory peridotites show more enriched isotopic signature. The Nd model age of the most primitive ASUS sample, which is considered as the sample without any influx of melt, is about 430 Ma. This age is consistent with K-Ar ages (421-480Ma) of amphiboles in intruded rocks which have been interpreted as emplacement age of this complex (Ozawa et al.,1988; Shibatta and Ozawa, 1992). Thus, the partial melting event was likely to happen just before the emplacement. Time corrected Nd isotopic compositions of the refractory ASUS are lower than those of the most primordial ASUS. It is suggested that the influxed melt had enriched isotopic composition compared to a source peridotite. Although the time corrected Nd isotopic ratios of most of CSUS overlap the range of the refractory ASUS, some of CSUS show more enriched characteristics. Thus, the formation of CSUS could be induced by more enriched melt influx. These observations may indicate that path of influxing melt was gradually shifted and composition of isotopic and trace elements for the influxed melt was more enriched with time.

In situ Sr isotop ratio of plagioclase phenocrysts of tholeiitic and calc-alkaline volcanic rocks from Zao volcano, Northeastern Japan.

T. Takahashi, ***Masako Yoshikawa, T. Shibata*** *and Y. Tatsumi*

Sr isotope ratio is basic and important geochemical tracer for studying magma generation and evolution processes. And, chemical compositions and texture of phenocrystic minerals can provide important constraints on magmatic processes, such as fractional crystallization, magma mixing and assimilation.

The Quaternary Zao volcano is located at the central part of the volcanic front of northeastern Japan arc. The Zao volcano has been active since 1Ma, and is divided into Stage 1 to Stage 4 (Sakayori, 1991). According to Sakayori (1991), the rocks of Stage 1 belong to tholeiitic series (TH), and all the other stages to calc-alkaline series (CA). Shibata et al. (2003) determined bulk Sr, Nd and Pb isotopic and rare earth element compositions for stage 1 and stage 3, and argued that four components are necessary to explain the chemical and isotopic characteristics of TH and CA from the Zao volcano. Thus, we selected the one sample from stage 1 and two from stage 3, and performed the In-situ Sr isotope analysis on plagioclase phenocrysts of TH and CA samples.

The In situ Sr isotope analysis was performed by combined method of microdrilling and Thermal

Ionization Mass Spectrometer (TIMS). The microdrilling is the sampling technique of drilling a sample mechanically with a small drill and collecting the sample powder milled. The diameter at the tip of the drills used for sampling is 0.1 and 0.27mm. The collected sample powder was dissolved with acid, and Sr was separated using columns cation-exchange resin. Sr isotope measurement was carried out on the TIMS.

The TH samples data suggest that plagioclase phenocrysts first grew in magma with stable chemical composition and Sr isotope ratios, and then, the magma was mixed with high Sr isotope ratio material. On the other hand, plagioclase phenocryst in CA has widely compositional range and Sr isotope ratios. Furthermore, dusty type was recording a change of Sr isotope ratio. Therefore, it is thought that two or more components participated in the magma evolution process of CA magma.

References

Sakayori, A. (1991) Magmatic evolution of Zao Volcano, Northeast Japan. *Bull. Volcanol. Soc. Japan*, 36, 79-92.

Shibata, T., Tatsumi, Y., Sakayori, A. (2003) Geochemistry of tholeiitic and calcalkaline volcanic rocks from Zao volcano, Northeastern Japan Arc. *Japan Earth and Planet. Sci. Joint Mtg. Abstr.*

Precise isotope determination of trace amount of Sr aims at the in situ Sr isotope analysis by microdrilling technique.

T. Takahashi and ***Masako Yoshikawa***

Sr isotope ratio is basic and important geochemical tracer for studying magma generation and evolution processes. In this study, we are aiming at the in situ Sr isotope analysis of plagioclase in volcanic rocks by combined method of microdrilling and Thermal Ionization Mass Spectrometer (TIMS). The microdrilling is the sampling technique of drilling a sample mechanically by a small drill and collecting the sample powder milled by it (e.g., Davidson and Tepley, 1997; Tepley et al., 1999). Tepley et al. (1999) reported that >5ng Sr was recovered from plagioclase using the microdrilling technique (the drill holes size are about 0.3 to 0.4mm). However, zoning order of chemical composition of the plagioclase in volcanic rocks are <0.3mm in many cases (e.g., Davidson et al., 2001). We aim at the in situ Sr isotope analysis of high resolution, for example a <0.3mm drill hole, and it is necessary to precise isotope determination of trace amount of Sr. In this report, we have improved analytical technique for the isotope measurement of trace amount of Sr employing the TIMS.

Sr isotope measurements was carried out on the Triton TI® (multicollector mass spectrometer) installed by Japan Marine Science & Technology Center (JAMSTEC) at Beppu Geothermal Research Laboratory (BGRL), Kyoto University. Sr sample solution was loaded on Re filament with a Ta solution. This procedure basically followed Birck (1986) and Yoshikawa and Nakamura (1993). Ta solution is the ionization activator for Sr, and it is used in order to obtain stable and high intensity Sr ion beams. The data were computed from 99 repeated measurements, comprising 9 scans in each of 11 blocks. The data acquisition time took about 40 min for each measurement. The $^{87}Sr/^{86}Sr$ ratios were normalized to $^{86}Sr/^{88}Sr$ ratio of 0.1194.

The stable and high ion beam is necessary for precise isotope measurement. However, it is difficult to simultaneously obtain stable and strong enough ion beam for trace amounts of Sr. We observed the relationship between average ^{88}Sr ion beam intensity during individual measurements and analytical precision for 100ng and 5ng Sr samples (Fig. 1). The analytical precision exponentially improved with increasing ion beam intensity. In 5ng analysis, a stable ion beam lasts for > 40 min at ^{88}Sr ion beam intensity of approximately 2V resulting in an analytical precision of from ±0.000014 to ±0.000018 ($2\sigma_m$). When the intensity was >2.5V, the ion beam intensity decayed rapidly, with the result that analytical precision is worse (Fig. 2). These results indicate that there is a limit to the analytical precision of approximately ±0.000016 for a 5ng Sr sample, and this value is smaller than the analytical precision for a 10ng Sr sample using the Finnigan MAT262® (± 0.000020) reported by Yoshikawa and Nakamura (1993).

In order to examine analytical precision, reproducibility and accuracy for the isotope measurement of trace amounts of Sr, consequently small ion beam intensity, repeated analyses of Sr reference material (NIST SRM 987) were conducted and results are shown in Fig. 3. The mean values and reproducibility for 100ng (at ion beam intensity > 3V), 100ng (at ion beam intensity < 3V) and 5ng samples are $^{87}Sr/^{86}Sr = 0.710257 \pm 0.000012$ (2σ, n = 25), $^{87}Sr/^{86}Sr = 0.710269 \pm 0.000018$ (2σ, n = 15) and $^{87}Sr/^{86}Sr = 0.710260 \pm 0.000022$ (2σ, n = 19), respectively, and agree within analytical error. These values are comparable to those obtained using other methods (Table 1). The reproducibility of 5ng Sr sample analysis was equivalent to previous result of 10ng Sr sample (Yoshikawa and Nakamura, 1993), and smaller than the result of 6ng Sr sample using the VG mass spectrometer (Tepley et al., 1999). Furthermore, reproducibility of isotope measurement with trace amount of Sr was comparable to the results of isotope measurements for ≥ 100ng, or smaller than those. These results indicate that our method is reliable even for trace amount of Sr as small as 5ng.

From the above result, it is concluded that the high precision isotope analysis of trace amount of Sr is possible, and our mass spectrometry is applicable to the in situ Sr isotope analysis of plagioclase by microdrilling technique.

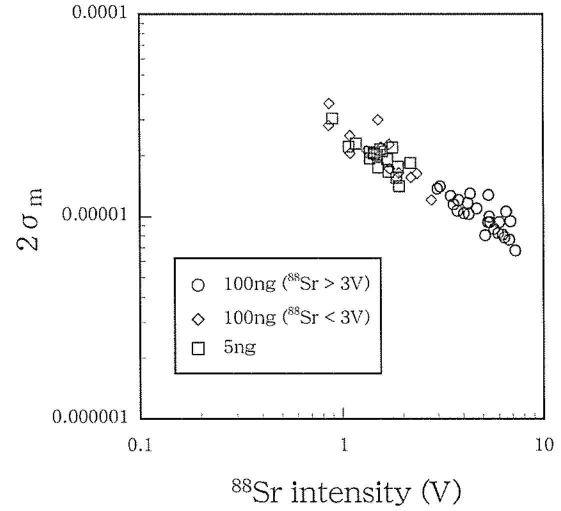

Fig.1. Relationship between ^{88}Sr ion beam intensity and analytical precision.

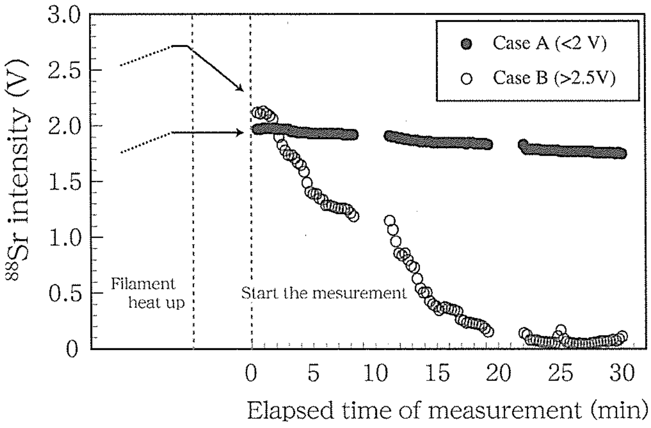

Fig.2. Relationship between time (min) and ^{88}Sr ion beam intensity. This diagram shows an example experiment using NIST SRM 987 (5ng). The arrows show the ion beam intensity before a measurement start.

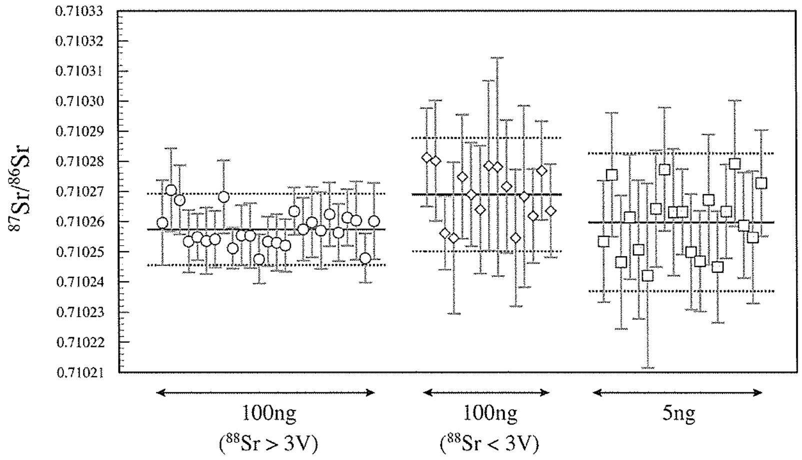

Fig.3. Variation in ^{87}Sr/^{86}Sr rations for sample sizes from 100 and 5ng. The vertical bar with symbol shows the error in 2σ m of each measurement. The horizontal solid and dotted lines show the average and range of error (2σ) in the ^{87}Sr/^{86}Sr ratios for sample sizes form 100 and 5ng.

Laboratory*[1]	Mass spectrometer		^{87}Sr/^{86}Sr	References
PML	MAT262	100ng loads	0.710239 ±0.000011 (2σ, n=5)	(1)
		50ng loads	0.710233 ±0.000014 (2σ, n=5)	
		10ng loads	0.710232 ±0.000022 (2σ, n=8)	
Niigata	MAT262		0.710251 ±0.000029 (2σ, n=51)	(2)
UCLA	VG	600ng loads	0.710234 ±0.000030 (2σ, n=11)	(3)
		6ng loads	0.710253 ±0.000050 (2σ, n=9)	
BGRL	MAT262	150ng loads	0.710261 ±0.000030 (2σ, n=17)	(4)
	Triton TI	150ng loads	0.710268 ±0.000019 (2σ, n=10)	
BGRL	Triton TI	100ng loads*[2]	0.710257 ±0.000012 (2σ, n=25)	(5)
		100ng loads*[3]	0.710269 ±0.000018 (2σ, n=15)	
		5ng loads	0.710260 ±0.000022 (2σ, n=19)	

Table 1. The comparison of Sr isotope analyses of NIST SRM 987.

References

(1) Yoshikawa and Nakamura (1993), (2) Miyazaki and Shuto (1998), (3) Tepley et al. (1999), (4) Shibata et al. (2002), (5) this study.

Laboratory*[1]: BGRL: Beppu Geothermal Research Laboratory, Graduate School of Science Kyoto University, Niigata: Department of Geology, Niigata University, PML: The Pheasant Memorial Laboratory, Institute for study of the Earth's Interior, Okayama University, Misasa, UCLA: University of California, Los Angeles, Department of Earth and Space Sciences.

100ng loads*[2] : Ion beam intensity > 3V, 100ng loads*[3] : Ion beam intensity < 3V

公表論文及び著書 Publications

<査読有>

Goto, S., M. Kinoshita, A. Schultz, R. P. Von Herzen (2003) Estimate of heat flux and its temporal variation at the TAG hydrothermal mound, Mid-Atlantic Ridge 26°N, J. Geophys. Res. 108(B9), 2434, doi:10.1029/2001JB000703.

Yamano, M., M. Kinoshita, ***S. Goto***, O. Matsubayashi (2003) Extremely high heat flow anomaly in the middle part of the Nankai Trough, Phys. Chem. Earth. 28, 487-497.

Hase H., T. Ishido, S. Takakura, T. Hashimoto, K. Sato, and Y. Tanaka, Zeta potential measurement of volcanic rocks from Aso caldera, Geophysical Research Letters, Vol. 30, No. 23, 2210, doi:10.1029/2003GL018694, 2003.

Inoue N., Kitada N., Itoh Y., Takemura K. and Nakagawa K., 2003, Integrated study of high resolution geophysical and geological information of Osaka Bay, Southwest Japan, Journal of Asian Earth Science, 22, 1-11.

Kawamoto, T., Hydrous phase stability and partial melt chemistry of H_2O-saturated KLB-1 peridotite up to the uppermost lower mantle conditions. Physics of Earth and Planetary Interior, 143-144, 387-395 (2004)

川本竜彦、マグマと水の間の臨界現象、日本高圧力学会誌, 2004(8月号印刷中)

Kawamoto, T., Matsukage, K. N., Mibe, K., Nishimura, K., Isshiki, M., Ishimatsu, N., Ono, S., Mg/Si ratios of aqueous fluids coexisting with forsterite and enstatite based on the phase relations in the Mg_2SiO_4-SiO_2-H_2O system. American Mineralogist. (2004) (5 pages in press, October 2004).

Kawamoto T., Matsukage, K., Nagai, T., Nishimura, K., Mataki, T., Ochiai, S., Taniguchi, T., Raman spectroscopy of cubic boron nitride under high temperature and pressure conditions: a new optical pressure marker. Review of Scientific Instruments, 75, 2451-2454 (2004)

Kawamoto, T., Ochiai, S., Kagi, H., Changes in the structure of water deduced from the pressure dependence of the Raman OH frequency. Journal of Chemical Physics (Communications section). 120, 5867-5870. (2004)

Matsukage, K.N., Ono, S., ***Kawamoto, T.***, Kikegawa, T., The compressibility of a natural apatite. Physics and Chemistry of Minerals. In press.

McCammon, C.A., Frost, D.J., Smyth, J.R., Lausten, H.M.S., ***Kawamoto,*** **T.**, Ross, N.L., van Aken, P.A. Oxidation state of iron in hydrous mantle phases: Implications for subduction and mantle oxygen fugacity, Physics of Earth and Planetary Interior, 143-144, 157-169 (2004)

三部賢治・神崎正美・***川本竜彦***・松影香子・費英偉・小野重明, 高温高圧X線ラジオグラフィ法による玄武岩-H_2O系の臨界状態に関する研究、地学雑誌 112, 970-978 (2003)

Mibe, K., Kanzaki, M., ***Kawamoto, T.***, Matsukage, K. N., Fei, Y., Ono, S., Determination of the second critical endpoint in silicate-H_2O systems using high-pressure and high-temperature X-ray radiography. Geochimica et Cosmochimica Acta. in press, December 2004.

Yamamoto M., Kawano Y., Imai A., ***Nishimura K.***, Miocene granites and Hishikari gold deposits in Kyushu, Hutton Symposium V, Field Guidebook, Geological Survey of Japan, Interim-Report, 2003, 28, 61-80.

千田 昇・*竹村恵二*・松田時彦・島崎邦彦・池田安隆・岡村 眞・水野清秀・松山尚典・首藤次男、大分平野直下に伏在する府内断層の位置と最新活動時期. 活断層研究, 23,93-108, 2003

北田奈緒子・斎藤礼子・*竹村恵二*、京都盆地の構造と地震による地盤災害. 地盤情報データベースからみた京都盆地浅部地質. 自然災害科学, 22, 216-220, 2003.

楠本成寿・*竹村恵二*、広域応力場とカルデラ形状の力学的関係. 火山, 48, 485-489, 2003.

Kusumoto, S. and ***Takemura, K.***, Numerical simulation of caldera formation due to collapse of a magma chamber. Geophysical Research Letters, 30, (24), 2278, doi:10.1029/2003GL018380, 2003.

中村洋介・岡田篤正・*竹村恵二*、富山平野西縁の河成段丘とその変形. 地学雑誌, 112,544-562, 2003.

中村洋介・金 幸隆・岡田篤正・*竹村恵二*、金沢市街地における河成段丘の形成時期と森本—富樫断層帯野町撓曲の第四紀後期における上下変位速度. 活断層研究, 23,69-76, 2003.

Sugiyama, Y., Mizuno, K.,Nanayama, F., Sugai, T., Yokota, H., Hosoya, T., Miura, K., ***Takemura, K.*** and Kitada, N. Study of blind thrust faults underlying Tokyo and Osaka urban area using a combination of high-resolution seismic reflection profiling and continuous coring. Annals of Geophysics, 46, (5), 1071-1085, 2003.

杉山雄一・七山 太・三浦健一郎・吉川 猛・横田 裕・末廣匡基・古谷正和・栃本泰浩・廣瀬孝太郎・横山芳春・北田奈緒子・*竹村恵二*、上町断層系の補足調査(その2)－新淀川北岸における追加ボーリングとS波反射法地震探査データの再解釈に基づく上町断層の活動性評価－. 活断層・古地震研究報告, 第3号, 117-143, 2003.

杉山雄一・七山 太・北田奈緒子・*竹村恵二*・横田 裕・末廣匡基、上町断層系の補足調査(その1)－石津川沿い沖積低地におけるP波及びS波反射法地震探査. 活断層・古地震研究報告, 第3号, 103-115, 2003.

竹村恵二、中部九州の地殻変動. 温泉科学会誌, 53(4), 143-150, 2004.

竹村恵二・香川敬生、近畿地方の活断層と強震動. 基礎工, 32, (3), 12-15, 2004.

竹村恵二・横田 裕・末廣匡基、京都盆地の構造と地震による地盤災害. 京都盆地の深部構造. 自然災害科学, 22, 220-225, 2003.

Yum J. G., ***Takemura, K.***, Tokuoka, T., and Yu K. M., Holocene Environmental changes of the Hwajinpo Lagoon on the eastern coast of Korea. Journal of Paleolimnology, 29 (2), 155-166, 2003.

Tatsumi, Y., Shukuno, H., Satho, K., ***Shibta, T.*** and ***Yoshikawa, M.***, The Petrology and Geochemistry of High-Magnesium Andesites at the Western Tip of the Setouchi Volcanic

Belt, SW Japan, J. Petrol, 44: 1561-1578, 2003.

Tatsumi, Y., Shukuno, H., ***Yoshikawa, M.***, Qing, C., Sato, K., and Lee, M.W. The npetology and geochemistry of volcanic rocks on Cheju island: plime magmatism along the Asian continental margin, J. Pterol. in press,

Mizukami T., Wallis S. R. and ***Yamamoto J.*** (2004) Natural examples of olivine lattice preferred orientation with a flow-normal a-axis maximum. Nature 427, 432-436.

Nishio Y., Nakai S., ***Yamamoto J.***, Sumino H., Matsumoto T., Prikhod'ko V. S., Arai S. and Kumagai H. (2004) Lithium isotopic systematics of the mantle-derived ultramafic xenoliths: implications for EM1 origin. Earth and Planetary Science Letters 217, 245-261.

Kawakami Y., ***Yamamoto J.*** and Kagi H. (2003) Micro-Raman densimeter for CO_2 inclusions of mantle-derived minerals. Applied Spectroscopy 57, 1333-1339.

Yamamoto J., Hirano N., Hanyu T., Kagi H. and Kaneoka I. (2003) Noble gases in mantle-derived xenocrysts in an alkali basalt from Japan Trench oceanward slope. In Plume and problems of deep sources of alkaline magmatism (edited by N.V. Vladykin), pp.39-50. Irkutsk State Technical University, Irkutsk.

<査読無>

Goto, S., H. Hamamoto, M. Yamano, K. Takahashi, Past environmental changes in southern Lake Biwa inferred from borehole temperature data, Proceedings, 2002 International Matsuyama Workshop "Geothermal/Dendrochronological Paleoclimate Reconstruction across Eastern Margin of Eurasia", Yamano, M., T. Nagao, T. Sweda (eds.), 50-56, 2003.

Hamamoto, H., M. Yamano, O. Matsubayashi, ***S. Goto***, Heat flow measurement in shallow seas through long-term temperature monitoring, Proceedings, 2002 International Matsuyama Workshop "Geothermal/Dendrochronological Paleoclimate Reconstruction across Eastern Margin of Eurasia", Yamano, M., T. Nagao, T. Sweda (eds.), 185-191, 2003.

Okubo, Y., H.-C. Kim, Y. Uchida, ***S. Goto***, J. Safanda, Borehole data and climate reconstruction in Korea, Proceedings, 2003 Korea-Japan Joint Seminar on Geophysical Techniques for Geothermal Exploration and Subsurface Imaging, 58-63, 2003.

長谷英彰・石戸経士・橋本武志・神田径・佐藤佳子, 九州4火山(開聞岳・九重山・猿葉山・雲仙岳)の岩石のゼータ電位測定, Conductivity Anomaly 研究会 2003 年論文集, in press.

長谷英彰・石戸経士・橋本武志・神田径・佐藤佳子, 九州火山の岩石のゼータ電位測定, 京都大学防災研究所年報, 第 46 号, B, 787-795, 2003.

川本竜彦、落合周吉、鍵裕之、ラマン分光法からみた高圧条件での水の構造変化、現代化学 2004 年 9 月号印刷中

Kawamoto, T., Mg/Si ratios of aqueous fluids in the Earth’s upper mantle, SPring-8 Research Frontiers 2003(印刷中).

大沢信二, 須藤靖明, 馬渡秀夫, 下田玄, 宇津木充, 網田和宏, 吉川慎, 山田誠, 岩倉

一敏, 恩田裕二、阿蘇火山の火口湖「湯溜まり」の地球化学的性質, 九大地熱・火山研究報告, 12, 62-65, 2003.

大沢信二、塚野鉱泉の水質形成機構. 大分県温泉調査研究会報告, **54**, 7-14, 2003.

大沢信二, 恩田裕二, 高松信樹、海地獄の呈色に関する色彩学的・地球化学的研究. 大分県温泉調査研究会報告, **54**, 15-24, 2003.

大沢信二, 須藤靖明, 馬渡秀夫, 下田　玄, 宇津木　充, 網田和宏, 吉川　慎, 山田　誠, 岩倉一敏, 恩田裕二、阿蘇火山の火口湖「湯溜り」の地球化学的性質. 九大地熱・火山研究報告, **12**, 62-65, 2003.

竹村恵二、プレート収斂域の水・熱フロー. 京大大学院理学研究科・理学部弘報, 166, 2-3, 2003.

竹村恵二, 三村　衛、京都盆地の構造と地震による地盤災害. はじめに. 自然災害科学, 22, 209, 2003.

竹村恵二, *井上直人*, *由佐悠紀*、由布院盆地の地下構造と堆積物. 大分県温泉調査研究会報告, 54 号, 1-6, 2003.

竹村恵二、書評　鎌田浩毅　著:火山はすごい.　PHP 新書. 文化財科学会誌, 46, 75-78, 2004.

竹村恵二、堆積環境と考古学.　環境考古学ハンドブック(安田喜憲編集), 朝倉書店,86-98, 2004.

竹村恵二、地域のための地球科学の樹立をめざして. 紅萌(京都大学広報誌) インタービュー記事, 4 号, 13-16, 2003.

大久保綾子、*田中良和*、*宇津木充*、*北田直人*、清水洋、松島健、雲仙火山における空中磁気観測について、京都大学防災研究所年報、第 46 号、739-747,2003.

田中良和、*宇津木充*、地磁気変化を利用した地熱の推移に関する研究(3),大分県温泉調査会研究報告、第 54 号、85-89,2003.

田中良和、繰り返し観測を思考した空中磁気測量について、科学研究費特定領域研究「火山爆発のダイナミクス」平成 14 年度成果報告書,35-38,2003

井口正人、神田径、石原和弘、*田中良和*、火山爆発場としての口永良部火山の浅部熱水系の推定、科学研究費特定領域研究「火山爆発のダイナミクス」平成 14 年度成果報告書,70-74,2003

神田径、*田中良和*、*宇津木充*、藤井郁子、地磁気から見た口永良部島火山の蓄熱場、科学研究費特定領域研究「火山爆発のダイナミクス」平成 14 年度成果報告書,63-69,2003

山田誠・大沢信二・由佐悠紀、湧水の水素と酸素の安定同位体比からみた九重火山地域の地下水の涵養と流動, 九大・地熱火山研究報告, 12, 66-74, 2003.

Yamamoto J., Kagi H., Kawakami Y., Kaneoka I., Lai Y., Prikhod'ko V. S. and Arai S. (2003) "Fossil pressures of fluid inclusions in mantle xenoliths: implications for geobarometry of mantle minerals using micro Raman spectroscopy" Geochimica Cosmochimica Acta 67 (18S), A551.

学会発表　Conference Presentations

後藤秀作、海底熱水域における放熱量の測定—大西洋中央海嶺 TAG 熱水マウンドでの例—, 第17回KS-WHAT研究会(熊本県長陽村, 2003年12月13日).

後藤秀作、地下温度に記録された過去の気候・環境変動, 地球研インキュベーション研究(沿岸都市地下環境)第2回インキュベーション研究会(京都, 2004年3月10-11日).

Goto, S., H. Hamamoto, M. Yamano, K. Takahasi, Past environmental changes in southern Lake Biwa inferred from borehole temperature data, The 23rd General Assembly of the International Union of Geodesy and Geophysics (IUGG2003) (Sapporo, June 30-July 11, 2003).

Goto, S., S. Kuramoto, J. Ashi, M. Yamano, Heat and fluid fluxes at a biological community site on the Nankai accretionary prism off Kii peninsula, The 23rd General Assembly of the International Union of Geodesy and Geophysics (IUGG2003) (Sapporo, June 30-July 11, 2003).

Goto, S., S. Kuramoto, J. Ashi, M. Yamano, Heat and fluid fluxes at a biological community site on the Nankai accretionary prism off Kii peninsula, Japan Earth and Planetary Science Joint Meeting (Chiba, May 26-29, 2003).

濱元栄起, 山野　誠, *後藤秀作*、海底堆積物中の長期温度計測による熊野トラフ海域における地殻熱流量の測定, 地球惑星科学関連学会 2003 年合同大会予稿集(千葉, 2003年5月26日-29日).

Hamamoto H., M. Yamano, O. Matsubayashi, ***S. Goto***, Heat flow measurement in shallow seas through long-term temperature monitoring, The 23rd General Assembly of the International Union of Geodesy and Geophysics (IUGG2003) (Sapporo, June 30-July 11, 2003).

Kinoshita, M., ***S. Goto***, H. Hamamoto, M. Yamano, Heat flow distribution and thermal regime across the Nankai accretionary complex, AGU Fall Meeting (San Francisco, December 8-12, 2003).

木下正高, 山野　誠, *後藤秀作*、熱流量観測等から推定された南海トラフ付加体の間隙水湧出の規模, 地球惑星科学関連学会2003年合同大会(千葉, 2003年5月26日-29日).

Kinoshita, M., M. Yamano, ***S. Goto***, S. Gulick, H. Mikada, Fluid flow regime along the western Nankai accretionary complex detected by closely-spaced heat flow measurement, The 23rd General Assembly of the International Union of Geodesy and Geophysics (IUGG2003) (Sapporo, June 30-July 11, 2003).

Okubo, Y., H.-C. Kim, Y. Uchida, ***S. Goto***, J. Safanda, Borehole data and climate reconstruction in Korea, 2003 Korea-Japan Joint Seminar on Geophysical Techniques for Geothermal Exploration and Subsurface Imaging (Daejeon, Korea, September 22-26, 2003).

Yamano, M., ***S. Goto***, Temperature monitoring in a borehole drilled into an active fault zone: water injection experiments and natural groundwater outflow, The 23rd General

Assembly of the International Union of Geodesy and Geophysics (IUGG2003) (Sapporo, June 30-July 11, 2003).

Yamano, M., ***S. Goto***, H. Hamamoto, Effects of water injection and groundwater outflow on the temperature profile in a borehole drilled into the Nojima fault zone, Japan Earth and Planetary Science Joint Meeting (Chiba, May 26-29, 2003).

Hase, H., T. Ishido, S. Takakura, K. Sato, T. Hashimoto and Y. Tanaka, Zeta potential measurement of various rocks on Aso volcano, IUGG2003, Sapporo, Japan, July, 2003.

Hase, H, T. Hashimoto, S. Sakanaka and Y. Tanaka, Hydrothermal system beneath Aso volcano as inferred from Self-potential mapping, IUGG2003, Sapporo, Japan, July, 2003.

井上直人・田中靖之・伊藤陽之・岩野祥子・北田奈緒子・福田洋一・*竹村恵二*：京都盆地における 2 次元重力解析より推定された堆積層の密度－堀川・巨椋池，久世橋，丸太町測線－，日本第四紀学会 2003 年大会（大阪市立大学，2003 年 8 月）

Kawamoto, T., Raman spectra of liquid H_2O under high temperature and high pressure. Goldschmidt Conference, Geochimica Cosmochimica Acta Supplement, p. A207, September, 2003, Kurashiki, Japan.

Kawamoto, T., Matsukage, K.N., Mibe, K., Nishimura, K., Isshiki, M., Ishimatsu, N., and Ono, S. (2003) H_2O-rich magmas or silicate-rich H_2O fluids? A perspective from high pressure and temperature experiments. European Geophysical Society, American Geophysics Union, European Union of Geoscience, Joint Assembly, p. EAE03-A-01670, April, 2003, Nice, France.

Mibe, K., Kanzaki, M., ***Kawamoto, T***., Matsukage, K.N., Fei, Y., and Ono, S. (2003) Direct observation of immiscible fluids using X-ray radiography. Goldschmidt Conference, Geochimica Cosmochimica Acta Supplement, p. A289, September, 2003, Kurashiki, Japan.

川本竜彦、マグマの発泡をその場観察する。2003年地球惑星科学関連学会合同大会、幕張メッセ、千葉、2003年5月

川本竜彦、松影香子、三部賢治、一色麻衣子、西村光史、石松直樹、小野重明、マントル鉱物と共存するH_2OフルイドのMg/Siの圧力変化のその場観察。2003年地球惑星科学関連学会合同大会、幕張メッセ、千葉、2003年5月

三部賢治、神崎正美、*川本竜彦*、松影香子、Y. Fei、小野重明、Direct observation of immiscible aqueous fluid and silicate melt using X-ray radiography. 2003年地球惑星科学関連学会合同大会、幕張メッセ、千葉、2003年5月

西村光史、杉本健、小林哲夫、山下茂、*川本竜彦*、雲仙火山噴出物中にみられる結晶急成長とメルト包有物の形成。2003年地球惑星科学関連学会合同大会、幕張メッセ、千葉、2003年5月

岡田卓、小松一生、日野原邦彦、*川本竜彦*、鍵裕之、ラマンスペクトルの圧力依存性からみた高圧下での水の構造変化。日本鉱物学会 2003 年度年会，仙台市戦災復興記念館、仙台市、2003 年 10 月

岡田卓、小松一生、日野原邦彦、*川本竜彦*、鍵裕之水のラマンスペクトル圧力依存性と水素結合状態の変化。第44回高圧討論会、慶応義塾大、東京、2003年11月

Nishimura K., Crystal capture and settling in granitic magma chambers, Fifth Hutton Symposium (Toyohashi, 2003)

西村光史・杉本健・小林哲夫・山下茂・川本竜彦, 雲仙火山噴出物中にみられる結晶急成長とメルト包有物の形成, 地球惑星科学関連学会 2003 年合同大会(幕張, 2003 年 5 月)

西村光史, 珪長質マグマ溜まりの固結前線における沈降結晶の捕獲, 地球惑星科学関連学会 2003 年合同大会(幕張, 2003 年 5 月)

Ohsawa, S., Yuji Onda, Nobuki Takamatsu : Change in color of thermal water of Umi-Jigoku hot pool in Beppu city, central Kyushu, Japan. 38th International Conference of SITH in collaboration with OMTh, Joint Conference with the 56th Meeting of the Balneological Society of Japan, B-con Plaza（Beppu）, September 25-October 1, 2003.

柴田知之・巽 好幸・酒寄 淳、史、東北日本孤蔵王火山に共存するソレアイト・カルクアルカリ両系列火山岩の地球化学、地球惑星科学関連学会合同大会、幕張、2003.

柴田知之・巽 好幸・酒寄 淳、東北日本孤蔵王火山に共存するソレアイト・カルクアルカリ両系列火山岩の成因、質量分析学会同位対比部会、伊東、2003.

巽好幸, 宿野浩司, 佐藤佳子, *柴田知之*, *芳川雅子*, The Petrology and Geochemistry of High-Mg Andesites at the Western Tip of the Setouchi volcanic belt, SW Japan, 地球惑星科学関連学会 2003 年合同大会, 幕張, 2003 年 5 月.

宮崎隆, *柴田知之*, *芳川雅子*, 表面電離型質量分析計による鉛同位体分析のための新しいシリカゲル合成方法, 質量分析学会同位体比部会, 伊東, 03 年 11 月

Chang, Q., ***Shibata, T.***, Shinotsuka, K., ***Yoshikawa, M.***, and Tatsumi, Y., Precise determination of rare earth elements and yttrium in GSJ standard rock sample JP-1 (Peridotite) by microconcentric desolvating nebulisation ICP-MS, Geochim. Cosmochim. Acta, *67-18S, A57* , *abs*. of Goldschmidt Conf. 2003, Kurashiki, Japan, 2003.

土志田正二・*竹村恵二*・岡田篤正： 京都盆地における地下構造の三次元解析. 地球惑星科学関連学会 2003 年合同大会 （幕張メッセ, 千葉, 2003 年 5 月）

兵頭智至・下山正一・*竹村恵二*:別府湾地溝の南側地塊における第四紀層序と地層変形形態について. 日本地質学会西日本支部(広島大学理学部:2004 年 2 月 14 日)

伊藤浩子・北田奈緒子・岩城啓美・諏訪靖ニ・*竹村恵二*・三田村宗樹:京都盆地の表層地質ーボーリングデータベースと地質分析からの検討. 日本第四紀学会 2003 年大会（大阪市立大学, 2003 年 8 月）

岩城啓美・伊藤浩子・北田奈緒子・諏訪靖ニ・林田 明・*竹村恵二*:磁気的手法を用いた神戸港沖コア試料の対比. 日本第四紀学会 2003 年大会大阪市立大学, 2003 年 8 月

Kaneda, H.., ***Takemura, K***. and Kanehara, M.: Pit Excavation on a Mountain Slope: A Possible Paleoseismic Investigation for Short and Low Slip-rate Faults without Suitable Sites for Trenching. XVI INQUA Congress, Reno, USA, July 2003

Kusumoto, S. and ***Takemura, K***.: Numerical simulation of caldera formation due to collapse of a magma chamber. IUGG, Sapporo, June 2003

楠本成寿・*竹村恵二*:マグマ溜りの崩壊に起因するカルデラ形成の数値モデリング. 地球惑星科学関連学会 2003 年合同大会 （幕張メッセ, 千葉, 2003 年 5 月）

楠本成寿・*竹村恵二*:カルデラの規模を決めるマグマ溜りの深さと収縮量の関係. 地震学会（京都国際会館:2003年10月）

楠本成寿・*竹村恵二*:カルデラ形成に必要なマグマ溜まりの収縮. 火山学会（九州大学, 福岡, 2003年10月）

金　幸隆・岡田篤正・*竹村恵二*:信濃川活褶曲帯における累積変位地形の3つの特徴. 地球惑星科学関連学会2003年合同大会（幕張メッセ, 千葉, 2003年5月）

北田奈緒子・斎藤礼子・伊藤浩子・岩城啓美・諏訪靖ニ・*竹村恵二*・三田村宗樹: 大阪平野部の沖積層について. 日本第四紀学会2003 年大会（大阪市立大学, 2003年8月）

北田奈緒子・伊藤浩子・三村　衛・*竹村恵二*:京都盆地の表層の地盤について－ボーリングデータベースを用いた検討－. 平成15年度京都大学防災研究所研究発表講演会（京都テルサ:2004年2月19日－20日）

中村洋介・金　幸隆・岡田篤正・*竹村恵二*:金沢市街地における河成段丘の形成時期と森本－富樫断層帯野町撓曲の第四紀後期における上下平均変位速度. 地球惑星科学関連学会2003年合同大会（幕張メッセ, 千葉, 2003年5月）

中西利典・*竹村恵二*・東郷正美ほか:ボーリング試料分析による養老断層の完新世の活動 地球惑星科学関連学会2003年合同大会（幕張メッセ, 千葉, 2003年5月）

中西利典・*竹村恵二*・岡田篤正:ボーリング試料分析による濃尾平野西麓断層帯の完新世の活動. 日本第四紀学会2003 年大会（大阪市立大学, 2003年8月）

Takemura, K., Hayashida, A. Nakagawa, T., Kitagawa, H., Yasuda, Y. : Lake Biwa Sediments in Japan: Recorders of Global Paleoenvironments during 450ka. Third Limnogeological Congress, Tucson, Texas, USA, March-April 2003.

Takemura, K., Hayashida, A., Nakagawa, T., Kitagawa, H., Yasuda, Y., Yokoyama, T., Horie, S. and Meyers, P. A.: Lake Biwa Sediments in Japan: Recorders of Global Paleoenvironment and Island Arc Tectonics since Pliocene. XVI INQUA Congress, Reno, USA, July 2003.

Takemura,K. Tectonic movements in the central Kyushu, Japan. 国際温泉科学会公開講演, (International Convention Center, Beppu, September, 2003)

竹村恵二・北田奈緒子・横田　裕・末廣匡基・中川信夫:京都盆地の深部構造について. 平成15年度京都大学防災研究所研究発表講演会（京都テルサ:2004年2月19日－20日）

谷美由起・堤　浩之・小松原　琢・*竹村恵二*ほか 1596年慶長伏見地震における有馬・高槻断層帯の破壊領域. 地球惑星科学関連学会2003年合同大会（幕張メッセ, 千葉, 2003年5月）

Okubo A., ***Y,Tanaka***, ***M. Utsugi***, ***N. Kitada***, H. Shimizu, T. Matsushima, Aeromagnetic survey over Unzen Volcano, IUGG 2003, 10, July, 2003, Sapporo Japan.

大久保綾子、*田中良和*、*宇津木充*、*北田直人*、清水洋、松島健、雲仙火山における空中磁気観測について、京都大学防災研究所講演会,2003.

大久保綾子、*田中良和*、*宇津木充*、*北田直人*、清水洋、松島健、雲仙火山における空中磁気観測、地球惑星科学関連学会合同大会,2003(幕張メッセ, 千葉, 2003年5月).

大久保綾子、*田中良和*、*宇津木充*、*北田直人*、清水洋、松島健、低高度な高密度空中磁気測量から推定される雲仙火山とその周辺の磁化構造、物理探査学会,2003(大阪)

大久保綾子、*田中良和*、*宇津木充*、*北田直人*、清水洋、松島健、低高度な高密度空中磁気測量から推定される雲仙火山とその周辺の磁化構造、地球電磁気学・地球惑星圏学会,2003(富山)

大久保綾子、*田中良和*、*宇津木充*、*北田直人*、清水洋、松島健、High-Resolution, Low-Altitude Helicopter-Bone Aeromagnetic Survey over Unzen Volcano, Kyushu Japan、CA 研究会講演会,2003(北海道)

Utsugi M., ***Y. Tanaka***, S. Sakanaka, K. MatsushimaKyusyu, T. Hashimoro, ***N. Kitada***, Height Resolution Helicopter-Borne Aeromagnetic Survey in Aso Volcano, Central Kyushu Island of Japan, IUGG 2003, 10, July, 2003, Sapporo Japan.

Utsugi M.,N. Shirai, H. Hamasaki, T Nishiki and S. Fujiwara, Regional model of the geomagnetic annual changes in and around Japan Island based on NOC and SCH analysis, IUGG 2003, 10, July, 2003, Sapporo Japan.

宇津木充, 田中良和、橋本武志、北田直人、阿蘇火山における高密度空中磁気観測、特定領域研究「火山爆発のダイナミックス」平成 15 年度シンポジウム(東京, 2004 年 3 月 1 日-3 日).

神田 径, 田中良和, *宇津木 充*, 北田直人, 後藤秀作, 大野正夫(2003)諏訪之瀬島火山における自然電位連続観測, 2003 年度 CA 研究会「火山流体の分布とその挙動」(北海道虻田町, 2003 年 12 月 2 日-4 日).

神田 径, 田中良和, *宇津木充*, 橋本武志, 北田直人, 後藤秀作, 大野正夫(2004)地磁気および自然電位による火山爆発場の観測的研究, 特定領域研究「火山爆発のダイナミックス」平成 15 年度シンポジウム(東京, 2004 年 3 月 1 日-3 日).

高橋俊郎・*芳川雅子*・*柴田知之*・巽好幸、 斜長石斑晶の高精度局所 Sr 同位体比分析、火山学会、福岡、03 年 10 月

巽好幸, 宿野浩司, *芳川雅子*, 常青, 佐藤佳子, 李文遠, 済州島火山岩類の岩石学・地球化学:東アジア東縁のマントルプルーム, 火山学会, 福岡, 03 年 10 月

高橋俊郎・*芳川雅子*・*柴田知之*・巽好幸、斜長石斑晶の高精度局所 Sr 同位体比分析、質量分析学会・質量分析学会同位体比部会、伊東市、03 年 11 月

山本順司, 流体包有物圧力計ー捕獲岩への適用ー. 2004 Spring Mantle Xenoliths Workshop in Kanazawa (石川, 2004 年 3 月

山本順司, マントルウェッジ中の水の在り処. 2004 Spring Mantle Xenoliths Workshop in Kanazawa (石川, 2004 年 3 月)

山本順司, 沈み込み由来流体の直接探査に向けて:地質圧力計や局所分析を用いたマントルウェッジの 3 次元構造の解明. 東北アジアマントル研究集会 (神奈川, 2004 年 1 月)

Yamamoto J. and Burnard P. G., Solubility controlled noble gas fractionation during magmatic degassing. 質量分析学会同位体比部会 (静岡, 2003 年 11 月)

Yamamoto J., Hirano N., Hanyu T., Kagi H. and Kaneoka I., Noble gases in mantle-derived xenocrysts in an alkali basalt from Japan Trench oceanward slope. Plume and problems of deep sources of alkaline magmatism, September 2003, Khabarovsk, Russia

Yamamoto J., Kagi H., Kawakami Y., Kaneoka I., Lai Y., Prikhod'ko V. S. and Arai S. Fossil pressures of fluid inclusions in mantle xenoliths: implications for geobarometry of mantle minerals using micro Raman spectroscopy. Goldschmidt conference, September 2003, Kurashiki, Japan

共同研究　Collaborations

国内

後藤秀作:熊野海盆泥火山における海底長期温度モニタリング(東大地震研・山野, 濱元, 東大海洋研・芦, 産総研・森田, 日大・藤野)

後藤秀作:熊野沖南海トラフ沈み込み帯の温度構造の推定(東大地震研・山野, 濱元, JAMSTEC・木下)

川本竜彦:東京大学地震研究所　一般共同研究、研究員

川本竜彦:愛媛大学地球深部ダイナミクス研究センター　客員研究員

川本竜彦:岡山大学固体地球研究センター　嘱託研究員

川本竜彦:スプリング８高輝度光科学研究センター　外来研究員

大沢信二:秋吉台の陸水の地球化学的・色彩学的研究　参加機関:東邦大学理学部化学科

大沢信二:河川に及ぼす温泉水の影響評価に関する環境化学的研究　参加機関:東邦大学理学部化学科

竹村恵二:「京都盆地の地盤に関する研究」関西地盤情報活用協議会

竹村恵二:「大阪湾海底地盤に関する研究」大阪湾海底地盤情報活用協議会:京都大学防災研究所一般共同研究　代表:地盤データベースを活用した堆積平野地盤の高精度地質学的分析と都市地盤防災への適用に関する研究 (担当者:三村　衛)

国際

後藤秀作:都市の地下環境に残る人間活動の影響(代表:地球研・谷口)

後藤秀作:韓国の地下温度データを利用した気候変動復元の研究(産総研・大久保, 内田, KIGAM・Kim Hyoung Chan)

井上(北田)直人:韓国全谷里遺跡周辺の電気探査(同志社大学・Hanyang University, 2003 年 9 月 23 日～28 日)

竹村恵二:「High resolution reconstruction of Holocene environmental changes from lagoonal sediments along the East Sea (the Japan Sea)」(Prof. Yu, Yonsei University, Korea)

竹村恵二:ICDP Project "Lake Biwa and Lake Suigetsu: Recorders of Global Paleoenvironments and Island Arc Tectonics"

田中良和・宇津木充:ロングバレーカルデラにおける電磁気観測(USGD)

定常観測 Routine Observations

Geophysical Monitoring Under Operation at AVL

Aso Volcanological Laboratory

Permanent Stations

Nakadake monitoring system

Seismic Stations : HNT, PEL, KSM, SUN, KAE, KAE; KAN, UMA, TAK(microwave telemetry)

Tiltmeters : HNT(water tilt 3-comp.), SUN, KAE, NAR, KAK (on-site logging)

Extensiometers : HNT(invar 3-comp.)

Microphone : HND(microwave telemetry)

Geomagnetic Stations : C1, C3, S0, W1, CS, NGD, FF1 (proton; on-site logging)
C223(fluxgate 3-comp.; on-site), newC223(fluxgate 3-comp.; online),
FF2 (proton; on line)

Ground Temperature : KAK (boreholes of 70 and 150 m deep; microwave telemetry)

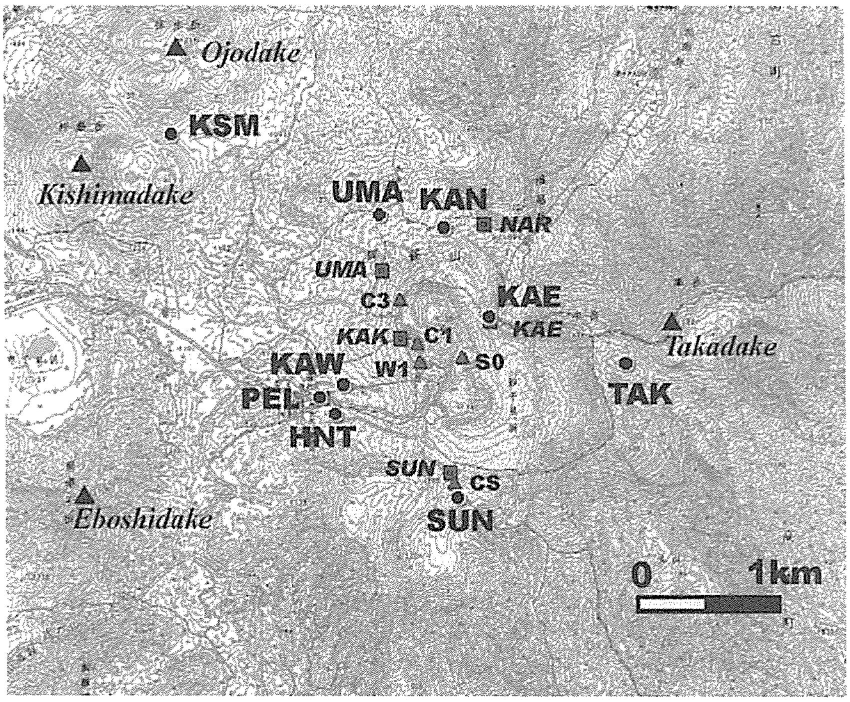

Seismic, geodetic and geomagnetic stations in the central part of Aso Volcano.

Kuju monitoring system

Seismic Stations : HNG(radio-telemetry), AKG, CJB, IOY(on-site logging)

Tiltmeters : H283, KSR (on-site logging)

Geomagnetic Stations : N2, E1, S0, SE (proton; on-site logging)

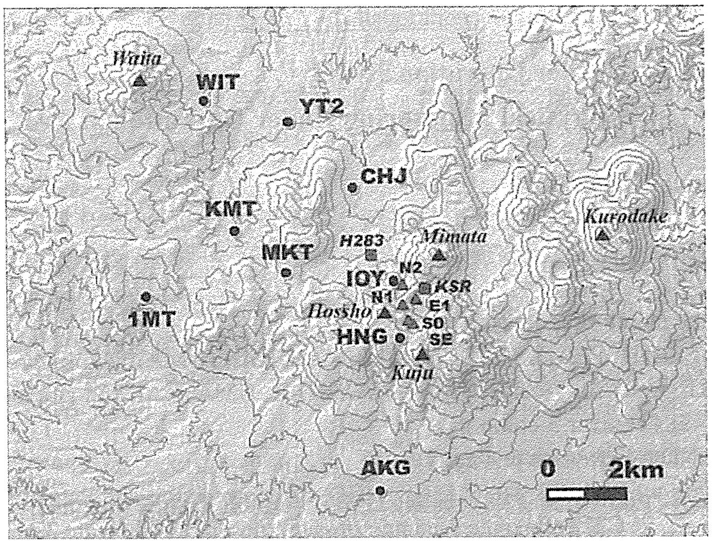

Seismic, geodetic and geomagnetic stations in the central part of KujuVolcano.

Central Kushu regional network

Seismic Stations : AVL(6), MAK, NBR, MKN, HDK, TAT, MGR(online telemetry),
ASJ, HNY, SKM, KBM, TRM(dial-up)

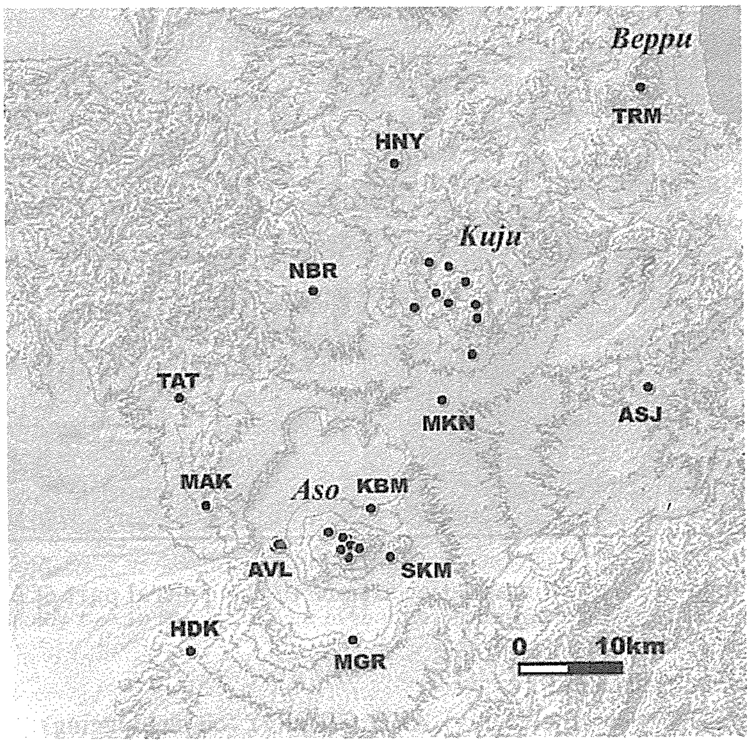

Seismic network in the central Kyushu

観測・実験システム　Observation and Experimental System

Analytical procedure of Sr, Nd, Pb isotopes from rock and mineral samples

***Masako Yoshikawa*, *Tomoyuki Shibata*,** *Takashi Miyazaki and Toshiro Takahasi,*
Yoshiyuki Tatusmi and ***Yuki Yusa***

The analytical procedure for chemical separation and mass spectrometry basically followed Yoshikawa et al. (2001) and Takahashi and Yoshikawa (in this report) for Sr isotopic ratio and Shibata et al. (2000) for Nd isotopic ratio and Koide and Nakamura (1990) and Miyazaki et al. (2003) for Pb isotopic ratio.

Sample decomposition

For Sr and Nd analyses, the samples were decomposed by HF + $HClO_4$ in a 7ml teflon beaker on a hot plate at 100C. The sample solution was evaporated to dryness. After that $HClO_4$ was add to the dried sample and evaporated to dryness. By this decomposition procedure, sample is decomposed completely without precipitation of a fluoride (Yokoyama et al., 1999), which prevents the chemical separation of Sr and Nd (Yoshikawa and Nakamura, 1993; Boer et al., 1993).

The samples for Pb analyses was decomposed by HF + HBr in a 7ml teflon beacker on hot plate at 100C. The dissolved sample was dried and the dried sample was dissolved in 0.5M HBr. After that the solution was centrifuged to remove fluoride deposits.

Chemical separation

The dried sample for Sr and Nd isotope analyses was dissolved with 1ml HCl (2.5M) to be loaded onto the ion-exchanged column. Sr and Nd were separated with 2.5M HCl and 6M HCl using 1ml cation-exchange chromatography in H^+ form (Muromac AG50W-X8 resin). Sr was purified with 0.06M DCTA in 0.5N pyridine, distilled water and HCl using 0.3ml cation-exchange chromatography in pyridinium form. Nd was purified with 0.22M hydroxy-alpha-isobutric acid using 0.3ml cation-exchange chromatography in pyridinium form.

Pb was separated with 0.5M HBr and distilled water using 0.1ml anion-exchange chromatography in Br^- form. Pb was purified using the same column with the same procedure described above. Total procedure blank of Sr, Nd, Pb are 1pg, 2 pg, and 5 pg, respectively. This low level, comparing to world widely, of blank is low enough to analyze the rock and mineral samples extremely depleted in Sr, Nd and Pb.

Mass spectrometry

Sr, Nd, Pb samples were loaded onto Re filaments with Ta-solution (Birck et al., 1986), HNO_3 and silica-gel (Miyazaki et al., 2003), respectively. Mass spectrometry was carried out on a Triton

TI instruments at BGRL installed by the Institute for Frontier Research on Earth Evolution, Japan Marine Science and Technology Center. The isobaric interference of 87Rb to 87Sr and 144Sm to 144Nd were corrected by monitoring 85Rb and 147Sm, respectively. The normalizing factors to correct for isotopic fractionation for Sr and Nd are $^{86}Sr/^{88}Sr = 0.1194$ and $^{146}Nd/^{144}Nd = 0.7219$, respectively. The averaged correction factor of 25 measurements relative to the values of NIST SRM 982 (Catanzaro et al., 1968) is 0.140 % per mass unit. Measured ratios for standard materials were $^{87}Sr/^{86}Sr = 0.710279 \pm 0.000028$ (2σ) for NIST SRM987 ($n = 5$) ,$^{143}Nd/^{144}Nd = 0.511851 \pm 0.000013$ (2σ) for La Jolla ($n = 9$), $^{208}Pb/^{204}Pb = 36.705 \pm 0.013$ (2sd.) $^{207}Pb/^{204}Pb = 15.493 \pm 0.004$ (2sd., and $^{206}Pb/^{204}Pb = 16.938 \pm 0.003$ (2sd.) for the NIST SRM981 (n = 20).

References

Birck, L. J. (1986) Precision K-Rb-Sr isotopic analysis: application to Rb-Sr chronology, *Chem. Geol.*, 56, 73-83.

Boer, R.H., Beukes, G.J., Meyer, F.M. and Smith, C.B. (1993) Fluoride precipitation in silicate wet-chemistry: implications on REE fractionation, *Chemi. Geol.*, 104, 93-98.

Catanzaro, E.L., Murphy, T.J., Shields, W.R. and Garner, E.L. (1968) Absolute isotopic abundance ratios of common, equal-atom, and radiogenic lead isotopic standard. Jour. Res. Nation. Bureau Stand. A, 72A, 261-267.

Koide, Y and Nakamura, E. (1990) Lead isotope analysis of standard rock samples. Mass Spectroscopy, 38, 241-252.

Miyazaki et al. (2003) New sysntesis method of silica-gel for lead isotope analysis. Proc. Japan Acad., 79, 58-62.

Shibata, T. Yoshikawa, M. and Tatsumi, Y. (2000) An analytical method for determing precise Sr and Nd isotopic compositions and results for thirteen rock standard materials, IFREE report, 1, 363-367.

Takahashi, T. and Yoshikawa, M. (in this report) Precise isotope determination of trace amount of Sr aims at the in situ Sr isotope analysis by microdrilling technique.

Yokoyama, T., Nakamura, E. and Makishima, A. (1999) Separation of thorium and uranium from silicate rock samples using two commercial extraction chromatographic resins, *Anal. Chem.*, 71, 135-141.

Yoshikawa, M. and Nakamura, E. (1993) Precise isotope determination of trace amounts of Sr in magnesium-rich samples, *J. Min. Pet. Econ. Geol.*, 12, 548-561.

Yoshikawa, M. and Shibata, T. and Y. Tatsumi (2000) The Sr, Nd and Pb isotopic ratios of GSJ standard rocks, Annual report of Institute for Geothermal Sciences, Kyoto-Univ., 30.

装置　Instruments

【別府】

ICP 発光分光分析装置

波長分散型電子プローブマイクロアナライザー

エネルギー分散型電子プローブマイクロアナライザ

波長分散型蛍光 X 線分析装置

エネルギー分散型蛍光 X 線分析装置

端末 X 線回折装置

液体シンチレーションシステム

イオンクロマトグラフ

ガスクロマトグラフ

Tiltmeters

自動滴定装置

ピストンシリンダー型高圧発生装置

ICP-MS 用レーザーアブレーション装置

四重極型 ICP-MS 装置

表面電離型質量分析装置

外熱式ダイアモンドアンビル

フーリエ変換型近赤外分光光度計

赤外顕微鏡

加熱ステージ

ラマン顕微鏡

【阿蘇】

阿蘇、九重火山連続地震観測システム

地殻変動観測坑道

孔中温度観測システム

ビデオ映像監視システム

プロトン磁力計

フラックスゲート磁力計

地磁気絶対観測システム

傾斜計

可搬型地震計(広帯域、短周期)

人工震源車

重力計

地磁気地電流測定装置(広帯域,ULF,ELF,VLF 型)

光波測距儀

水準測量システム(自動読み)

【Beppu】

ICP emission Spectrometer

Wavelength dispersive electron mincroprobe

Energy dispersive electron mincroprobe analyzer

Wavelength dispersionty type X-ray Fluorescence analyzer

Energy dispersionty type X-ray Fluorescence analyzer

Power X-ray diffractometer

Liquids scintillation system

Ion chromatography

Gas chromatography

Automatic titration system

Piston cylinder type high pressure apparatus

Laser ablation system

Inductively coupled plasma mass spectrometer(ICP-MS)

Thermal ionization mass spectrometer(TIMS)

Externally heated diamond anvil cell

FT-NIR spectrometer

IR microscope

Heatings stage

Raman microscope

【Aso】

Continuous seismic monitoring system for Aso and Kuju Volcanoes

Observation tunnel for ground deformation

Borehole temperature monitoring system for Aso

Video monitoring system of Aso and Kuju Volcanos

Proton and Fluxgate magnetometers

Geomagnetic absolute measurement system

Portable seismometers (broadband and short period)

Car-mounted seismicsource

Cravimeters

Magneto-Telluric measurement system (broadband, ULF, ELF, VLF-band)

Electronic distance measurement system

Leveling survey system (automatic reading)

設備　Facilities

【別府】

岩石粉砕・鉱物分離室

パックミル・ディスクミルによる岩石粉砕やアイソダイナミックセパレータによる鉱物分離行う。

器具洗浄室

実験に用いる器具の洗浄を行う。ドラフト2台、イオン交換筒、Milli-Qが設置されている。

クリーンルーム

HEPAフィルターを設置し極力金属使用を控えた設計で、クラス100のクリーン度を達成している。Sr・Nd・Pb同位体比分析のための化学処理(試料の分解・イオン交換クロマトグラフィーによる目的元素の抽出)を行っている。

【阿蘇】

地下観測坑道(阿蘇火山地殻変動観測坑道)

阿蘇中岳第一火口から南西1km、地下30mに設けられた直角三角形の水平坑道で,1987年度に竣工した。現在は、水管傾斜計(25m)、伸縮計(20,25m)、短周期地震計、長周期地震計、広帯域地震計が設置されている。

火山研究センター構内地震観測システム

火山センター構内では、従来からトリパタイトによる地震観測を行ってきたが、平成13年度にノイズ軽減の為約200mのボーリング孔を4本掘削し、孔底に地震計を導入した。これにより、S/N比は大幅に改善され、従来識別できなかった中岳の長周期微動が検出されるようになった。また、ボーリングコアを採取した事により、研究センターの丘、高野尾羽根(あかのおばね)火山について地質学的に新たな知見が得られつつある。これは、阿蘇中央火口丘の噴火氏を研究する上でも貴重な資料である。

火山研究センター地磁気基準観測システム

火山研究センターの北西側斜面には、オーバーハウザー型磁力計及びフラックスゲート磁力計が設置されており､それぞれ1秒及び0.1秒サンプリングで地磁気全磁力及び磁場3成分の連続観測が行われている。フラックスゲート磁力計は、温度変化の影響を除くため、約50mの水平坑の最深部に設置されている。それぞれの測定精度は全磁力が0.01nT、磁場3成分が0.1nTである。

研究費 Funding

科学研究費補助金

大沢信二　科学研究費補助金　基盤研究（C）「水文化学的手法による火山湧水からのマグマ起源二酸化炭素の流出フラックスの評価」1700 千円

田中良和　科学研究費補助金　特定領域研究(2)「火山爆発の発生場と発生過程」 58700 千円

田中良和　科学研究費補助金　基盤研究(B)「空中磁気測量による火山性磁場変動の検出」 3800 千円

受託研究

竹村恵二　科学技術振興調整費　雲仙掘削　雲仙地溝の活構造解析 3, 090 千円

田中良和　科学技術振興調整費　雲仙掘削　雲仙地溝の活構造解析　1626 千円

田中良和　文部科学省独創的革新技術開発研究提案公募研究
「総合空中探査システムを用いた大規模災害の防災技術に関する研究」

奨学寄附金等

川本竜彦：日産科学振興財団研究助成（奨励研究）富士火山の下でのマグマとH_2Oフルイドの間の超臨界現象 4, 000 千円

川本竜彦　倉田奨励金（倉田記念日立科学技術財団）高温高圧力条件における立方晶窒化ホウ素の状態方程式とラマン散乱 1, 500 千円

川本竜彦　京都大学教育研究振興財団・海外派遣助成　高温高圧力条件における水とマグマの分光学（IPGP、フランス）2,550 千円

共同研究等

大沢信二　産業総合技術研究所深部地質環境研究センター受託費「地層処分にかかる広域地下水流動系の研究」2216 千円

竹村恵二　京都大学防災研究所一般共同研究　（代表：竹村恵二, 担当者：三村　衛）850 千円

竹村恵二　経済産業省原子力保安院　「地表断層の形状の三次元化及び高精度化と深部起震断層との相関」（代表：岡田篤正）8, 369 千円

教育活動　Education

学位審査

須藤靖明
（審査員）吉川美由紀（博士　京都大学大学院理学研究科）
竹村恵二
（審査員）金　幸隆（博士　京都大学大学院理学研究科）
（審査員）金田平太郎（博士　京都大学大学院理学研究科）
（審査員）中村洋介（博士　京都大学大学院理学研究科）
（審査員）中西利典（博士　京都大学大学院理学研究科）

（審査員）土志田正二（修士　京都大学大学院理学研究科）
（審査員）木下朋和（修士　京都大学大学院理学研究科）
（審査員）井上　勉（修士　京都大学大学院理学研究科）
（審査員）松岡　暁（修士　京都大学大学院理学研究科）
田中良和
（審査員）長谷英彰（博士　京都大学大学院理学研究科）
（審査員）相沢広記（博士　京都大学大学院理学研究科）
（審査員）吉川美由紀（博士　京都大学大学院理学研究科）

講義・実習

科目	担当教官
（学部）	
地球熱学	由佐悠紀・竹村恵二・大沢信二・古川善紹
課題演習 D3　地下構造と活構造・地表変動	岡田篤正・竹村恵二・堤　浩之・赤松純平・福岡　浩・岩田知孝
課題研究 T8 地表変動・固体地球物理・火山物理	岡田篤正・竹村恵二・須藤靖明・堤　浩之・入倉孝次郎・佐々恭二
（大学院・修士課程）	
第四紀地質学	竹村恵二
地球熱学・地熱流体学 II	竹村恵二・須藤靖明・古川善紹・大倉敬宏
応用地球科学ゼミナール I	岡田篤正・竹村恵二・堤浩之・小松原　琢

応用地球科学ゼミナール II	岡田篤正・竹村恵二・堤浩之・小松原　琢
地球惑星科学特殊研究(修士論文)	

(大学院修士課程および博士後期課程)

地球熱学・地熱流体学ゼミナール II	竹村恵二・須藤靖明・古川善紹・大倉敬宏
応用地球科学ゼミナール I	岡田篤正・竹村恵二・堤浩之・小松原　琢
応用地球科学ゼミナール II	岡田篤正・竹村恵二・堤浩之・小松原　琢
地球生物圏史セミナー	増田富士雄・前田晴良・竹村恵二・ 大野照文

野外実習

地熱学野外実習

応用地球科学現地実習　(6 月 1 日～6 月 4 日)

講義・セミナー(他機関など)

大沢信二　非常勤講師:大分大学教育福祉科学部「環境科学入門」(2003 年 7 月 28 日-31 日)

竹村恵二　集中講義:九州大学総合理学特別講義 VI

芳川雅子 「造山帯幌満かんらん岩体の地球化学的進化過程」、セミナー『衝突型造山運動、島弧地殻形成論、西太平洋三角地帯』、東工大地球史資料館、5月

芳川雅子 「上部マントル物質に記録されたスラブ由来流体による化学・同位体組成変化」「リソスフェアの流体:地質学・水理学・地球化学の接点」ワークショップ」1 月　京都大学理学研究科附属地球熱学研究施設セミナー室

柴田知之、放射起源同位体・微量元素組成を用いた沈み込み帯における物質循環の研究、21 世紀 COE(KAGI)J2 ミニシンポジウム、別府、2004.

招待講演

Kawamoto, T., "Direct observations of water and magmas beneath volcanoes" 2, March, 2004, Laboratoire Magmas et Volcans, Univ. Blaise Pascal, Clermont-Ferrand, France

地熱学ゼミナール

平成 15 年

4 月 16 日　大沢信二「台風の地球化学」

5 月 7 日　川本竜彦「地球内部条件でのマグマと水の観察」“Direct observation of magmas

and aqueous fluids under high pressure and temperature conditions"

5月21日　柴田知之　「東北日本弧蔵王火山に共存するソレアイト・カルクアルカリ両系列火山岩の地球化学」

6月4日　山田「九重火山周辺湧水に溶け込む火山性CO_2」

6月18日　中川毅「花粉分析　伝統的手法が変貌するとき」

7月2日　網田和宏「別府地域における電磁気学的研究」

9月24日　China Chen" What did I do?　What shall I do?"
　　中川毅「気候変動の入れ子構造、および製品紹介」

10月15日　Jianguo Du ″Carbon isotope compositions of gases produced from Lignite pyrolysis at HDT″

10月29日　西村光史「雲仙1991-1995噴出物中のメルト包有物の形成条件とマグマ溜まりダイナミクス」

11月5日　共同研究紹介　高橋俊郎・芳川雅子・柴田知之・巽好幸「第四紀蔵王火山の斜長石局所Sr同位体比」

11月19日　竹村恵二「西南日本の第四紀テクトニクスの画期」

12月3日 Jianguo Du　″Introduction for Tengchong volcanic area and analyzing purpose″

平成16年

1月21日　山田「火山地域におけるマグマ起源流体の浅層地下水系への影響」
　　山本順二「プレート沈み込み域のマントルに存在する流体の起源」"The origin of fluid in mantle wedg "

特別セミナー

11月25日　谷健一郎（IFREE）「丹沢複合深成岩体－海洋性島弧火成活動の深部プロセスへのアプローチー」

12月3日　鍵山恒臣（東大地震研）「火山の構造と火山流体の蓄積・移動－九州火山地域研究の課題と展望」

1月30日　鈴木勝彦（IFREE）　「中国のマントルゼノリスのRe-Os同位体」

学会活動 Activities in Scientific Societies

大沢信二

国際交流・広報委員：日本温泉科学会

編集委員：日本地熱学会

川本竜彦

Associate editor for Geochemical journal

須藤靖明

編集委員：日本地震学会

竹村恵二

評議員:日本第四紀学会

編集幹事:第四紀研究

社会活動 Public Relations

大沢信二

大分県温泉調査研究会理事

大分県温泉監視調査委員会委員

京都大学地球熱学研究施設一般公開講演講師（2003年8月1日，ニューライフプラザ）

須藤靖明

桜島運営協議会委員

火山噴火予知連絡会委員

阿蘇火山ガス安全対策専門委員会委員

くじゅう山系(硫黄山)防災協議会委員

九重山系火山砂防基本検討委員会委員

火山研究センター一般公開特別公演講師

竹村恵二

文部科学省　科学技術政策研究所　科学技術動向研究センター　専門調査員

『関西国際空港（二期地区）地盤挙動調査委員会』委員

『京都府地域活断層調査委員会』委員

『地震調査研究推進本部地震調査委員会北日本活断層分科会』委員

『大阪府地下構造調査委員会』委員

『大分県地域活断層調査委員会』委員

『三重県伊勢平野地下構造調査委員会』委員

平成15年（2003）11月9日（土）ふるさと地盤診断ウオーク講師　地盤工学会関西支部.

平成15年(2003)9月12日（金）Univ. Michigan Geological Sciences lecture: Recent progress on active fault research and paleoseismology in Japan after 1995 Kobe Earthquake.

平成15年（2003）8月7日(木)平成15年度九州地区消防実務講習「大分の活断層と地震」

平成15年（2003）8月1日（金）　オープンハウス地球熱学研究施設　講演　「由布・鶴見火山はいつどのような活動をしてきたか？」

平成15年（2003）5月20日(火)　日本文理大学「大分学」講師.「大分の活断層」.

田中良和

測地学審議会火山部会委員

火山噴火予知研究協議会委員

火山噴火予知研究委員会委員

地磁気観測作業委員会委員

火山研究センター一般公開特別公演講師

オープンハウス報告

【別府】

オープンハウス（別府）は以下のように、セミナーと施設内の見学の２本立てで行いました（川本）。

第１回京都大学地球熱学夏休みセミナー

小学生以上を対象に第１回京都大学地球熱学夏休みセミナーを開催しました。

場所　ニューライフプラザ２階視聴覚教室

日時　７月３０日（水曜日）ー８月１日（金曜日）

開場１８時、開演１８時３０分、終演２０時。入場無料。

７月３０日（水曜日）由佐悠紀教授　「南極に温泉はあるか？」

川本竜彦助手　「火山の下で何がおこっているか？」

７月３１日（木曜日）柴田知之助手　「岩石の輪廻転生」

由佐悠紀教授　「温泉のしくみとなぞ」

８月１日（金曜日）大沢信二助教授　「海地獄の色は何の色？」

竹村恵二教授　「由布・鶴見火山はいつ・どのような活動をしてきたか？」

第３回京都大学地球熱学研究施設　一般公開

８月２日（土曜日）９時から１６時まで、第３回京都大学地球熱学研究施設（別府）を一般に公開しました。

【阿蘇】

1. 目的

地域住民、関係機関等に、当センターの活動内容を知って頂くことでセンターに関する関心・理解を得る。また、社会へ学術的知識の還元、啓蒙を図る。

2. 開催日時

平成 15 年 10 月 25 日(土) 9:30～16:00

3. 内容

- ポスター展示(約 30 点)による研究内容の紹介・火山学の一般向け解説
- 公開実験
  - 「地震計のデモンストレーション」(大倉)
  - 「簡易方位磁石による地磁気方位測定」(宇津木)
  - 「火山工作」(吉川美由紀)
  - 「間欠泉実験」(吉川慎、大沢)
- 施設備品展示(旧型地震計等各種観測装置の展示・解説)
- 火山に関するビデオ上映・書籍展示
- パソコンによる展示
  「九州の地震活動リアルタイムモニター」
  「海底観測艇による海底探査の映像」
- 特別公演（午前:須藤靖明、午後:田中良和)
- 見学者パンフレット(大人用、子供用)配布

4. 社会告知の方法

- A3, A4 版ポスターを作成
- 火山研究センターホームページによる告知
- 日の長い一日の村美術館(長陽村秋季イベント)総合パンフレットに掲載

来訪者　Visitors

【別府】

平成15年4月6日（月）松山尚典（応用地質九州）

平成15年4月6日（日）－16日（水）宮田佳樹（東大地震研究所）

平成15年4月7日（月）・8日（火）中川　毅（国際日本文化研究センター）

平成15年4月9日（水）副田宣夫（西日本技術開発）

平成15年4月30日（水）　荒金大琳（別府大学）

平成15年4月30日（水）松山尚典・藤沢康弘（応用地質九州）

平成15年5月18日（日）九州第四紀露頭見学会32名（松田時彦・首藤次男・下山正一・大木公彦・宮田雄一郎・坂井　卓・檀原　徹ほか九大学生・鹿児島大学生・山口大学生・応用地質・復建設計・西日本技術開発など）

平成15年)6月6日（金）岡田篤正ほか10名（京大地球物理）

平成15年6月8日（日）—9日（月）岡田篤正ほか6名（京大地球物理）

平成15年6月11日（水）－12日（木）楠本成寿（東海大海洋）

平成15年6月23日（月）石川祐介（梅林建設）

平成15年８月２－３日　町田　忍

平成15年８月２日　オープンハウス

平成15年８月６－９　学生実習　（地球熱学B）13名

平成15年８月８日　別府市土木部ほか3名

平成15年８月９－１０日　淡路敏之・余田成男

平成15年　　　　近畿地質（株）　　　中津工業高校　立石

平成15年８月21日　大分大学教育福祉科学部附属中学１年生　首藤卓登・工藤詩瑞砂

平成15年８月23－24日　京都教育大学武蔵野実ほか学生

平成15年８月21－22日　九大大学院比較文化研究院酒井治孝ほか院生学生

平成15年８月29日～9月7日　東邦大学　高松信樹、他１名

平成15年９月15－16日　島根大学理工学部横田修一郎ほか院生学生

平成15年９月29-30日　大阪府立大学総合科学部伊藤康人

平成15年10月８日　明大工業江川龍一郎ほか２名

平成15年10月９日　基礎地盤コンサルタント籾倉克幹・永川

平成15年10月17日－19日　京大地質学鉱物学平島崇男，三宅　亮，下林典正，小畑正明，防災研大見士郎，地球物理学中西一郎

平成15年11月16日－17日防災研共同研究集会　（三村衛，末廣匡基，北田奈緒子，山本浩司，佐藤（京都市），松山尚典，植村善博）

平成15年11月21日～23日　京都大学大学院理学研究科地球物理学教室　余田成男，他7名
平成15年12月14日　九大地球惑星：下山正一，兵頭
平成16年1月22日～24日　東邦大学　高松信樹、他1名
平成16年1月23日　京大経理部　竹下・松井・菅野
平成16年2月9日　応用地質（株）松山尚典，川本康司
平成16年2月25日　京大保健管理センター　高山宏江・宇治昭代
平成16年3月4日～8日　東邦大学　高松信樹、他1名
平成16年3月7日－9日　京大地球物理　中西利典
平成16年3月20日　井上（京大総合人間），古川（京大人間環境）
平成16年3月21日～22日　小畑・成瀬ほか学生7名（京大地鉱）（上田，亀井，山本，古崎・藤本・岡本・佐藤），古川（火山研）ほか学生8名（由井，上垣，仲本，宇野，古川，井上，三井，原田）
平成16年3月22日～23日　原口強　（大阪市立大）
平成16年3月23日～24日　横井悟・川田耕二（石油資源）
平成16年3月28日～31日　島根大学沢田順弘ほか学生・院生5名
平成16年3月31日～4月1日　　里村雄彦・内藤陽子（京大地球物理）

【阿蘇】
平成15年5月20－24日　東大地震研　川勝均、東工大　金島聡、高木憲明
平成15年7月11日　渡辺一徳氏他２名、火山博物館 池辺伸一郎 研究打ち合わせ
平成15年7月12日　読売新聞社 宇佐美氏　取材
平成16年7月12－18日　京都大学防災研究所　大久保綾子
平成15年7月13日　RKK熊本放送 黒田氏他3名 取材
平成15年8月3－6　学生実習　（地球熱学A）16名
平成15年8月4－10日　京都大学大学院　人間・環境学研究科院生　古川邦之
平成15年8月9－18日　東工大　金島聡、高木憲明
平成15年8月20-27日　地球電磁気学実習生 3名
平成15年9月10日　財務局内牧支社　東辻ほか2名
平成15年9月15日　産業総合研究所　星住英夫
平成15年10月20日　JAMSTEC 後藤忠徳、笠谷貴史　見学
平成15年10月25日　オープンハウス
平成15年1月15日　火山博物館 池辺伸一郎 研究打ち合わせ
平成15年1月16日　読売新聞社 宇佐美氏　取材
平成16年2月13－16日　京都大学防災研究所　大久保綾子
平成16年3月25-27日　経理部主計科(吉田、中村、馬場)　施設調査